Russian Original Vol. 42, No. 2, February, 1977

August, 1977

SATEAZ 42(2) 91-190 (1977)

SOVIET ATOMIC ENERGY

АТОМНАЯ ЭНЕРГИЯ
(ATOMNAYA ÉNERGIYA)

TRANSLATED FROM RUSSIAN

c/b CONSULTANTS BUREAU, NEW YORK

SOVIET ATOMIC ENERGY

Soviet Atomic Energy is a cover-to-cover translation of *Atomnaya Énergiya*, a publication of the Academy of Sciences of the USSR.

An agreement with the Copyright Agency of the USSR (VAAP) makes available both advance copies of the Russian journal and original glossy photographs and artwork. This serves to decrease the necessary time lag between publication of the original and publication of the translation and helps to improve the quality of the latter. The translation began with the first issue of the Russian journal.

Consultants Bureau journals appear about six months after the publication of the original Russian issue. For bibliographic accuracy, the English issue published by Consultants Bureau carries the same number and date as the original Russian from which it was translated. For example, a Russian issue published in December will appear in a Consultants Bureau English translation about the following June, but the translation issue will carry the December date. When ordering any volume or particular issue of a Consultants Bureau journal, please specify the date and, where applicable, the volume and issue numbers of the original Russian. The material you will receive will be a translation of that Russian volume or issue.

Subscription
$117.50 per volume (6 Issues)
2 volumes per year
Prices somewhat higher outside the United States.

Single Issue: $50
Single Article: $7.50

CONSULTANTS BUREAU, NEW YORK AND LONDON

227 West 17th Street
New York, New York 10011

Published monthly. Second-class postage paid at Jamaica, New York 11431.

Soviet Atomic Energy is abstracted or indexed in *Applied Mechanics Reviews, Chemical Abstracts, Engineering Index, INSPEC—Physics Abstracts and Electrical and Electronics Abstracts, Current Contents,* and *Nuclear Science Abstracts.*

SOVIET ATOMIC ENERGY

A translation of *Atomnaya Énergiya*

August, 1977

Volume 42, Number 2 February, 1977

CONTENTS

CONTENTS

(continued)

The Russian press date (podpisano k pechati) of this issue was 1/24/1977. Publication therefore did not occur prior to this date, but must be assumed to have taken place reasonably soon thereafter.

ARTICLES

THIRTIETH ANNIVERSARY OF THE FIRST SOVIET NUCLEAR REACTOR

V. V. Goncharov

UDC 621.039.5

In 1943, by the decision of the Party and the Government in Moscow, in order to solve the nuclear problem, a special scientific establishment was set up – Laboratory No. 2 of the Academy of Sciences of the USSR, (now, the I. V. Kurchatov Institute of Atomic Energy). I. V. Kurchatov was appointed its scientific director. The main task of Laboratory No. 2 was to carry out research which would permit a chain reaction in a nuclear reactor to be achieved. The reactor would have to be a system of uranium and graphite, moderating the neutrons, in which the release of nuclear energy took place spontaneously. It was postulated that the graphite would make possible the use of natural uranium (with a content of fissile U-235 to a total of 0.7%).

Even in 1940, I. V. Kurchatov produced a report at the All-Union Conference on the Physics of the Atomic Nucleus and published the paper "Fission of Heavy Nuclei." He arrived at the optimistic conclusion that a chain reaction by slow neutrons was entirely feasible. It might have been assumed to be practicable after the discovery in 1939 of the fission reaction of uranium by the action of neutrons. However, in 1941, after the start of the Great Fatherland War (Second World War), work in this direction completely ceased in the Soviet Union and was renewed only in 1943.

A grandiose program for constructing a reactor and for achieving a controlled chain reaction could be carried out only by solving three basic problems: 1) to develop a detailed reactor theory with subsequent experimental verification of the theoretical data; 2) to produce graphite of a high degree of purity to the amount of hundreds of tons and 3) to produce tens of tons of pure metallic uranium. Such graphite and uranium had never been produced in the Soviet Union.

In Laboratory No. 2, theoretical and experimental investigations of the physical constants were developed, especially the cross sections of capture by poisons of thermal (moderated) neutrons in graphite. A method of measuring the absorption cross section for neutrons was found as a result of theoretical work by Ya. B. Zel'dovich, I. Ya. Pomeranchuk and I. I. Gurevich, and experimental investigations carried out by I. V. Kurchatov jointly with I. S. Panasyuk, on the moderation and diffusion of neutrons in graphite. After the development of a method of measuring such small cross sections, physical tests were started on the absorption of neutrons in prisms of mass up to 5 tons, in different batches of graphite (graphitized electrodes), developed by industry.

The first results proved to be one hundred times worse than expected, and caused a great disappointment. Then better batches of graphite were chosen for the tests but they also proved to be unsuitable. The graphite absorbed so many neutrons that it was impossible to achieve a chain reaction. The presence in the graphite of impurities was then established, which were poison-absorbers of neutrons. The impurity content, determined by the amount of ash which remained after ignition of the samples, amounted to 1%.

Kurchatov himself, together with colleagues from Laboratory No. 2, left for the factory and endeavored under his direction to produce the purest graphite. The workers of the factory considered this a completely unachievable desire of the scientists. They maintained that it was not possible to manufacture graphite blocks whose purity must be significantly higher than for diamond (also carbon). Kurchatov and his assistants did not lose faith in their ability to produce graphite of the required purity. But to accomplish this, the technological process for the manufacture of the graphite blocks would have to be improved considerably.

As a result of physical investigations in Laboratory No. 2, in November 1944 the first stringent requirements for reactor graphite were compiled – the content of impurities, i.e., boron, must be not more than a few parts per million.

Translated from Atomnaya Énergiya, Vol. 42, No. 2, pp. 83-86, February, 1977. Original article submitted December 13, 1976.

After a detailed analysis of the existing production technology of graphitized electrodes in the factory, and familiarization with the technical literature, in February 1945 the technical conditions were formulated and measures were developed, recommended by Laboratory No. 2, for solving this difficult and important problem. From March 1945, jointly with Laboratory No. 2, scientific-research and pilot-plant projects were developed in the factory for the purpose of a test production of six experimental batches of pure graphite blocks of 5 tons. The complexity of the problem was aggravated by the fact that the graphitization process lasted about two weeks and the duration of the whole technological cycle was approximately two months. On the first occasion the physical tests of the graphite blocks (measurement of the neutron absorption cross section) were carried out in Laboratory No. 2 and then they were carried out in the factory.

As a result of intensive and self-consolidated work by the factory, jointly with Laboratory No. 2 with the support of the National Committee for Nonferrous Metals of the USSR, by August 1945 a special technological process had been developed successfully and in October the industrial startup of production of the necessary quality was started. Thus, the critical assignment of the State Committee for Defense of the USSR was accomplished ahead of schedule. At the same time, the planning of a new factory was started. Thus, for the first time in the USSR, a method for the production of graphite blocks for reactors had been developed in an exceptionally short period; the basic principle was the use of low-ash raw material and pure materials in electric graphitized furnaces and the achievement of improved processes of thermal and gas refining in graphite furnaces of the normal type, reequipped for this purpose.

It can be seen from the American official report published in 1945, that the production of pure graphite in the USA was considered to be one of the most important and difficult problems, as before 1940 carbon (graphite) had never been produced in such quantity and with such a degree of purity as were required for the moderator in a reactor. At the beginning of summer 1940, there was no guarantee that it was possible for graphite to have such purity and in the required quantity. At the beginning of 1942, the position was still unsatisfactory, and only by the middle of 1942 was the problem mainly resolved. By the autumn of 1942 in Chicago sufficient graphite was produced to make an attempt to construct a reactor. Thus, in the USA, the development of a method to produce pure graphite required more than two years (from the beginning of summer 1940 to the middle of 1942), and only after this was it possible to start the production of graphite for the first reactor, CP-1.

In the Soviet Union, the problem posed was solved successfully in an extremely short time – in all, six months (from March to August 1945), which permitted the industrial production of high-grade graphite blocks to be organized, for the F-1 reactor.

In the reports presented by the USA at the International Conference on the Peaceful Uses of Atomic Energy in Geneva (1955), data were given about the quality of the American graphite. It was found that the impurity content (ash) in the best kind of nuclear graphite, AGOT, was greater by a factor of 3.7 than in the Soviet graphite. The content and cross section of thermal neutron poison-absorbers in this graphite was also found to be higher than in the Soviet graphite. Thus, the quality of the American graphite was significantly less than that of the Soviet Union.

Together with the graphite researchers, a study of the physical characteristics of the small quantity of available uranium was started. The investigations showed that in order to achieve a chain reaction, pure uranium is required in which the content of impurities (boron, cadmium, rare-earth elements) amounted to only negligible fractions. Physicotechnical requirements were formulated for the production of uranium, designed to ensure a high chemical purity and density, and a requirement was established for the capture cross section, taking into account the neutron absorption in the uranium itself and in all impurities. Consequently, the immediate problem was the development of a technology for the manufacture of blocks of uranium metal which did not contain strongly neutron-absorbing poison-impurities.

The problem of uranium p oduction was solved in many establishments: in the scientific-research institutes, in the mines, concentration plants, chemical production plants and factories.

At first, experimental work on the production of uranium was undertaken by Giredmet Narkomtsvetmet SSSR* under the direction of Prof. N. P. Sazhina. I. V. Kurchatov was moved for a short time to Giredmet to offer assistance and to accelerate the accomplishment of the work. At the end of 1945, the decision was taken to organize the production of uranium metal at one of the factories, but by another technology. Thanks to strenuous measures and after overcoming many difficulties, the production of uranium steel metal blocks was successfully started primarily for the F-1 reactor.

*State Rare Metals Research Institute of the National Committee for Nonferrous Metals of the USSR.

When carrying out in Laboratory No. 2 a series of experiments in prisms with different uranium–graphite lattices, it was discovered that certain batches of uranium blocks which were completely acceptable according to the results of chemical and spectroscopic analyses, gave an unsatisfactory neutron multiplication factor. Because of this, a physical quality control was set up in Laboratory No. 2 for all batches of uranium blocks issued by industry. The very great importance of the development of a procedure for the chemical analysis of impurities in the uranium should be mentioned. These procedures did not exist for the majority of elements and their development represented a difficult problem, due to the insignificantly small quantity of impurities which it was required to determine. These analytical methods were developed under the direction of Academician A. P. Vinogradov.

After the arrival of the graphite and uranium blocks in Laboratory No. 2, the conduct of the physical experiments was extended sharply. Day and night in tents and dug-outs, the graphite prisms were assembled with the uranium and then they were disassembled and reassembled. Tens of experiments were carried out, and according to the accumulation of experimental data the physical parameters were refined and reactor theory was improved. The most exact thermal neutron capture cross sections were determined for graphite and uranium. Certain physical characteristics of the uranium blocks were studied also, the optimum parameters were chosen, and the pitch of their arrangement in the space lattice in the graphite. By means of these numerous experiments, after the production of a large amount of graphite and uranium, and the study of their properties, four subcritical models of the reactor were chosen, investigated and dismantled. The calculations permitted the approximate critical dimensions of the reactor to be estimated and the required number of uranium (up to 50 tons) and graphite blocks (approximately 500 tons) to be estimated for its construction.

A special building with a concrete foundation pit 7 m deep and an underground laboratory with a control desk for remote control were designed and constructed. When a sufficient number of uranium and graphite blocks were produced, the quality of which was controlled by physical methods, assembly was started. The active zone of the F-1 reactor was a sphere with a diameter of 6 m, built of graphite blocks with dimensions 100 × 100 × 600 mm. It was surrounded by a reflector, 800 mm thick, also made of graphite blocks. In the graphite blocks about 30,000 openings for the uranium were drilled, forming a space lattice with a defined pitch. Three vertical channels were provided in the reactor, for the rods of the safety and control system, and also six horizontal experimental channels.

The F-1 reactor was started up on December 25, 1946. It startup was conducted by I. V. Kurchatov himself with the participation of assistants. Thus, it was 30 years ago that a controlled fission chain reaction in uranium was accomplished. In 1958, Kurchatov wrote: "I recall the emotion with which, for the first time on the continent of Europe, myself and a group of co-workers successfully achieved a chain fission reaction in the Soviet Union in a uranium–graphite reactor."

The construction, under the direction of Kurchatov, of the F-1 reactor was the greatest achievement of Soviet science and technology, the first stage in the solution of the most complex and difficult of the nuclear problems. The work was carried out under incredibly difficult conditions by the utmost strenuous efforts and genuine enthusiasm of all participants. This was an enormous labor feat of Soviet scientists, engineers, and workers who built the first reactor, and for the uranium and graphite industry.

The startup of the first nuclear reactor in the Soviet Union ensured the feasibility of obtaining many more important theoretical, experimental and methodological results.

The investigations carried out in the F-1 reactor were of enormous importance. Measurements were made of the principal nuclear constants, the optimum lattice was determined for the first commercial reactor and its calculated characteristics were refined, problems of control and safety were studied, and means of shielding from radiation. The small quantity of plutonium produced in the reactor allowed its chemical properties to be studied, and a technology to be developed for its extraction from irradiated uranium. The investigations in the F-1 reactor made possible in every way the further development of reactor theory.

With the aid of the reactor, a method was developed for the quantitative monitoring (by the change of reactivity) of the physical qualities of uranium, graphite and uranium–graphite lattices. The quality of the uranium, graphite and other industrial articles issued for commercial reactors was checked by this method.

The exceptionally valuable experience obtained on the first reactor, and the investigations undertaken in it, permitted progress toward the designing and construction of other reactors and, in its turn, toward the construction of a commercial reactor. Thus, the startup of the first F-1 reactor served as the beginning of the birth of the Soviet nuclear industry.

In comparing the history of construction of nuclear reactors, it should be noted that in the USA the Uranium Committee started operation in October 1939, and the first experiments with carbon (graphite) were commenced in April-May 1940, in Columbia University (from this time, all operations on the uranium problem were classified secret). The chain reaction in the first USA reactor CP-1 was accomplished in December 1942. In the Soviet Union, the first reactor F-1, installed in a special building, was constructed more rapidly than the American reactor and its experimental capabilities proved to be considerably broader than of the Amercian reactor. The power of F-1 reached 4000 kW, but the American reactor did not exceed 200 W. It should be noted that in the Soviet Union, the problem was solved during the war and in the first year of recovery of the national economy, which had suffered enormous material and manpower losses. Also, it was solved only by the efforts of the Russians themselves. In the USA, in a country possessing a highly developed industry, not having suffered from the war, the investigations and construction of the reactor were accomplished with the participation of eminent scientists who had emigrated from Europe.

The F-1 reactor is functioning at the present time in the I. V. Kurchatov Institute of Atomic Energy and it not only of historical value, but also provides for the carrying out of certain researches which are useful even at the present time.

As mentioned, in the USA the first reactor, CP-1, was started up in December 1942. Before the startup of the first production reactor in Hanford, three further research reactors were constructed: at Argonne, with a power of 20 kW (March 1943), CP-2; Clinton, 1000 kW (November, 1943); and X-10 at Oakridge, 3800 kW (November 1943).

After the startup of the first Soviet reactor, F-1, the first production reactor was built and brought into operation in record time in 1948, omitting the construction stage of intermediate expensive facilities.

As the Americans themselves wrote, from the time of the decisive experiments on the chain reaction, the USA required 3.5 yr to the construction of the plutonium reactor at Hanford. In the Soviet Union, this problem was solved in 2.5 yr.

The construction of the F-1 reactor served as the start of the general development of work on the peaceful use of atomic energy. The world's first nuclear power station was started up in the USSR (in April 1954). Then reactors were built with a unit power from 240 MW to 1000 MW for nuclear power stations, reactors for icebreakers, etc. The Soviet Union is operating nuclear power stations and is continuing, with ever-increasing tempo, the construction of new nuclear power stations. Among them are nuclear power stations with high capacity reactors: Leningrad, Novovoronezh, Kursk, Chernobyl'sk, Smolensk, Ignalinsk, Rovensk, Kol'sk, Armyansk, etc. With the assistance of the Soviet Union, nuclear power stations have been constructed and continue to be constructed in the countries of the CMEA countries and in Finland. In the Tenth Five-Year Plan, the capacities of the nuclear power stations brought into operation in the USSR will be increased by almost a factor of four, by comparison with the previous five-year plan.

DIFFERENCE-SCHEME SOLUTION OF HETEROGENEOUS-REACTOR EQUATIONS

B. P. Kochurov and V. M. Malofeev

UDC 539.125.52:621.039.51.12

The equations of a heterogeneous reactor with point sinks and sources were first formulated in [1, 2], and the literature devoted to heterogeneous methods of calculation is now very extensive. General heterogeneous equations, taking into account the finite dimensions of the blocks and including the dipole formulation, are given in [3, 4]. The equations of heterogeneous theory are in matrix form, so that the calculation time and the demands on computer storage capacity increase quadratically with the number of blocks, and hence reactors with more than a few blocks cannot be effectively calculated even using up-to-date computers.

The homogeneous equations have a finite-difference form and so can be applied to large reactors with several thousand lattice points. In [5, 6], a finite-difference formulation of the sink–source equations was proposed. The main terms of these equations have the usual finite-difference "homogeneous form," while the correction terms depend on more distant points and take into account heterogeneous effects.

Recently, the so-called quasialbedo method was proposed [7]: Elementary solutions are constructed in each cell and combined so as to give maximum smoothness of the total solution in the reactor. This method allows heterogeneous reactors with a large number of blocks to be calculated. However, the derivation of these equations is rather complex, and furthermore their relation to heterogeneous theory is not sufficiently clear.

The present paper proposes a method for the direct transformation of the heterogeneous equations to finite-difference form. The approach employed is similar to that of [5, 6], but the formal transformation of the initial heterogeneous equations considerably simplifies the procedure. The use of difference operators with free parameters, chosen as so to give the most complete elimination of distant terms, leads at once to difference equations directly related to the initial heterogeneous equations. These equations are derived without resorting to concepts such as the mean flux in the reactor cells.

The appropriate difference operator providing sufficient (and in fact very high) accuracy is found to be broader than the traditional Laplace operator (the difference scheme for a square lattice should include not less than nine points, which agrees with the results of [7]), so that a member of widely used "homogeneous" algorithms for the solution are inapplicable. However, the Chebyshev iterational method is completely suitable in this case, and was successfully used in the present work.

Formulation of Heterogeneous-Reactor Equations

In place of the point theory of sinks and sources, a general formulation of the heterogeneous equations in the small-group (with a total of G groups) approximation is used (see [3, 4, 8]). The distance between the surfaces of the blocks is assumed to be several times larger than the free-path length of the neutrons in the moderator, while the boundary conditions at the block surfaces are specified in sufficiently general form by the matrix Λ

$$dN = \Lambda N; \quad d \equiv \rho \, (\partial/\partial r) \, |_{r=\rho}. \tag{1}$$

Here N is the vector of extrapolated values of the neutron flux, of dimensionality G × K; K is the number of blocks; Λ is a matrix diagonal in **k**, consisting of G × G matrices for blocks of each kind; ρ is the matrix of block radii. The group fluxes in the moderator satisfy the system of equations

Translated from Atomnaya Energiya, Vol. 42, No. 2, pp. 87-90, February, 1977. Original article submitted April 23, 1976.

TABLE 1. Dependence of Results for Eq. (14) on z for Nine-Point Scheme in Square Lattice

z	α_1	β	R_0	R_1	R_2	K_0	ε
0,1	0,6425	0,9966	—7,730	2,732	0,7614	2,427	$1{,}634^{-3}$
0,5	0,6437	1,020	—2,846	1,706	0,4719	0,924	$1{,}535^{-3}$
1,0	0,6477	1,086	—1,259	1,283	0,3441	0,421	$1{,}279^{-3}$
2,0	0,6624	1,385	—0,330	0,906	0,2122	0,114	$0{,}667^{-3}$
3,0	0,6834	2,039	—0,100	0,731	0,1362	0,035	$0{,}259^{-3}$
4,0	0,7080	3,381	—0,032	0,636	0,0876	0,011	$0{,}081^{-3}$

$$(\Delta - \xi_g)\, n_g = -\xi_{g-1} n_{g-1}; \quad g = 1, \ldots G, \tag{2}$$

where $\xi_g = 1/\tau_g$; $\xi_G = 1/L^2$; and the parameters n_g ($g < G$) differ from the corresponding moderator densities by a factor τ_g/D_G (D_G is the diffusion coefficient of the thermal neutrons; τ_g, and L^2 are the squares of the deceleration and diffusion lengths in the moderator). The general solution of the system in Eq. (2) for a reactor height H is

$$N = C \mathcal{F} A, \tag{3}$$

where the triangular matrix (assuming that energy losses in neutron–moderator collisions are less than the group width) consists of the elements

$$\begin{aligned} &C_{gg} = 1; \quad C_{gg'} = v_{gg'} C_{g-1,\, g'}; \\ &v_{gg'} = \xi_{g-1}/(\xi_g - \xi_{g'}) \; (g > g'); \end{aligned} \tag{4}$$

A is an arbitrary vector of dimensionality K × G; the matrix $\mathcal{F}$ of dimensionality (K × G) × (K × G) (diagonal in g, $1 \leq g \leq G$) consists of weighting functions depending on the boundary conditions at the external surface of the reactor. Since the boundary conditions may be formulated using hypothetical sinks and sources situated outside the reactor in an infinitely extended moderator, while boundary conditions are taken directly into account in the difference formulation, it is sufficient to take the weighting function in an infinite moderator. In this case the use of the summation theorem for Bessel functions gives

$$\mathcal{F} = K_0 + I_0 F, \tag{5}$$

where K_0 and I_0 are matrices diagonal in k with elements

$$K_0 (x_g \rho_k), \quad I_0 (x_g \rho_k);$$

$x_g^2 = \xi_g^2 + \pi^2/H^2$; and the elements of the matrix F are

$$F_{kl}^g = K_0 (x_g \,|\, \mathbf{r}_k - \mathbf{r}_l \,|) \, (1 - \delta_{kl}). \tag{6}$$

Applying the boundary conditions in Eq. (1) to Eq. (3), we find

$$\left.\begin{aligned} dN &= dC \mathcal{F} A = C d\mathcal{F} A; \\ d\mathcal{F} &= dK_0 + dI_0 I_0^{-1} (I_0 F + K_0 - K_0) = \\ &= -I_0^{-1} + dI_0 I_0^{-1} C^{-1} C \mathcal{F}; \\ dN &= -C I_0^{-1} A + C dI_0 I_0^{-1} C^{-1} N = \Lambda N; \\ A &= \gamma N; \quad \gamma = -I_0 C^{-1} \Lambda + dI_0 C^{-1}. \end{aligned}\right\} \tag{7}$$

Here the expression for the Wronskian of a Bessel function is used

$$dK_0 - dI_0 I_0^{-1} K_0 = -I_0^{-1}.$$

Substituting A in Eq. (3) gives

$$N = C \mathcal{F} \gamma N.$$

TABLE 2. Basic Reactor Characteristics

Parameter	Reactor		
	1	2	3
No. of groups	2	3	3
Reactor radius, cm	650	500	105
Spacing, cm	26	20	8,5
Growth of neutrons, cm^2	100	40; 80	80; 40
Square diffusion length, cm^2	10000	5000	10000
No. of channels	55; 2	124; 20; 77	124; 97
Fuel-channel radius, cm	5,7; 2.9	5; 3; 5	3; 3

Equations of similar structure in which N appears but A does not were formulated in [3, 4] in a rather different form.

If we separate out from γ a part γ_1 proportional to the source of fission neutrons and divide it by the eigennumber, the effective multiplication factor λ making the reactor critical (i.e., if we make the substitution $\gamma \to \gamma_1/\lambda - \gamma_2$), the equation for N takes the form

$$N = (C\mathcal{F}\gamma_1/\lambda - C\mathcal{F}\gamma_2)\,N. \tag{8}$$

Note that the matrix γ is related to the matrix Λ by the simple transformation in Eq. (7), affecting each type of block individually.

Transformation of Heterogeneous-Reactor Equations to Difference Equations

We now pass to a difference formulation of Eq. (8). Introducing an arbitrary (diagonal in **k** and g) matrix D* and bearing in mind Eq. (5), Eq. (8) may be transformed to give

$$UN = (I_0^{-1}K_0 + F)\,(\gamma_1/\lambda)\,N - (F + D)\,\gamma_2 N; \quad U \equiv I_0^{-1}C^{-1} + (I_0^{-1}K_0 - D)\,\gamma_2. \tag{9}$$

For the variable $\tilde{N} = UN$, we obtain the equation

$$\tilde{N} = (I_0^{-1}K_0 + F)\,(\tilde{\gamma}_1/\lambda)\,\tilde{N} - (F + D)\,\tilde{\gamma}_2\tilde{N}; \tag{10}$$

$$\tilde{\gamma}_{1,2} = \gamma_{1,2}U^{-1}. \tag{11}$$

The matrices $\tilde{\gamma}_{1,2}$ are related to $\gamma_{1,2}$ by simple transformations individually for each type of block and serve as effective characteristics for $\tilde{N}$. Note that Eq. (10) has the structure of the equation for point blocks, although this was not assumed in the initial theory; characteristics associated with finite blocks are included in $\tilde{\gamma}_{1,2}$.

The aim of the transformation leading to Eq. (10) is to obtain the matrix F in Eq. (6) as the first operator in the left-hand side.

Replacing $\mathbf{r}_k$ by an arbitrary vector **r** in the elements F leads to the condition (if $\mathbf{r} \neq \mathbf{r}_l$)

$$(\Delta_r - x_g^2)\,F^g(\mathbf{r}, \mathbf{r}_l) = 0.$$

This equation will be approximately satisfied if a difference operator which contains the operator Δ_1 acts on the variables $\mathbf{r}_k$. The operator Δ_1 replaces the Laplacian in the grid of lattice points (a is the lattice spacing)

$$(\Delta_1 - x_g^2a^2)\,F^g(\mathbf{r}_k, \mathbf{r}_l) \approx 0; \quad |k_i - l_i| > 1;$$
$$\Delta_1 : f_k \to \Big(\sum_Q f_{k+Qe_i} - 4f_k\Big)/|\mathbf{e}_i|^2, \tag{12}$$

*The matrix D is introduced so as to preserve the structure of the equation, but may affect the rate of convergence of the iterative process; so far it has been assumed that D = 0.

where $\mathbf{e}_1 = (1, 0)$, while Q specifies rotation of the vector by 0, 90, 180, and 270°.

We now drop the requirement that the operator in Eq. (12) be exactly the Laplace operator on the grid, and demand simply that it be constructed "locally," i.e., relate only a few adjacent points. In addition, of course, it is required to be symmetric with respect to rotations around lattice points k on the grid that return it to its original position. For a square lattice, we may take an operator P (diagonal in g, with elements P_g) relating to values of the functions on adjacent blocks

$$\begin{gathered} P_g : f_{\mathbf{k}} \to (-\alpha_1\Delta_1 - \alpha_2\Delta_2 - \ldots - \alpha_I\Delta_I + \\ + \beta x_g^2 a^2) f_{\mathbf{k}}; \\ \sum_{i=1}^{I} \alpha_i = 1; \quad \alpha \equiv (\alpha_1, \ldots, \alpha_{I-1}). \end{gathered} \tag{13}$$

The operator Δ_2 differs from Δ_1 in the replacement of $\mathbf{e}_1 = (1, 0)$ by $\mathbf{e}_2 = (1, 1)$, i.e., Δ_2 includes the series of blocks immediately following k, etc. For example, in the case of a nine-point scheme, P_g contains only Δ_1, Δ_2, and $\alpha_2 = 1 - \alpha_1$. We denote by $U_{\mathbf{k}}$ the set of adjacent indexes covered by the operator P_g.

The parameters α and β in Eq. (13) are required to provide the most complete elimination of the elements $F_{\mathbf{kl}}$ outside $U_{\mathbf{k}}$. Since $F_{\mathbf{kl}}$ is invariant with respect to shifts of the lattice, to find α and β it is sufficient to consider the case $\mathbf{k} = 0$. It is possible to adopt various criteria, but previously two have been used in the metrics L^∞ and L^2

$$\max_{\mathbf{l}} |P_g(\alpha, \beta) F^g_{0,\mathbf{l}}| \to \min, \quad \mathbf{l} \notin U_0; \tag{14}$$

$$\sum_{\mathbf{l}} [P_g(\alpha, \beta) F^g_{0,\mathbf{l}}]^2 \to \min, \quad \mathbf{l} \notin U_0, \tag{15}$$

where $\mathbf{l}$ runs through a sufficiently large set of points, including the point 0. If the operator $P(\alpha, \beta)$ obtained from Eqs. (14) and (15) operates from the left on both sides of Eq. (10) then, for each k, it results in approximately complete elimination of all the elements of the matrix in Eq. (10) outside the region $U_{\mathbf{k}}$. On the other hand, the elements of $F_{\mathbf{kl}}, \mathbf{l} \in U_{\mathbf{k}}$, are not eliminated. We denote by R the result obtained when $P(\alpha, \beta)$ operates on $F_{\mathbf{kl}}, \mathbf{l} \in U_{\mathbf{k}}$

$$R = P(\alpha, \beta)(F + D). \tag{16}$$

In place of Eq. (10) we obtain

$$(P + R\tilde{\gamma}_2)\tilde{N} = [P(I_0^{-1}K_0 - D) + R](\tilde{\gamma}_1/\lambda)\tilde{N}, \tag{17}$$

neglecting the results obtained when P operates on $F_{\mathbf{kl}}$, $\mathbf{l} \notin U_{\mathbf{k}}$.

The structure of Eq. (17) is that of a difference equation: for each k, the effect of the operators P and R is concentrated in the region $U_{\mathbf{k}}$, and the other matrices – $\tilde{\gamma}_1$, $\tilde{\gamma}_2$, $(I_0^{-1}K_0 - D)$ – are diagonal in k. Note that the structure of the matrix $R\tilde{\gamma}_2$ is triangular in g.

By extending the region $U_{\mathbf{k}}$, i.e., adding new series of blocks and correspondingly enlarging the set α, β with new parameters, it is possible in principle, to eliminate the operator F ever more precisely outside $U_{\mathbf{k}}$. If F is a short-range operator (i.e., in epithermal groups), it may be left in the initial form, as in Eq. (10).

Although the given theory was developed in a monopole approximation, it may also be used for heterogeneous equations in a dipole formulation. Symbolically, Eqs. (8) and (10) are unchanged, but the matrix F must be extended by elements of the form

$$K_n(x_g|\mathbf{r}_{\mathbf{k}} - \mathbf{r}_{\mathbf{l}}|)\exp(in\,\psi_{\mathbf{kl}}); \quad n = \pm 1, \tag{18}$$

where $\psi_{\mathbf{kl}}$ may be taken to be the angle between some fixed direction and the vector $(\mathbf{l} - \mathbf{k})$; it is again possible to apply a procedure of the form of Eq. (14) or (15), leading to a difference equation similar to Eq. (17). Evidently the theory is also applicable to reactors with blocks at the points of a triangular or hexagonal lattice.

The solution of Eq. (14) or (15) depends only on a single parameter $z \equiv x_g a$. Table 1 gives solutions of Eq. (14) (the parameters α_1 and β; the elements of the operator R at the points 0, $\mathbf{e}_1$, and $\mathbf{e}_2$; values of the Bessel function $K_0(z)$; the maximum error $\varepsilon = \max|PF|$, $\mathbf{l} \in U_{\mathbf{k}}$ for various values of z, for a nine-point scheme in a square lattice. The difference of β from 1 characterizes the extent to which the operator P differs from the operator $\Delta_1 - z^2$; the value of $K_0(z)$ shows how far the effect of the initial operator F extends. Note that the elements of the operator R are of opposite sign to the elements of P and on the whole, as is clear from a comparison with the homogeneous equations, $R\tilde{\gamma}_2$ characterizes the mean-square migration length of the neutrons in the reactor lattice (and not purely in the moderator).

Method of Solving Difference Equation

The solution of Eq. (17) was programmed in a monopole, small-group approximation for a square lattice using nine- and five-point schemes. Iteration of sources was used, with acceleration by the Chebyshev method in conjunction with the Chebyshev method for internal iteration [9]. The set of Chebyshev parameters for internal iteration was determined after a preliminary estimate of the limits of the operator spectrum

$$A_g = P_g + R_g\tilde{\gamma}_{2,gg}. \tag{19}$$

As shown by trial calculations, the limits of the operator spectrum A_g always lie on the real axis of the complex plane and are positive, which is necessary for convergence of the internal iteration. Adding the operator $R_g\tilde{\gamma}_{2,gg}$ to P_g leads to narrowing of the limits of the spectrum and improved convergence.

Numerical Comparison with the Direct Method

The solution of Eq. (17) was compared numerically with results obtained by direct solution of Eq. (8) by a modification of the DIGGER program [8] for a BÉSM-6 computer and FORTRAN for a cylindrical reactor of radius R_r with correspondingly altered weighting functions.

For a five-point scheme, the error ε is large – two orders of magnitude higher than the corresponding figures in Table 1 for the nine-point scheme. This leads to considerable disagreement with the direct method – usually up to a few percent in the neutron flux, and an order of magnitude higher in the eigennumber.

However, the accuracy obtained using the nine-point scheme is good: As a rule, the differences in the group fluxes of neutrons (thermal and epithermal) do not exceed a few tenths of a percent, and those in the effective multiplication factor for the neutrons amount to a few hundredths of a percent. Table 2 gives basic characteristics for three reactors. The differences in the multiplication factor and the maximum difference in the neutron flux by Eq. (8) (the direct method) and Eq. (17) (the difference method) are as follows: for the first and second reactors, less than 10^{-4} and less than 10^{-3}; for the third reactor, $2.5 \cdot 10^{-4}$ and $1.4 \cdot 10^{-3}$, respectively. In the first reactor, the active zone had channels typical for a heavy-water reactor using natural uranium with gas cooling [10] and two asymmetrically positioned regulators; the reflector was taken to be large enough to exclude small differences in the description of conditions at the external reactor boundary in the direct and difference methods (in the latter case, the circular boundary was approximated by a discontinuous line). In the active zone of the second reactor, blocks with a moderator and a certain number of light absorbing rods and hollow tubes were used. The third reactor was small, and contained blocks with a moderator and some heavy regulators.

Thus, by means of the proposed difference method, it is possible to obtain the solution of heterogeneous-reactor equations (for a square lattice, a scheme with no less than nine points should be used) with an accuracy that is entirely satisfactory in practice.

LITERATURE CITED

1. A. D. Galanin, in: Proc. International Conference on the Global Use of Atomic Energy (Geneva, 1955) [Russian translation], Vol. 5, Izd. AN SSSR, Moscow (1958), p. 571.
2. S. M. Feinberg, ibid., p. 578.
3. T. Auerbach, EIR-200, Eidg. Inst. f. Reaktorforschung, Würenlingen, Switzerland (1970).
4. A. D. Galanin, Theory of Heterogeneous Reactors [in Russian], Atomizdat, Moscow (1971).
5. D. Blackburn, in: Proc. EAES Symposium on Advances in Reactory Theory, Vol. 2, Karlsruhe (1963).
6. D. Blackburn and C. Griggs, in: Proc. Conference on Applications of Computing Methods to Reactor Problems, ANL-7050, Illinois, May 17-19 (1965), p. 231.
7. S. S. Gorodkov, Preprints IAÉ-2251 and IAÉ-2296 [in Russian], Moscow (1973); Preprint IAÉ-2502 [in Russian], Moscow (1975).
8. B. P. Kochurov, Preprint ITÉF-2 [in Russian], Moscow (1974).
9. V. I. Lebedev and S. A. Finogenov, Zh. Vychisl. Mat. Fiz., 13, No. 1, 18 (1973).
10. V. M. Abramov et al., At. Energ., 36, No. 2, 113 (1974).

GAS-THERMAL TREATMENT OF NUCLEAR POWER-STATION FUEL ELEMENTS TO SEPARATE THE CORE FROM THE CAN

G. P. Martynovskikh, A. T. Ageenkov, M. M. Arduanov, A. F. Bogatov, E. M. Valuev, V. F. Savel'ev, V. A. Chemezov, G. I. Chechetin, and Yu. V. Yastrebov

UDC 621.039.546.3:66.094.16.0015

The removal of irradiated fuel-element cans has been considered in a large number of investigations, and a great deal of laboratory and experimental equipment for mechanical, chemical, electrochemical, pyrochemical, pyrometallurgical, and combined test methods has been developed [1].

In order to remove the cans of nonirradiated, unconditioned fuel elements, mechanical cutting is usually employed [2]. Such methods fracture a considerable number of the fuel briquets, which become unfit for a second charging; this seriously harms the technological-economic indices of fuel-element production.

The aim of the present investigation is to study methods of processing unconditioned fuel elements of the VVÉR and RBMK types so as to be able to extract the fuel briquets from the cans without damage.

As a means to this end we took the method of hydrogen treatment (hydrogenation of the fuel elements) [3-5], which produces considerable changes in the physicochemical and mechanical properties of cans made from the zirconium alloy Zr–1% Nb [6, 7] and at the same time creates favorable conditions for freely emptying the fuel briquets by enlarging the annular gap between the core (oxide fuel briquets) and the hydrogenated can.

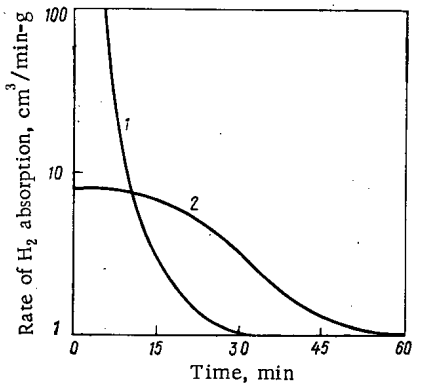

Fig. 1

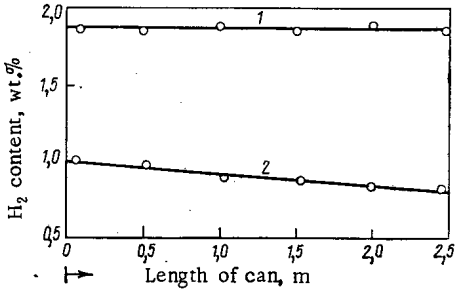

Fig. 2

Fig. 1. Kinetics of the absorption of hydrogen by the Zr–1% Nb alloy can; 1, 2) at 770° and 700°C for a hydrogen pressure in the apparatus of 200-500 and 10-30 mm Hg, respectively.

Fig. 2. Hydrogen distribution in a Zr–1% Nb alloy can after saturation for 60 min. Notation as in Fig. 1; arrow indicates point of hydrogen supply.

Translated from Atomnaya Energiya, Vol. 42, No. 2, pp. 91-93, February, 1977. Original article submitted June 21, 1976.

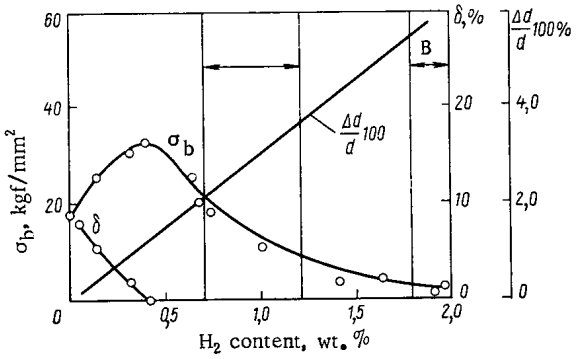

Fig. 3

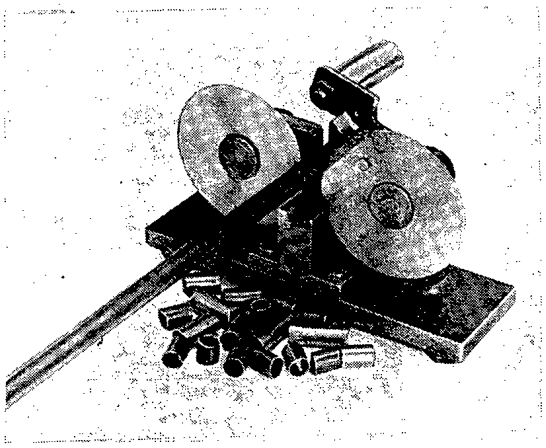

Fig. 4

Fig. 3. Effect of hydrogen content on the tensile strength σ_b and relative elongation δ of the alloy Zr–1% Nb and increment in the can diameter $(\Delta d/d) \cdot 100$.

Fig. 4. Mechanism for removing the end sections from the fuel elements after hydrogen saturation of their cans.

TABLE 1. Final Hydrogen Content of Can Material after Thermal Degassing at Rarefaction of $5 \cdot 10^{-2}$ mm Hg

Exptl. conditions		Hydrogen content of can, wt.%
temp.	duration, h	
600	1,0	0,90
600	3,0	0,29
800	1,0	0,03
800	3,0	0,01
900	1,0	$<$ 0,01

Under earlier-proposed conditions of treatment [4] the hydrogenation process took place very intensively (Fig. 1, curve 1). The absorption of more than 30 wt. % of hydrogen by the can required only 10-15 min. This led to the local overheating of the can and curved the fuel elements, which prevented the free movement of the fuel briquets inside the can. A fair number of the briquets were also fractured or cracked.

The zirconium alloy can was almost completely saturated with hydrogen (corresponding to the composition ZrH_2) along the whole length of the fuel element (Fig. 2, curve 1). The zirconium alloy became so weak (Fig. 3, region B) that the cans easily broke on removal from the apparatus or during transportation. It was therefore necessary to choose hydrogen treatment parameters such as would exclude the deformation of the fuel elements during hydrogen absorption, and mechanical damage during charge-transfer and transportation.

Our tests showed that the optimum hydrogen concentration in the can was 0.7-1.2 wt. % (Fig. 3, region A). Hydrogen was therefore introduced into the can at 650-700°C and a hydrogen pressure of around 15 mm Hg for 60 min (Fig. 1, curve 2). This mode of hydrogen absorption also enabled us to create an annular gap between the core and the can sufficient to allow the free extraction of the fuel briquets.

In experiments on the simultaneous hydrogenation of a group of fuel elements, a prespecific hydrogen concentration was created along the whole length of the case to an accuracy of ±0.15 wt. %. The hydrogen absorption of the can at 700°C diminished on moving away from the point of gas supply (Fig. 2, curve 2), but even in the case of a unilateral supply of the gas from the end the nonuniformity of hydrogen absorption was no greater than 0.3 wt. %. On feeding hydrogen in both from the ends and in the middle of the can, the nonuniformity of saturation was no greater than ±0.1 wt. %.

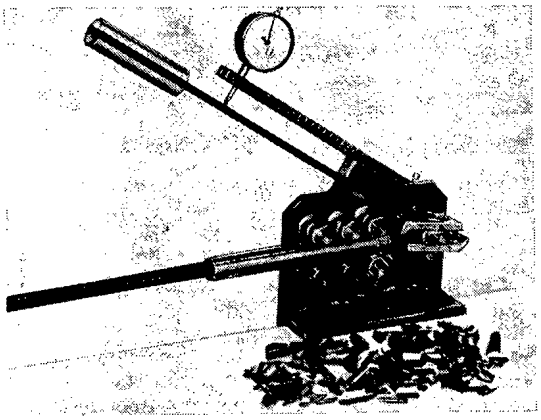

Fig. 5. Rotor-type mechanism for crushing the embrittled fuel-element cans.

The subsequent technology of processing the fuel elements included the separation of the end sections, the extraction of the fuel briquets from the can, the crushing of the embrittled shell, and the deactivation and reuse of the can fragments. In order to execute these technological operations we created and tested various experimental devices and investigated the deactivation of the cans and the removal of hydrogen from the latter.

Tests confirmed the suitability of our experimental device for separating the end sections of the fuel element with disk cutters (Fig. 4). The torque required for cutting was no greater than 1.5 kgf·m, and the angular velocity of the leading edge of the disk amounted to 8-12 rpm. Experimental tests on a vibrational system for removing the fuel briquets showed that the rate of extracting the briquets depended very largely on the vibration frequency. The optimum rate of displacement of the briquets in a can inclined at an angle of 3-6° (35-120 mm/sec) was achieved for a vibration amplitude of 1-3 mm and a frequency of 9-17 Hz.

The impact strength of the hydrogenated cans was ~ 1 kgf · m/cm^2, bearing witness to their embrittled state. However, in mechanical rupture tests on a hydrogenated can 13.9 mm in diameter and 1.1 mm thick the tensile strength was ~ 16 kgf/cm^2. The retention of a moderately high strength by the can prevents deformation of the fuel elements and ensures execution of the charge-transfer operations without any danger of premature mechanical failure.

Analysis of various crushing techniques (with rollers, jawbreakers, etc.) showed that the rotor mechanism of Fig. 5 crushed the hydrogenated fuel-element cans most efficiently. In this method the can is moved along a guide made in the form of rollers or tube and is broken with a rotating rotor. The length of the can fragments lies in the range 15-110 mm, the better uniformity being achieved on using a guide in the form of a tube.

In order to utilize the hydrogen-containing can fragments, we carried out some experiments which confirmed the possibility of deactivating the contaminated inner surface of the can fragments with carbonate-peroxide solutions at 50-60°C.

The deactivated zirconium fragments were remelted after preliminary thermal degassing. The experimental data (Table 1) show that 99% of the hydrogen is removed in 3 h at 800°C, the residual hydrogen content of the alloy being 0.01 wt. %. If necessary a higher degree of purification of the zirconium scrap from hydrogen may be achieved.

The degassed zirconium scrap was remelted in electron-beam and vacuum-arc furnaces. The hydrogen content of the resultant material was $8 \cdot 10^{-4}$-$5 \cdot 10^{-5}$ wt. % while the oxygen and nitrogen content remained at the original level.

We have thus successfully demonstrated the use of one procedure for regenerating nonirradiated fuel elements of the VVÉR- and RBMK types, incorporating the following stages: saturation of the Zr–1% Nb alloy cans with hydrogen in order to embrittle the cans and increase the annular gap between them and the core; mechanical removal of the metal parts at the ends; vibrational extraction of the fuel briquets and crushing of the can; chemical deactivation of the can fragments with a carbonate-peroxide solution; thermal degassing of the can fragments in vacuo, and metallurgical remelting of the zirconium scrap so degassed.

LITERATURE CITED

1. A. T. Ageenkov, V. F. Savel'ev, and E. M. Valuev, Preparation of Irradiated Nuclear Fuel for Chemical Reprocessing [in Russian], TsNIIatominform (Central Scientific-Research Institute of Atomic Information), Moscow (1975).
2. V. B. Shevchenko (editor), Reprocessing the Fuel of Power Reactors (Reference Book) [in Russian], Atomizdat, Moscow (1972).
3. U. S. Patent No. 2962371 (1960).
4. A. T. Ageenkov and V. F. Savel'ev, At. Energ., 32, No. 6, 474 (1972).
5. U. S. Patent No. 3135697 (1961).
6. A. T. Ageenkov et al., Izv. Akad. Nauk SSSR, Metally, No. 4, 160 (1973).
7. A. T. Ageenkov and V. F. Savel'ev, At. Energ., 37, No. 1, 58 (1974).

BEHAVIOR OF HIGHLY ACTIVE WASTE PRODUCTS OBTAINED WHEN REGENERATING THE FUEL ELEMENTS OF FAST REACTORS BY THE GAS-FLUORIDE METHOD

A. P. Kirillovich, Yu. G. Lavrinovich, O. V. Skiba, M. P. Vorobei, and D. I. Starozhukov

UDC 621.039.59:621.039.75

Nonaqueous methods of regenerating nuclear fuel in the irradiated condition have recently been developed and experimentally verified, as being the most promising methods of reprocessing the fuel elements of fast reactors. The gas-fluoride technique constitutes one of these procedures [1, 2]. Further development of these methods is largely determined by the problem of isolating the highly active waste products and storing them safely. The solution depends on the large number of factors, and primarily on a knowledge of the properties and behavior of the highly active waste, as well as methods of preparing the waste for prolonged storage or burial. Studies of this nature have already been carried out with model and labeled waste products [3]. In view of the newness of the fuel-regeneration methods which have been developed, hardly any such information has been obtained in relation to real waste products.

This paper presents a certain amount of information regarding the properties and behavior of highly active waste products obtained in regenerating briefly held fuel elements of the BOR-60 reactor by the gas-fluoride method.

Characteristics of the Test Device and Experimental Method. Tests were carried out in a special experimental device mounted in a hot chamber. Constructionally this was composed of a number of individual instruments and devices for determining the energy evolution, the radiation and thermal resistance, the thermal conductivity and diffusivity, the volatility of the fission products and the degree of contamination of the gas phase for various methods of storing the waste products, corrosive effects on the construction materials, the conditions and feasibility of hermetizing the waste, methods of verifying hermetization, and other properties determining the safety and reliability of the isolated storage of highly radioactive materials. The tests system is furnished with manipulators.

For measuring the energy evolution of irradiated fuel and highly active waste products, a double (differential) calorimeter of the heat-conducting type was employed [4]. Chromel–nickel thermopiles acted as sensors for recording the thermal flux. The measuring system comprised a dc amplifier, a matching chain

Translated from Atomnaya Énergiya, Vol. 42, No. 2, pp. 94-98, February, 1977. Original article submitted May 24, 1976.

TABLE 1. Forms and Characteristics of Solid High-Activity Waste Products Obtained in the Experimental Regeneration of the Fuel Elements of the BOR-60 Reactor

Form of waste	Fuel-element cooling time, months	Yield of waste, kg/kg UO_2	Bulk density, kg/m³	Spec. heat evolution	Activity		Content of radionuclides, Ci/kg										
					specific, Ci/kg	orig. fuel activity, %	$^{144}Ce - ^{144}Pr$	^{141}Ce	$^{106}Ru - ^{106}Rh$	^{103}Ru	^{137}Cs	^{134}Cs	^{95}Zr	^{95}Nb	^{90}Sr	^{129m}Te	^{129}Te
Irradiated fuel	3	—	—	95,8	28 740	100	6 500	680	210	250	17,0	13,0	3 150	6 900	224,7	—	—
	6	—	—	16,9	5 600	100	2 590	3,9	126	8,0	4,1	1,8	230	460	—	—	—
Fluorination ashes	3	0,147	2540	552,3	165 690	85	30 000	3 000	540	640	86	64	16 000	3 800	1578	—	—
	6	0,18		75,5	24 900	81	12 200	6,0	290	8,3	22	2,76	900	288	—	—	—
Purifying sorbent	3	1,0	710	3,97	1 191	4,3	4,8	0,64	150	100	0 64	0,34	0,89	59	0,29	—	—
	6	0,62		2,3	760	8,4	26,3	1,2	310	4,7	2,1	0,81	3,78	290	—	—	—
Sorbent of sorption–desorption cycle	3	1,477	715	2,56	768	5,3	3,1	0,21	1,4	0,35	0,041	0,01	1,55	12,5	—	—	—
	6	2,260		0,391	129	5,2	24,1	0,043	26	0,284	0,065	0,036	1,89	6,3	—	—	—
	3	2,18		0,07	21	0,1	0,17	0,013	1,6	1,2	0,01	0,01	0,016	0,002	—	3,9	2,0
Chemical absorbent	6	1,8	1060	0,391	129	4,2	0,028	0,007	8,35	0,10	0,14	0,007	0,21	0,39	—	—	—

TABLE 2. Thermal Balance of the Fission Products

Form of Product	Amount, kg	Spec. heat evolution, W/kg	Total heat evolution, W
Irradiated fuel	1.896	95.8	181.6
Purifying sorbent	1.890	4.0	7.6
Sorbent of the sorption–desorption cycle	2.800	2.6	7.3
Chemical absorbent	4.100	0.1	0.4
Ashes	0.280	552.3	154.6
Total			169.9

of resistances, and a recording instrument. The sensitivity remained constant with changing power of heat evolution in the calorimeter cell (from thousandth parts to several watts). The error in measuring the specific thermal power of the radioactive materials was ±5%. The minimum heat evolution recorded in the apparatus was $\sim 0.9 \cdot 10^{-7}$ W.

The radiative gas evolution was determined from the amount of evolving gas and the pressure increment in the closed system, as recorded by a differential micromanometer of the membrane type.

The degree of contamination of the gas phase was estimated by measuring the aerosol activity collected in a filter of the AFA-RMP-20 type. The radionuclide composition of the aerosols and the concentration of fission products in these were determined by measuring the γ spectra with DGDK lithium drift detector and an AI-4096 multichannel analyzer. The spectrometer was calibrated by reference to standards of the OSGI type, and the area and intensity of the photopeaks were calculated by means of a BÉSM-3 computer.

The thermal stability of the samples was studied by differential thermal analysis [5]. The furnace was heated at 8-10°C/min, the limiting temperature being 800-850°C. The phase transformations taking place in the material while heating were recorded by means of a Kurnakov pyrometer of the NTR-70 type in the form of simple and differential recordings on photographic paper. The temperature of the phase transformations were determined from a calibration curve to an accuracy of ±3°C. Calcined aluminum oxide served as indifferent material.

Results and Discussion. The principal forms and characteristics of the waste products are shown in

TABLE 3. Passage of Radionuclides from the Solid Waste into the Gas Phase as a Function of Time

Form of waste	Holding time, h	Activity of radionuclides, Ci					
		$^{144}Ce-^{144}Pr$	^{137}Cs	^{103}Ru	$^{106}Ru-^{106}Rh$	^{95}Zr	^{95}Nb
Sorbent	96	$7,0\cdot10^{-6}$	$1,1\cdot10^{-7}$	$3,8\cdot10^{-7}$	$1,7\cdot10^{-6}$	$6,8\cdot10^{-7}$	$1,3\cdot10^{-6}$
	192	$3,2\cdot10^{-6}$	$1,2\cdot10^{-7}$	$1,3\cdot10^{-7}$	$7,9\cdot10^{-7}$	$5,2\cdot10^{-7}$	$1,3\cdot10^{-6}$
	336	$1,9\cdot10^{-6}$	$2,3\cdot10^{-8}$	$2,9\cdot10^{-8}$	$2,4\cdot10^{-7}$	$6,7\cdot10^{-8}$	$7,0\cdot10^{-7}$
	936	$2,5\cdot10^{-7}$	$4,3\cdot10^{-9}$	$6,0\cdot10^{-10}$	$9,8\cdot10^{-8}$	$1,4\cdot10^{-8}$	$3,8\cdot10^{-8}$
Chemical absorbent	72	$1,6\cdot10^{-6}$	$3,2\cdot10^{-8}$	$2,0\cdot10^{-7}$	$1,7\cdot10^{-6}$	$2,5\cdot10^{-7}$	$5,6\cdot10^{-7}$
	96	$1,5\cdot10^{-6}$	$2,7\cdot10^{-8}$	$8,4\cdot10^{-8}$	$1,0\cdot10^{-6}$	$1,4\cdot10^{-7}$	$3,9\cdot10^{-7}$
	336	$1,1\cdot10^{-6}$	$2,2\cdot10^{-8}$	$3,7\cdot10^{-8}$	$3,8\cdot10^{-7}$	$5,4\cdot10^{-8}$	$3,2\cdot10^{-7}$
	936	$3,1\cdot10^{-7}$	$4,2\cdot10^{-9}$	—	$4,9\cdot10^{-8}$	$2,1\cdot10^{-8}$	$5,2\cdot10^{-8}$
Ashes	96	$5,8\cdot10^{-6}$	$1,3\cdot10^{-8}$	$6,8\cdot10^{-7}$	$4,6\cdot10^{-6}$	$8,1\cdot10^{-7}$	$1,9\cdot10^{-6}$
	192	$4,0\cdot10^{-6}$	$5,8\cdot10^{-8}$	$4,8\cdot10^{-7}$	$1,9\cdot10^{-6}$	$4,4\cdot10^{-7}$	$1,8\cdot10^{-6}$
	336	$5,9\cdot10^{-7}$	$8,2\cdot10^{-9}$	$3,8\cdot10^{-8}$	$2,0\cdot10^{-7}$	$5,8\cdot10^{-7}$	$2,3\cdot10^{-7}$

*Self-heating temperature of ashes.

TABLE 4. Passage of Radionuclides from the Waste Products into the Gas Phase as a Function of Temperature

Form of waste	Holding time, h	Heating temp. °C	Activity of radionuclides, Ci							
			$^{144}Ce-^{144}Pr$	^{137}Cs	^{103}Ru	$^{106}Ru-^{106}Rh$	^{95}Zr	^{95}Nb	^{155}Eu	^{125}Sb
Sorbent	24	25	$1,6\cdot10^{-6}$	$2,0\cdot10^{-8}$	$8,0\cdot10^{-8}$	$3,8\cdot10^{-7}$	$1,5\cdot10^{-7}$	$2,7\cdot10^{-7}$	—	—
		100	$1,6\cdot10^{-6}$	$2,4\cdot10^{-8}$	$1,6\cdot10^{-7}$	$5,1\cdot10^{-7}$	$1,5\cdot10^{-7}$	$5,9\cdot10^{-7}$	—	—
		200	$2,4\cdot10^{-6}$	$8,5\cdot10^{-8}$	$1,0\cdot10^{-7}$	$7,9\cdot10^{-7}$	$1,9\cdot10^{-7}$	$1,3\cdot10^{-6}$	—	—
Chemical absorbent	72	25	$1,6\cdot10^{-6}$	$3,2\cdot10^{-8}$	—	$1,7\cdot10^{-6}$	$2,5\cdot10^{-7}$	$5,6\cdot10^{-7}$	—	—
		100	$2,8\cdot10^{-5}$	$3,1\cdot10^{-7}$	—	$8,7\cdot10^{-6}$	$8,7\cdot10^{-8}$	$2,6\cdot10^{-7}$	—	—
		200	$2,5\cdot10^{-5}$	$3,6\cdot10^{-7}$	—	$6,6\cdot10^{-6}$	$3,7\cdot10^{-7}$	$3,2\cdot10^{-7}$	—	—
Ashes	96	78	$2,8\cdot10^{-4}$	$3,8\cdot10^{-6}$	—	$2,8\cdot10^{-5}$	$9,4\cdot10^{-7}$	$2,4\cdot10^{-6}$	$7,0\cdot10^{-7}$	$1,5\cdot10^{-6}$
	10	400	$9,0\cdot10^{-3}$	$1,2\cdot10^{-4}$	—	$1,0\cdot10^{-3}$	$3,6\cdot10^{-5}$	$9,1\cdot10^{-5}$	$1,6\cdot10^{-5}$	$1,8\cdot10^{-3}$

Note: The difference in the yield of aerosols from the surface of the ashes (Table 3) is due to the experimental conditions: In the first case the aerosol yield was determined under steady-state conditions, in the second under dynamic conditions (in selecting the gas phase for mass-spectrometric analysis).

Table 1. For comparison the first line presents some experimental data obtained for irradiated fuel. Tests showed that 80-85% of the activity of the fission products was concentrated in the fluorination residue (ashes), the specific heat evolution of which was 75.5 and 552.3 W/kg and the β activity over 20 and 160 thousand Ci/kg (depending on the form of the reprocessed fuel).

The remaining 10-15% of the activity was distributed in the sorbent (NaF) and chemical absorbent (KhP-I), the heat evolution of which fluctuated in the range 0.07-4 W/kg. The solid waste products formed in the gas-fluoride reprocessing of nuclear fuel constituted loose powdered (ash) or granulated (sorbents, chemical absorbent) materials, having various bulk densities (Table 1). The main long-lived radionuclides were concentrated in the ash.

Table 2 (based on calorimetric measurements) illustrates the thermal balance of the fission products during the reprocessing of the fuel; the 11.7 W (6.5%) balance discrepancy is explained by the fact that samples from the filters and services were not analyzed. The calorimetric method was sufficiently reliable when studying energy evolution and the activity of the irradiated fuel and high-activity waste.

The self-heating temperature of the waste products and the variation in temperature with time during the natural cooling of the containers (volume 1 liter, diameter 105 mm, wall thickness 2.5 mm) are given in Fig. 1. The high temperature drop between the center and wall of the container accommodating the ashes arising from fluorination is due to the low thermal conductivity of the ash.

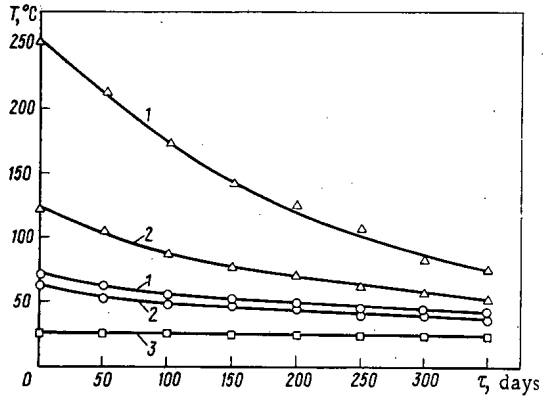

Fig. 1. Change in the temperature of the waste products and walls of the container during the experiments: 1, 2) ashes with masses of 0.280 and 0.435 kg and heat evolution of 552.3 and 75.5 W/kg; Δ, ○) center and wall of the container, respectively; 3) sorbents of mass 0.72 kg; □) center and wall of the container.

During the tests on radiative gas evolution (~ 8700 h) no development of an excess pressure in the containers filled with the exhausted sorbent and chemical absorbent was recorded. In the container filled with the ashes, the maximum pressure increment was $6.08 \cdot 10^3$ P, which corresponded to the gas evolution already established (~ 0.23 cm^3/g).

Mass-spectrometric analysis of the gas phase revealed the existence of fluorine, hydrogen fluoride, and fluorocarbons. Gaseous fluorine may be evolved from the ash as a result of radiochemical and thermal transformations of the intermediate fluorides in the fission products; this is further confirmed by the results of thermographic analysis.

Figure 2 shows the thermographs of the highly active waste products arising from the experimental reprocessing of irradiated uranium oxide fuel by the gas-fluoride method. An analysis of the thermographic indicates the thermal instability of the ashes (Fig. 2e, f). The effects taking place at 150, 155, and 210°C are due to the dehydration of the samples. The presence of moisture is attributable to its absorption from the air during the storage of the samples. Remembering the extremely complicated composition of the ashes it is difficult to classify the character of each of the effects observed on the thermographs; however, the existence of these effects specifically indicates the occurrence of phases transformations. Analysis of the thermographs of the chemical absorbent (Fig. 2a, b) indicates that the latter is only thermally stable at 25-450°C. The effects in the region of 480-530°C are due to the decompostion of the KhP-I, the most probable reaction being $Ca(OH)_2 = CaO + H_2O$ [6].

The thermographs of the sorbents (Fig. 2c, d) show that the thermal stability of the sorbent is determined by its storage conditions. Without moisture the sorbent remains stable at 25-800°C. A study of the thermal stability of the fluoride waste products shows these to be hygroscopic.

The activity of the gas phase is due to the same radionuclides as in the solid waste. With increasing waste holding period the proportion of the activity carried away with the aerosols diminishes (Table 3). This is evidently associated with the enlargement of the aerosol particles and their partial deposition on the walls of the container, and also with the gradual depletion of the surface layer of the waste products with respect to the radionuclides. With increasing temperature the activity in the gas phase is augmented (Table 4). This latter may be due to a number of factors: an increase in the volatility of the fluorides of several fission products, intensification of the convective flows due to the thermal expansion of the gas, and so on. The rate of volatilization of the radionuclides from the end surface of the waste products, calculated from the expression $a'/a\,\tau^{-1} \cdot F^{-1}$ (where a' is the activity of the nuclides passing into the gas phase in Ci; a is the specific activity of the test product in Ci/g; τ is the test period in days; F is the end surface area of the waste products in cm^2) at 25-200°C was $3 \cdot 10^{-8}$-$5 \cdot 10^{-8}$ and $8.7 \cdot 10^{-7}$-$6.6 \cdot 10^{-6}$ for the sorbent and chemical absorbent respectively, while for the ashes it was $3 \cdot 10^{-10}$-$5 \cdot 10^{-7}$ g/(cm^2 · day) at 190 and 400°C.

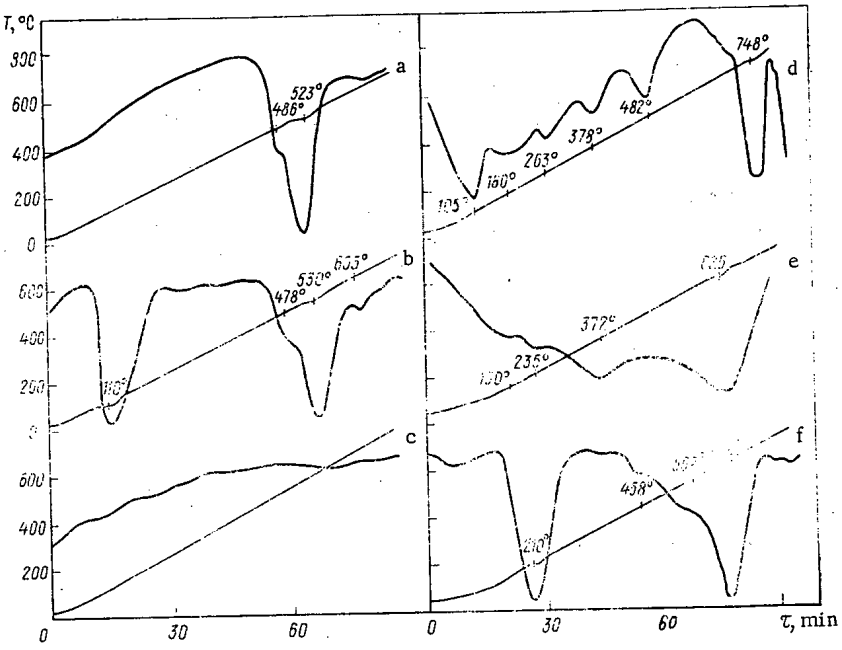

Fig. 2. Thermographs of highly active waste products: a) chemical absorbent, dry; b) chemical absorbent, moist; c) sorbent, dry; d) sorbent, moist; e) ash, dry; f) ash, moist.

Thus the rate of volatilization was either much smaller than or close to 10^{-6} g/(cm^2·day). A study of the extraction of the radionuclides (with water) from the solid waste products showed that a considerable proportion of the activity of the fission products passed into the water even after a brief contact period. The extraction rate of ^{137}Cs reached $3.8 \cdot 10^{-4}$–$8.0 \cdot 10^{-1}$ g/(cm^2·day).

The foregoing results enable us to determine the conditions relating to the storage of waste products arising from the reprocessing of fast-reactor fuel elements by the gas-fluoride method.

When such waste products (especially the ashes) are to be stored for a long time without preliminary reprocessing, it is essential to allow for rapid evolution of radionuclides from the ashes, as well for their hygroscopic properties and inadequate thermal stability and the existence of fluorine-containing gases over the ash. All this makes it a vital matter to hermetize the vessels used for storing the waste products, to select corrosion-resistant materials for the vessels, and to provide for their hydraulic insulation and heat release.

The foregoing experimental data regarding the properties and behavior of the waste products may also be useful in preparing waste for prolonged burial.

LITERATURE CITED

1. L. J. Anasatia et al., US Patent No. 3753920 (1973).
2. J. Peka, in: Third COMECON Symposium on the Reprocessing on Irradiated Fuel, Marianske Lazne (April 22-26, 1974), Paper No. ML 74/2.
3. V. V. Kulichenko, N. V. Krylova, and Yu. P. Martynov, in: COMECON Symposium on the Reprocessing of Irradiated Fuel, Vol. 1, Atomic-Energy Commission, Czechoslovakian SSR, Prague (1972), p. 60.
4. A. P. Kirillovich, P. S. Gordienko, and V. P. Buntushkin, At. Energ., 40, No. 5, 427 (1976).
5. L. G. Berg, Introduction to Thermography [in Russian], Nauka, Moscow (1969).
6. Yu. G. Lavrinovich et al., Zh. Prikl. Khim., No. 12, 2083 (1975).

PHYSICOCHEMICAL PROPERTIES OF MELTS COMPRISING MIXTURES OF URANIUM TETRACHLORIDE WITH THE CHLORIDES OF ALKALI METALS

V. N. Desyatnik, S. F. Katyshev, and S. P. Raspopin

UDC 532.148.608

The density and surface tension of molten mixtures of uranium tetrachloride with chlorides of the alkali metals were measured by the "maximum gas-bubble pressure" method over the whole range of uranium tetrachloride concentrations.

It is well known that molten halides of the alkali metals form typically ionic liquids; their structure may be represented as a mixture of complex ions of the MeX_4^{3-} type (Me = cation of an alkali metal, X = halide F, Cl, Br, or I), "free" Me cations, and vacancies, the mutual disposition of which obeys no special order but is governed by the laws of statistical distribution [1, 2].

The intrinsic complex structure may also be extended to the molten chlorides of polyvalent metals. However, in contrast to the halides of monovalent metals, the existence of "free" cations, U(IV) in particular, is improbable because of their high polarizing capacity. It is more likely that in this case the melt will consist of complex anions, complex cations, and vacancies.

When uranium tetrachloride is mixed with the chlorides of alkali metals there should be a considerable redistribution of the bonds in the complex groupings. This in turn should reflect on the physicochemical properties of the mixtures. Thus the melting diagrams of mixtures of uranium tetrachloride with the chlorides of the alkali metals are characterized by both congruently (Me_2UCl_6) and incongruently (Me_3UCl_4, $MeUCl_5$) melting compounds [3-5].

The density and surface tension are important physicochemical characteristics, a knowledge of which is essential in the solution of both practical and theoretical questions; in particular they enable us to establish the manner in which uranium tetrachloride interacts in the molten mixtures and to assess the most probable form of existence of the complex uranium ions in these melts.

The density of mixtures of uranium tetrachloride with the chlorides of alkali metals was earlier studied by the method of hydrostatic weighing [6]. The density of pure uranium tetrachloride was measured by means of a quartz pycnometer [7] and also by measuring the maximum pressure in a gas bubble [8].

TABLE 1. Density of the Molten Chlorides

Molten salt	$\rho = a - bT$, g/cm³			Temp. range, °K
	a	$b \cdot 10^3$	$S \cdot 10^4$	
LiCl	1,8807	0,4317	11	888—1102
NaCl	2,1332	0,5405	10	1076—1273
KCl	2,1751	0,6030	9	1050—1240
RbCl	3,1069	0,8799	13	1012—1142
CsCl	3,7776	1,0716	11	922—1125

TABLE 2. Density of Uranium Tetrachloride, g/cm³

Temp., °C	Expt.	[6]	[7]
590	3,647	3,571	3,50
600	3,624	3,552	3,48
650	3,509	3,454	3,40
700	3,394	3,357	3,30
750	3,280	3,260	3,20

Translated from Atomnaya Énergiya, Vol. 42, No. 2, pp. 99-103, February, 1977. Original article submitted March 29, 1976.

TABLE 3. Density and Surface Tension of Molten Mixtures of Uranium Tetrachloride with Chlorides of the Alkali Metals

Concn. of HCl_4, mole %	$\rho = a - bT \pm S$, g/cm^3			$\sigma = \sigma_0 - cT \pm S$, mJ/m^2			Temp. range, °K
	a	$b \cdot 10^3$	S	σ_0	c	S	
			System	$LiCl-UCl_4$			
0,0	1,8807	0,4317	0,0011	—	—	—	888—1082
0,0	—	—	—	185,64	0,06309	0,04	902—1075
5,0	2,3445	0,5692	0,0012	132,53	0,04473	0,04	885—985
11,8	2,9844	0,8920	0,0015	113,43	0,04230	0,08	845—937
20,8	3,3512	0,9437	0,0014	102,37	0,03469	0,03	812—908
24,3	3,9846	0,9846	0,0021	101,15	0,03492	0,05	787—926
33,2	3,8140	1,1146	0,0012	96,14	0,03513	0,05	748—871
42,8	4,0705	1,2063	0,0014	86,43	0,03008	0,04	773—920
54,7	4,3478	1,3966	0,0030	83,27	0,03419	0,03	785—905
63,0	4,4816	1,4555	0,0014	86,51	0,04165	0,06	778—904
69,0	4,6067	1,5373	0,0016	86,79	0,04664	0,09	806—926
82,0	5,0017	1,8313	0,0011	100,17	0,06338	0,08	829—941
100,0	5,6251	2,2924	0,0021	105,94	0,07567	0,10	891—998
			System	$NaCl-UCl_4$			
0,0	2,1332	0,5405	0,0010	—	—	—	1076—1273
0,0	—	—	—	193,63	0,07403	0,02	1090—1242
3,0	2,4533	0,7141	0,0009	169,74	0,06191	0,05	1086—1176
10,0	2,9055	0,8700	0,0012	138,92	0,05481	0,04	1062—1165
20,0	3,2593	0,9002	0,0023	116,26	0,04180	0,05	995—1104
30,0	3,6016	1,0076	0,0013	107,17	0,03878	0,03	826—950
33,3	3,6492	1,0020	0,0012	100,87	0,03474	0,04	772—926
40,1	3,9074	4,1469	0,0008	100,78	0,04005	0,04	741—904
50,0	4,0630	1,1922	0,0024	89,75	0,03594	0,02	793—893
60,1	4,1815	1,2188	0,0017	88,06	0,04030	0,04	762—917
69,1	4,3855	1,3380	0,0018	89,44	0,04479	0,04	773—898
70,1	4,4030	1,3384	0,0021	—	—	—	814—898
80,6	5,0030	1,8630	0,0015	94,72	0,05771	0,05	811—899
90,0	5,1948	1,9930	0,0017	99,70	0,06596	0,05	843—948
			System	$KCl-UCl_4$			
0,0	2,1751	0,6060	0,0009	170,61	0,06922	0,05	1050—1240
5,0	2,4133	0,6467	0,0018	140,40	0,05408	0,06	1041—1160
16,0	2,9156	0,7978	0,0005	124,18	0,04886	0,04	987—1087
25,0	3,1907	0,8607	0,0015	112,78	0,04110	0,05	843—994
33,3	3,3889	0,8917	0,0015	105,41	0,03982	0,03	925—1054
39,7	3,5880	0,9879	0,0016	—	—	—	823—947
40,0	3,5373	0,9260	0,0006	96,44	0,03715	0,01	827—946
47,5	3,7947	1,0816	0,0018	—	—	—	657—909
50,0	3,8454	1,1017	0,0012	96,76	0,04424	0,04	688—917
57,0	4,1073	1,2821	0,0020	95,23	0,04770	0,03	758—887
60,0	4,1743	1,3098	0,0010	96,96	0,05050	0,02	744—933
71,0	4,5403	1,5502	0,0024	94,92	0,05339	0,02	808—919
75,6	4,7108	1,6705	0,0014	98,55	0,05830	0,04	816—933
89,0	5,2549	2,0808	0,0019	101,70	0,06610	0,05	867—960
			System	$RbCl-UCl_4$			
0,0	3,1069	0,8799	0,0013	155,59	0,06434	0,07	1012—1141
11,6	3,3316	0,8589	0,0013	131,36	0,05733	0,07	957—1079
19,9	3,4593	0,8559	0,0014	119,79	0,04821	0,03	859—989
24,3	3,5412	0,8804	0,0015	—	—	—	835—991
25,0	3,5449	0,8759	0,0010	109,56	0,04177	0,06	872—1020
33,3	3,7453	0,9834	0,0011	106,37	0,04120	0,07	914—1018
36,5	3,7730	0,9800	0,0015	—	—	—	—
40,0	3,7992	0,9820	0,0016	100,33	0,03900	0,06	823—940
48,3	4,0739	1,2061	0,0020	—	—	—	678—828
50,0	4,0464	1,1597	0,0021	90,30	0,03539	0,07	700—909
59,8	4,3307	1,3808	0,0019	85,43	0,03718	0,05	680—921
64,4	4,4903	1,5080	0,0028	88,67	0,04217	0,07	729—897
82,9	5,0041	1,8418	0,0016	94,38	0,05670	0,07	800—918
			System	$CsCl-UCl_4$			
0,0	3,7776	1,0716	0,0013	155,50	0,07208	0,06	922—1125
9,7	3,9260	1,1237	0,0014	141,70	0,06707	0,06	898—1049
15,2	3,9739	1,1288	0,0015	133,42	0,06344	0,03	849—937
17,1	3,9961	1,1328	0,0017	—	—	—	813—933
20,7	4,0390	1,1549	0,0033	119,32	0,05351	0,06	837—938
27,8	4,0940	1,1554	0,0020	120,46	0,05536	0,07	883—978
33,2	4,0992	1,1519	0,0021	117,62	0,05523	0,02	941—1041
38,0	4,2199	1,2576	0,0020	110,61	0,05060	0,03	889—980
45,1	4,3147	1,3206	0,0027	96,73	0,03982	0,06	853—937
50,0	4,3038	1,2881	0,0019	97,17	0,04362	0,08	804—916
56,6	4,3872	1,3380	0,0012	92,32	0,04090	0,07	768—922
60,3	4,4550	1,3972	0,0010	88,28	0,04025	0,06	729—912
67,2	4,8184	1,7390	0,0041	86,69	0,04147	0,09	816—895
77,0	5,0408	1,9083	0,0013	95,87	0,05648	0,09	837—898
85,3	5,3414	2,1268	0,0033	99,14	0,06255	0,09	854—916

In this paper we shall present the results of our own measurements of the density and surface tension of binary mixtures of uranium tetrachloride with the chlorides of the alkali metals over the whole range of UCl_4 concentrations. For these experiments we first prepared the alkali metal chlorides and uranium tetrachloride in pure form. The melting points of these original samples agreed closely with published data [9]; to an error of ±2°C they were equal to 610, 800, 770, 715, 645, and 590°C for LiCl, NaCl, KCl, RbCl, CsCl and UCl_4 respectively.

The density and surface tension of the molten mixtures were studied by a method based on the maximum pressure in a gas bubble. The working gas was argon, carefully purified from any traces of moisture or oxygen by passing over titanium and zirconium sponge at 800-900°C and over metallic calcium heated to 600-650°C. The height of the liquid column in the manometer was measured with a KM-8 cathetometer to an error of ±0.015 mm. As capillaries we used beryllium oxide tube with an internal diameter of 1.5-2.0 mm. The depth of vertical immersion of the capillary into the melt was regulated with a micrometer screw having a scale division of 0.01 mm. The vertical positioning of the capillary was verified before each experiment. Before the beginning of the experiment the capillary walls were sharpened to form a knife-edge no thicker than 0.1 mm. The time required for the formation of a bubble was 40-60 sec.

The density was calculated from the well-known equation

$$\rho = (\Delta H/\Delta h)\,\rho_M, \tag{1}$$

where ΔH is the difference between the maximum pressure in the bubble of manometric liquid at different levels (cm); Δh is the difference between the capillary immersion levels at which the maximum bubble pressure was measured (cm); ρ_M is the density of the manometric liquid (g/cm^3).

The surface tension was calculated from the Schrödinger equation

$$\sigma = \frac{r\rho_M hg}{2}\left(1 - \frac{2}{3}\frac{rg}{h\rho_M}\right), \tag{2}$$

where r is the radius of the capillary (cm); h is the rise height of the manometric liquid (cm); ρ is the density of the melt (g/cm^3); g is the gravitational acceleration (cm/sec^2).

In calculating the density we introduced corrections for the thermal expansion of the capillary and for the change in the level of melt in the crucible on immersing the capillary [10], while in calculating the surface tension we also made a correction for the depth of immersion of the capillary in the melt. The maximum relative error of the density measurement was 1.0% and of the surface of erosion measurement 1.5%.

The temperature range of the measurements was limited by the high vapor tension of the tetrachloride at relatively high temperatures, which naturally led to a considerable change in its composition during the measurement. The composition of the mixtures was determined by chemical analysis after the experiment.

Within the limits of experimental error, the temperature dependence of the density of the chlorides and chloride mixtures may be described by the equation $\rho = a - bT$. The numerical values of the coefficients determined from the experimental data by the method of least squares are given in Tables 1 and 2. The values obtained for the pure chlorides (Table 1) agree closely with the results of other authors [9].

The standard deviations were calculated for all the salts and mixtures studied from the equation

$$S = \sqrt{\Sigma (X_{expt} - X_{calc})^2/(n-p)}, \tag{3}$$

where X_{expt} and X_{calc} are the experimental and calculated densities at each temperature; n is the number of experimental points; p is the number of coefficients in the equation.

The values obtained for the density of molten uranium tetrachloride agree most closely with those given in [6] (Table 2).

The results of our measurements of the density and surface tension are presented in Table 3. If we construct the density isotherms for the systems in question, we find that the density of the mixtures increases monotonically as the concentration of uranium tetrachloride in the melt increases; the experimental values deviate from the additive law in the sense of greater values for the systems incorporating LiCl, NaCl, and KCl, while the density isotherms of the $RbCl-UCl_4$ and $CsCl-UCl_4$ systems have an S configuration.

On analyzing the molar volumes we find a relative deviation from the linear relationship in the direction of higher values; the maximum deviation occurs at about 60 mole % UCl_4 in each system. The similar behavior of the isotherms representing the deviations from additivity in clearly implies monotypic structural changes in all these systems.

It is quite evident that on mixing melts containing different cations there is a preferential formation of complex groupings based on the cation with the greater polarizing capacity. In this case the positive deviations of the molar volumes from additivity are associated with the formation of complex uranium ions of the $UCl_x^{(x-4)-}$ type. The formation of complex uranium ions in molten uranium chloride mixtures with the chlorides of the alkali metals is confirmed by the results of a study of other physicochemical properties and also by theoretical calculations [3, 5-7, 11-15]. Thus when studying the absorption spectra of mixtures of the alkali metal chlorides with uranium tetrachloride at least two forms of complex uranium ions were encountered: UCl_6^{2-}, $UCl_x^{(x-4)-}$ (x = 0-4) [11, 13].

The maximum deviation of the molar volumes from additivity increases linearly with increasing radius of the alkali metal cation. The negative deviations of the thermodynamic properties [3, 12] and the equivalent electrical conductivity [6] are augmented with increasing radius of the alkali metal cation, while the diffusion coefficients decline [14]. This indicates that with increasing radius of the alkali metal cation the interaction of uranium tetrachloride with the alkali metal chlorides intensifies. The complex uranium groupings will, in fact, be more stable if a cation with a smaller ionic moment appears in the second coordination sphere.

The results show that the surface tension falls sharply with increasing proportion of UCl_4 in the mixtures. We may conclude from the character of the surface-tension isotherms that UCl_4 is a surface-active substance in all the systems studied. There is a slight bend on the surface-tension isotherms corresponding to the chemical compound Me_2UCl_6 on the phase diagrams. This is evidently associated with the formation of complex UCl_6^{2-} ions in the melt, these being surface-active with respect to the chlorides of the alkali metals but being surface-active with respect to the chlorides of the alkali metals but inactive with respect to uranium tetrachloride. The surface-tension values close to the bend differ very little from one another, which indicates the concentration of monotypic complex uranium ions in the surface layer.

On the basis of the foregoing experimental data we determined the adsorption of uranium tetrachloride in the surface layer from the well-known equation

$$\Gamma = -\frac{N(1-N)}{RT}\frac{d\sigma}{dN}, \quad (4)$$

where N is the molar proportion of the surface-active component in the volume; σ is the surface tension. The adsorption curves for the melts of all the systems have two considerably differing maxima. As the ionic moment of the alkali metal cation increases from Cs^+ to Li^+, the maximum adsorption of uranium ions in the range 0-20 mole % UCl_4 increases from 1.26 to $2.99 \cdot 10^{-6}$ mole/m, the maximum being displaced in the direction of smaller UCl_4 concentrations. This agrees closely with V. K. Semenchenko's conclusions [16] to the effect that the surface activity of the components is determined by the ratio of their generalized moments. The cations with a large ionic moment have a greater "displacing" power with respect to the uranium ions, and saturation of the surface layer with the surface-active component takes place at smaller concentrations of the latter in the interior of the melt.

The second maximum on the adsorption isotherms corresponds to the adsorption of more complex uranium groupings of the UCl_6^{2-} type.

Thus we have demonstrated on the basis of density and surface-tension measurements carried out on molten mixtures of uranium tetrachloride with the chlorides of the alkali metals, together with computed data, that complex uranium groupings of the $UCl_x^{(x-4)-}$ type are formed in the molten mixtures, their stability increasing with increasing radius of the alkali metal cation; the grouping with the greatest stability is UCl_6^{2-}.

LITERATURE CITED

1. M. V. Smirnov, O. M. Shabanov, and A. P. Khaimenov, Elektrokhimiya, 2, No. 11, 1240 (1966).
2. M. V. Smirnov, Electrode Potentials in Molten Chlorides [in Russian], Nauka, Moscow (1973).
3. A. Bogacz and W. Trzebiatowski, Rocz. Chem., 38, No. 5, 729 (1964).
4. V. N. Desyatnik et al., Zh. Fiz. Khim., 46, No. 8, 2159 (1972).
5. T. Kuroda and T. Suzuki, J. Electrochem. Soc. Jpn., 26, Nos. 7-9, 140 (1958).
6. A. Bogacz and B. Ziolek, Rocz. Chem., 44, No. 3, 665 (1970).
7. T. Kuroda and T. Suzuki, J. Electrochem. Soc. Jpn., 29, No. 4, 215 (1961).
8. V. N. Desyatnik, S. P. Raspopin, and I. F. Nichkov, Izv. Vyssh. Ucheb. Zaved., Tsvet. Metal., No. 5, 95 (1969).
9. A. G. Morachevskii (editor), Reference Book on Molten Salts, Vol. 1 [Russian translation], Khimiya, Leningrad (1971).
10. B. N. Linchevskii, Technique of Metallurgical Experiments [in Russian], Metallurgizdat, Moscow (1967).

11. J. Morrey, Inorg. Chem., 2, No. 1, 163 (1963).
12. A. Kisza, Bull. Acad. Poln. Sci., Ser. Sci. Chem., 12, No. 3, 177 (1964).
13. O. V. Skiba, V. V. Gushchin, and A. N. Korzh, in: Physical Chemistry and Electrochemistry of Molten Salts and Slags, Part I [in Russian], Naukova Dumka, Kiev (1969), p. 49.
14. M. V. Smirnov, Elektrokhimiya, 10, No. 5, 770 (1974).
15. V. N. Desyatnik, S. P. Raspopin, and K. I. Trifonov, Zh. Fiz. Khim., 48, No. 3, 776 (1974).
16. V. K. Semenchenko, Surface Phenomena in Metals and Alloys [in Russian], Gostekhteorizdat, Moscow (1957).

PECULIARITIES IN THE CHEMICAL ETCHING OF POLYETHYLENE TEREPHTHALATE, IRRADIATED WITH RADIATIONS WITH VARIOUS LINEAR ENERGY LOSSES

N. S. Moshkovskii, L. N. Gaichenko, and Ya. I. Lavrentovich

UDC 541.64+678

Polyethylene terephthalate (PETP) is one of the polymers widely used in various fields of technology. In certain cases materials based on PETP may be subjected to the influence of intense fluxes of ionizing radiation with various linear energy losses (LEL) and may be in contact with aggressive media during use. Therefore, the study of processes of interaction of the irradiated polymer with such media is of substantial interest. The literature contains information concerning nonirradiated PETP. Thus, e.g., the mechanism of hydrolysis of PETP by solutions of alkali has been studied in the greatest detail [1]; the mechanism of the action of solutions of sulfuric acid on the polymer has been investigated [2]. There is practically no information on the chemical influence of aggressive media on PETP preliminarily irradiated with various types of ionizing radiation.

In this work we investigated the peculiarities of chemical etching of PETP irradiated with radiations with various LEL, in solutions of potassium hydroxide.

Experimental Method. Industrially produced PETP (M_V = 27,000, d = 1.38 g/cm^3) was used for the investigation in the form of films 12, 50, and 125 μ thick. The molecular mass M_V was determined according to the formula $\log M_V = 1.176 \log [\eta] + 3.036$ on the basis of data on the viscosity (η) of solutions of PETP in a mixture of phenol and dichloroethane (40 : 60) at 20°C [3]. The samples were irradiated under vacuum (10^{-4}–10^{-5} atm) at room temperature. For the irradiation we used the γ radiation of ^{60}Co, deuterons (13 MeV), and γ particles (23 MeV), which permitted variation of the LEL within broad limits (0.2–50 keV/μ).

The absorbed dose in γ irradiation was determined with dosimeters of cellulose diacetate and colored cellophane [4, 5]. In the irradiation of PETP with heavy charged particles, the absorbed dose was calculated on the basis of data on the linear energy losses by the particles in the polymer and the value of their integral flux [5].

After the irradiation of the film, the PETP was subjected to chemical treatment in aqueous solutions of potassium hydroxide of various concentrations at the temperatures 20–95°C. In this case samples of the same size (circles 38 mm in diameter) were loaded into a thermostatically controlled glass flask with the solution (300 ml), equipped with a reflux condenser. The substantial excess of the alkali solution and mixing ensured constancy of the alkali concentration near the surface of the sample. After definite time intervals, the samples were removed from the solution, washed thoroughly in distilled water, dried to constant mass at 60°C, and weighed with an error of $4 \cdot 10^{-5}$ g.

Translated from Atomnaya Énergiya, Vol. 42, No. 2, pp. 104-107, February, 1977. Original article submitted January 7, 1976.

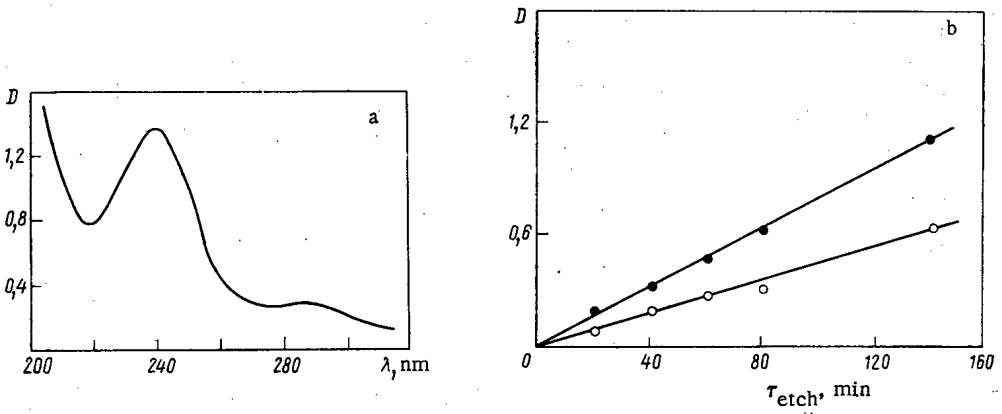

Fig. 1. Absorption spectrum of hydrolysis products of PETP (a) after etching in 3 N KOH solution with an addition of ethanol; variation of the optical density (b) at 240 nm with the time of etching for solutions in which irradiated (●) and non-irradiated (○) polymers were exposed.

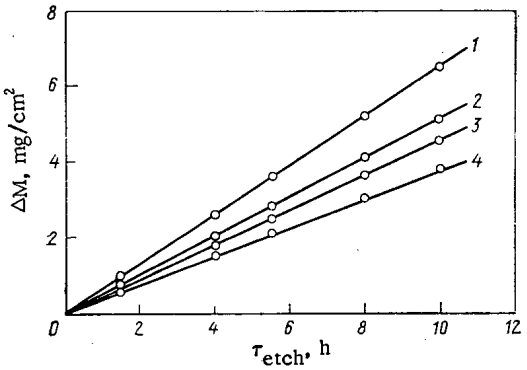

Fig. 2

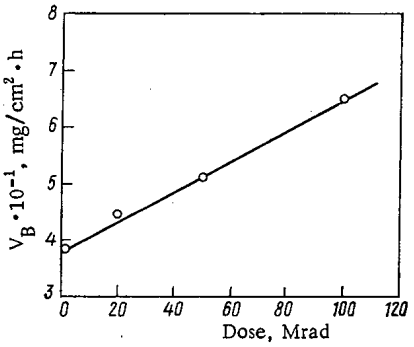

Fig. 3

Fig. 2. Change in the mass of samples of PETP irradiated with the γ radiation of ^{60}Co during hydrolysis in 3 N KOH solution at 85°C. 1, 2, 3) PETP irradiated with a dose of 20, 50, and 100 Mrad, respectively; 4) nonirradiated.

Fig. 3. Dependence of the rate of etching of γ irradiated PETP on the absorbed dose (3 N solution of KOH at 85°C).

We also investigated the products of etching of PETP that passed into solution. For this purpose, in several experiments we collected samples of the solution and determined their UV absorption spectra on a Specord spectrophotometer. The change in the surface of the samples during etching was observed visually with an MBI-8m microscope in transmitted light.

Results and Discussion. The experiments showed that after chemical etching of irradiated and non-irradiated samples of PETP in KOH solution, products are detected that absorb light in the UV region of the spectrum (Fig. 1a). The concentration of these products increases with increasing time of contact of PETP with the KOH solution (Fig. 1b). According to the literature data [1, 6], it can be assumed that a salt of terephthalic acid, which is formed in the hydrolysis of the polymer macromolecules, is accumulated in the solution. It must be noted that the nature of the UV spectra is the same for solutions in which the PETP samples irradiated with radiations with various LEL were treated. Evidently the LEL of the radiation does not affect the composition of the water-soluble products.

The surface of nonirradiated samples and those irradiated with the γ rays of ^{60}Co remains practically the same throughout the entire period of etching. In the case of etching of samples irradiated with heavy charged particles, in the initial period the formation of a microcontour is observed on the surface, and it subsequently remains unchanged. In this case, the surface of the samples becomes dull, since the heavy charged particles create regions of especially strong radiation damage in the polymer along their track, and these regions are etched at a higher rate than the remainder of the surface.

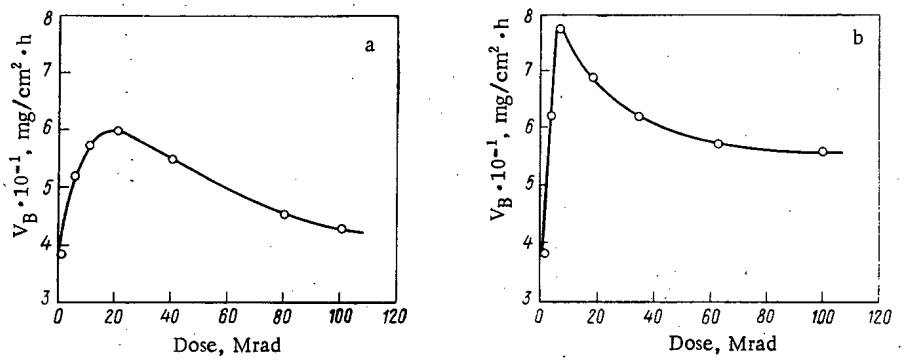

Fig. 4. Dependence of the rate of etching on the absorbed dose for PETP irradiated with deuterons (a) and α particles (b) (3 N solution of KOH at 85°C).

TABLE 1. Influence of Temperature on the Rate of Etching of PETP by a 3 N Solution

Temp., °C	Dose, Mrad	Wt. rate of etching, mg/cm^2 · h	Ratio of rates of irrad. and initial samples
65	0	0,09	1,83
65	5	0,16	
75	0	0,23	1,96
75	5	0,46	
85	0	0,38	2,05
85	5	0,78	
95	0	0,76	2,40
95	5	1,83	

Figure 2 presents the kinetic data on the change in the mass of samples of PETP irradiated with the γ radiation of ^{60}Co, and kinetic data for a nonirradiated sample, from which it can be seen that the change in the mass of the samples during etching is directly proportional to the time of contact. Analogous data were also obtained for samples irradiated with deuterons and α particles, according to which the weight rate of etching V was calculated.

From Fig. 3 it can be seen that the rate of etching of the samples increases with increasing absorbed dose of the γ radiation of ^{60}Co; moreover, a linear relationship is observed in the region of 1-100 Mrad.

Figure 4 presents the dose dependence of the rate of etching of samples irradiated with heavy charged particles, which differs substantially from the dependence obtained for γ irradiated samples. In the region of low absorbed doses, the rate of etching increases very sharply, reaching a maximum value in the interval 5-15 Mrad, but then gradually decreases with increasing dose. A comparison of the curves of the dependence of the rate of etching on the absorbed dose for samples irradiated with deuterons and α particles shows that in the region of the maximum, the rate of etching of α-irradiated samples is significantly higher than for samples irradiated with deuterons. This can be explained by the fact that α particles, possessing a larger LEL than deuterons, more substantially disrupt the polymer along their track. The general nature of the change in the rate of etching as a function of the dose of heavy particles may be due to the fact that in the region of low doses the polymer is etched, and a microcontour is formed on account of the separated tracks of the particles. In the case of large absorbed doses, when the track of the particles merge with one another, the rate of etching may decrease on account of a smoothing out of microinhomogeneities. It is also possible that in the region of large doses of heavy charged particles, a three-dimensional structure is formed in the PETP on account of cross-linking of macromolecules; moreover, the effectiveness of this process at the same dose may be substantially higher in the case of irradiation with heavy charged particles than in the case of γ irradiation. The formation of supplementary cross-links between macromolecules may increase the chemical stability of PETP. A comparison of the results shows that the absorbed dose in the track of the heavy charged particle may exceed 100 Mrad (Figs. 3 and 4).

TABLE 2. Influence of Additives on the Rate of Etching of PETP

Compos. of solution	Temp., °C	Dose, Mrad	Wt. rate of etching, mg/cm²·h	Ratio of wt. rates of etching for irrad. and initial samples
3 N solution of KOH	85	0	0,38	2,05
		5	0,78	
3 N solution of KOH + 1% sodium dodecylsulfate	85	0	0,21	2,13
		5	0,45	
C_2H_5OH + 3 N KOH (2:3)	65	0	0,46	1,74
		5	0,80	

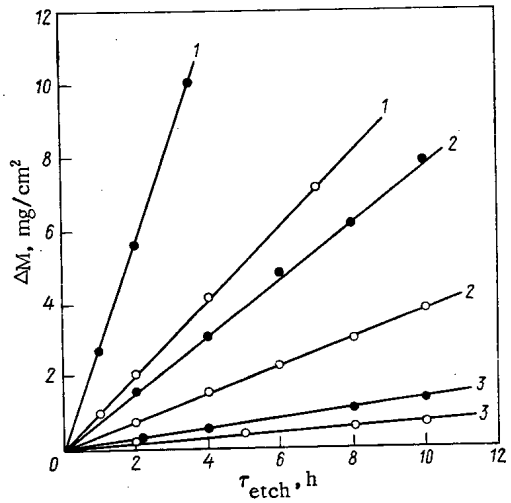

Fig. 5. Change in the mass of PETP samples irradiated with α particles (●) and nonirradiated (○), in the process of etching in KOH solution at 85°C: 1) 1 N; 2) 2 N; 3) 6 N solution.

Table 1 presents the results for samples of PETP irradiated with α particles with a dose of 5 Mrad and generalizes the data on the influence of temperature on the process of etching of PETP.

From Table 1 it can be seen that with increasing temperature, the rate of etching of nonirradiated and irradiated samples of PETP increases substantially, and their ratio increases. On the basis of data on the dependence of the rate of etching on the temperature, we calculated the effective activation energies [7]; they proved equal to 17.0 and 19.7 kcal/mole for the initial PETP and a sample irradiated with α particles with a dose of 5 Mrad, respectively.

Figure 5 presents the kinetic curves of the change in the mass of PETP samples treated in aqueous solutions of KOH of various concentrations, from which it can be seen that an increase in the concentration of the solution increases the rate of etching and the ratio of the rates of etching of irradiated and nonirradiated samples.

In an investigation of the influence of additives on the rate of etching of PETP in KOH solution, surface-active substances were introduced, e.g., sodium dodecylsulfate or sodium stearate, and ethanol was also added. Data on the influence of these additives are cited in Table 2, from which it follows that additions of surface-active substances to the solution decrease the rate of etching of the initial and irradiated PETP. But these additives negligibly increase the ratio of the rates V_{irr}/V_{init}. Ethanol increases the rate of etching of the initial and irradiated samples; however, in this case the V_{irr}/V_{init} ratio changes negligibly. The increase in the rate

of etching by a solution with ethanol may be a consequence of dissolution of hydrolysis products of the polymer macromolecules by the alcohol and their more rapid passage from the surface into the solution.

Thus, the stability of irradiated PETP in aqueous solutions of potassium hydroxide depends not only on the absorbed dose, but also on the type and energy of the exciting radiation. In the case of irradiation of PETP with radiations with increased LEL, its stability is sharply decreased in the region of low absorbed doses, while in the case of high doses it is somewhat increased and stabilized.

The influence of temperature and alkali concentration on the rate of etching was determined. The data obtained must be taken into consideration in the use of materials based on PETP subjected to irradiation and the influence of aggressive media.

LITERATURE CITED

1. T. E. Rudakova et al., Vysokomol. Soedin., A12, No. 2, 449 (1972).
2. T. E. Rudakova et al., Vysokomol. Soedin., A16, No. 6, 1356 (1974).
3. A. F. Nikolaev, Synthetic Polymers and Plastics Based on Them [in Russian], Khimiya, Moscow–Leningrad (1966), p. 695.
4. Ya. I. Lavrentovich et al., in: Summaries of Reports at the Fifth All-Union Coordination Conference on the Dosimetry of Intensive Fluxes of Ionizing Radiation [in Russian], Izd. VNIIFTRI, Moscow (1974), p. 18.
5. Ya. I. Lavrentovich et al., Khim. Vys. Energ., 3, No. 2, 147 (1969).
6. H. Paretzke, in: Proc. Intern. Conf. on Nuclear Photography and Solid State Track Detectors, Bucharest, Vol. 1 (1972), p. 322.
7. N. M. Émanuél' and D. G. Knorre, Course in Chemical Kinetics [in Russian], Vysshaya Shkola, Moscow (1969), p. 48.

CALCULATION OF THE CHARACTERISTICS OF A TOKAMAK REACTOR WITH INJECTION OF DEUTERIUM AND TRITIUM IONS

N. V. Karetkina

UDC 533.992

The authors of [1] described for the first time the possibility of building a thermonuclear reactor in which nuclei are synthesized by stopping a beam of fast deuterium ions in a cold tritium plasma. This type of thermonuclear reactor was termed a two-component scheme. Its efficiency in terms of energy was previously studied in [2, 3] in which the dependence of the ratio of thermonuclear power to injected power upon the energy of both the injected particles and the plasma temperature was determined.

A three-component scheme of a thermonuclear reactor was described in [4], according to which beams of high-energy deuterons and tritons are simultaneously injected into a deuterium–tritium plasma with hot electrons. The investigations included the relatively low electron temperature [4] at which the change in the distribution function of the deuterium and tritium ions depends upon the slowing down at electrons; but the collisions of the fast ions among themselves were disregarded.

The problem of plasma heating by a beam of high-energy particles was solved in a linear approximation [4-6], i.e., the injected ions and the plasma ions were separately described. This is correct when the intensity of the particles injected is smaller than the plasma density.

We consider in the present article the possibility of building a thermonuclear reactor with intense injection of deuteron and triton beams at a rather high electron temperature. In this case the ions need not be

Translated from Atomnaya Energiya, Vol. 42, No. 2, pp. 108-112, February, 1977. Original article submitted March 3, 1976.

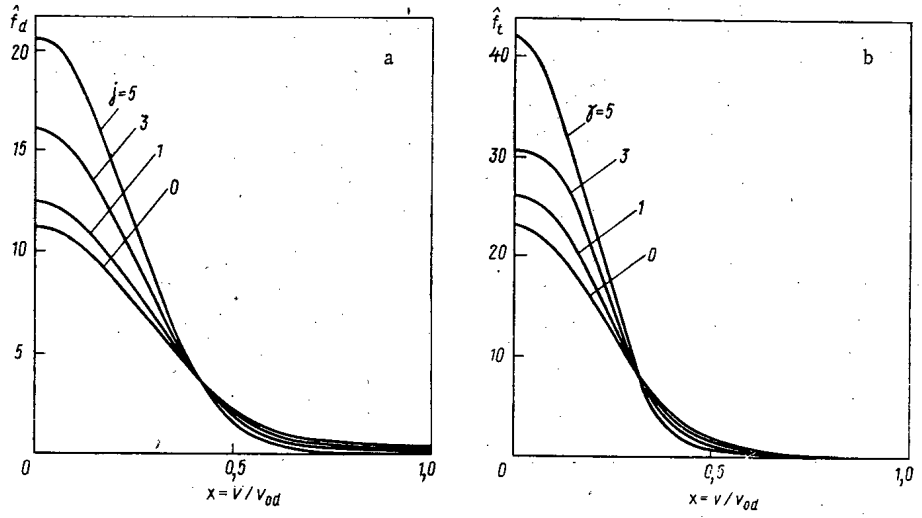

Fig. 1. Dependence of the distribution functions of a) the deuterons and b) the tritons upon $x = v/v_{0d}$ for various γ values at $E_d = 200$, $E_t = 40$; $T_e = 15$ keV, $\tau_{N,t} = \tau_{N,t} = 2$ sec; $N_d = N_t = 4 \cdot 10^{13}$ cm^{-3}.

TABLE 1. Dependence of the Effective Cross Section of the Thermonuclear Reaction D + T = ^{4}He + n upon the Deuteron Energy (fixed tritium)

E, keV	σ·10²⁴, cm²	E, keV	σ·10²⁴, cm²	E, keV	σ·10²⁴, cm²	E, keV	σ·10²⁴, cm²	E, keV	σ·10²⁴, cm²
20	0,05	70	2,60	120	5,00	170	3,50	300	1,30
30	0,20	80	3,50	130	4,90	180	3,20	350	1,00
40	0,60	90	4,30	140	4,50	190	3,00	400	0,85
50	1,00	100	4,80	150	4,20	200	2,80	450	0,70
60	1,80	110	4,90	160	4,00	250	1,80	500	0,60

separated into plasma ions and injected ions, but the collisions of the fast ions among themselves must be brought into account. One therefore obtains a system of two nonlinear kinetic equations for the distribution functions of the deuterium and tritium ions.

Let us consider the simplest form of the problem. Assume that both the sources and the losses are described by isotropic functions of the angle in velocity space and that the distribution functions depend only upon the absolute value of the velocity. Then the stationary state of the reactor using an intense injection of deuterium and tritium ions is given by the following system of equations for the distribution functions of particles of type α (α = d, t) [7]:

$$\sum_{\beta=d,\ t,\ e} \frac{4\pi e_\alpha^2 e_\beta^2 L N_\beta}{m_\alpha^3} \frac{1}{v^2} \frac{\partial}{\partial v} \left\{ \frac{T_\beta}{m_\beta} \frac{a_\beta}{v} \frac{\partial}{\partial v} f_\alpha(v) + \frac{m_\alpha}{m_\beta} b_\beta f_\alpha(v) \right\} - \nu_\alpha(v) f_\alpha(v) + p_\alpha F_{0\alpha}(v - v_{0\alpha}) = 0. \quad (1)$$

The notation is interpreted as follows: α denotes deuterons and t, tritons; N_β and T_β denote the density and the temperature (average kinetic energy) of the corresponding type of particles:

$$N_\beta = 4\pi \int_0^\infty f_\beta(v)\, v^2\, dv; \quad (2)$$

$$T_\beta = \frac{4\pi}{3} \frac{m_\beta}{N_\beta} \int_0^\infty f_\beta(v)\, v^4\, dv. \quad (3)$$

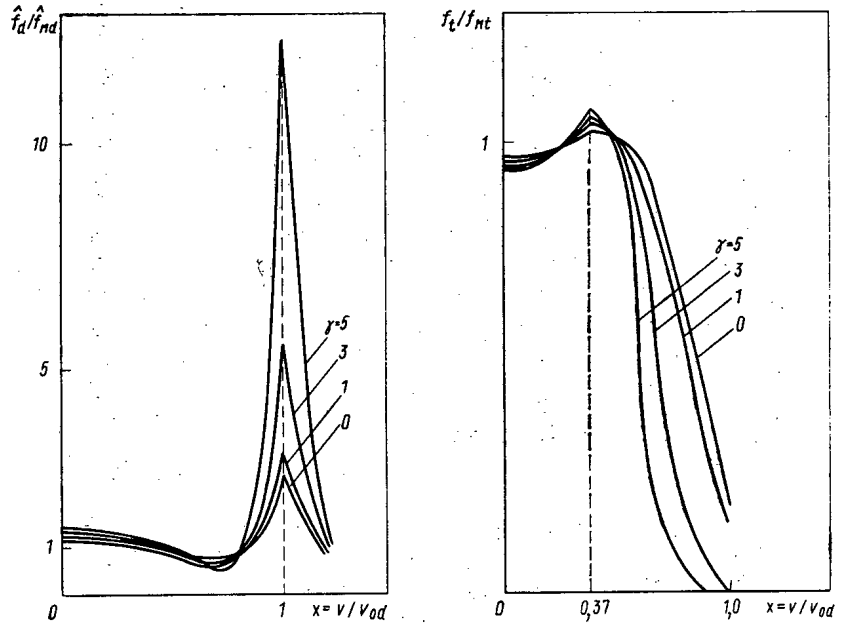

Fig. 2. Ratio of the distribution functions of deuterons and tritons to the corresponding Maxwell distributions at equal temperatures and densities.

TABLE 2. Characteristics of the Tokamak Reactor with Intense Injection of Deuterium and Tritium*

γ	τ_N, c	$\tau_{E,d}$	$\tau_{E,t}$	T_d	T_t	Q_{de}	Q_{te}	Q
		sec		keV		W		
0	1,2	1,20	1,20	33	23	0,61	0,22	2,0
1		0,96	0,93	31	21	0,56	0,19	1,8
3		0,60	0,62	27	18	0,44	0,13	1,5
5		0,36	0,49	23	15	0,32	0,08	1,1
0	2,0	2,00	2,00	26	19	0,40	0,15	2,5
1		1,61	1,57	25	18	0,37	0,14	2,3
3		0,99	1,04	22	16	0,31	0,10	1,9
5		0,59	0,80	19	14	0,23	0,06	1,5

* $E_d = 200$; $E_t = 40$; $T_e = 10$ keV; $N_d = N_t = 4 \cdot 10^{13}$ cm^{-3}.

The coefficients a_β and b_β are expressed by the distribution functions $f_\beta(v)$ as follows:

$$a_\beta = \frac{4\pi}{3} \frac{m_\beta}{N_\beta T_\beta} \left\{ \int_0^v f_\beta(w)\, w^4\, dw + v^3 \int_v^\infty f_\beta(w)\, dw \right\};$$

$$b_\beta = \frac{4\pi}{N_\beta} \int_0^v f_\beta(w)\, w^2\, dw.$$

The summation in Eq. (1) is extended over all types of particles, including the α. The second term on the right side of each of the equations of system (1) describes the loss of the particles α, whose intensity is given by the function $\nu_\alpha(v)$; the last term on the right side describes the source of the particles α; the source intensity is p_α; the energy distribution is characterized by the function $F_{0\alpha}(v - v_{0\alpha})$, where $v_{0\alpha}$ denotes the beam particle velocity corresponding to the characteristic injection energy $E_\alpha = m_\alpha v_{0\alpha}^2/2$. The function $F_{0\alpha}$ is normalized to unity:

$$4\pi \int_0^\infty F_{0\alpha}(v - v_{0\alpha})\, v^2\, dv = 1, \quad \alpha = d,\ t.$$

TABLE 3. Characteristics of the Tokamak Reactor with Intense Injection of Deuterium and Tritium*

ν	τ_N,	$\tau_{E,d}$	$\tau_{E,t}$	T_d	T_t	Q_{de}	Q_{te}	Q
		sec		keV		W		
0	1,2	1,20	1,20	46	34	0,46	0,18	2,7
1		0,93	0,89	42	30	0,40	0,14	2,5
3		0,65	0,59	36	25	0,30	0,08	2,2
5		0,43	0,47	30	20	0,20	0.04	1,6
0	2,0	2,00	2,00	36	29	0,32	0,13	3,9
1		1,64	1,50	34	27	0,28	0.11	3,6
3		1,08	0,96	30	22	0,21	0,07	3,0
5		0,70	0,75	25	19	0,15	0,04	2,5

* $E_d = 200$; $E_t = 40$; $T_e = 15$keV; $N_d = N_t = 4 \cdot 10^{13}$ cm^{-3}.

When each of the equations of system (1) is multiplied by $4\pi v^2$ and $2\pi m_\alpha v^4$ and integrated over the velocity, the following equations are obtained:

$$p_\alpha - (N_\alpha/\tau_{N,\alpha}) = 0, \quad \alpha = d, t; \tag{4}$$

$$Q_\alpha - \sum_\beta Q_{\alpha\beta} - (\varepsilon_\alpha/\tau_{E,\alpha}) = 0, \quad \alpha = d, t. \tag{5}$$

Equation (4) describes the particle balance, with $\tau_{N,\alpha}$ denoting the lifetime of the particles given by the formula

$$\tau_{N,\alpha} = \left\{ \frac{4\pi}{N_\alpha} \int_0^\infty f_\alpha(v)\, \nu_\alpha(v)\, v^2\, dv \right\}^{-1}, \quad \alpha = d, t. \tag{6}$$

Equation (5) expresses the energy balance. In Eq. (5), $\varepsilon_\alpha = 3/2\, N_\alpha T_\alpha$ denotes the energy of the particles of type α; $\tau_{E,\alpha}$ denotes the lifetime at that energy; $Q_{\alpha\beta}$ denotes the power of injection into the plasma; and α to particles β:

$$\tau_{E,\alpha} = \left\{ \frac{2\pi m_\alpha}{\varepsilon_\alpha} \int_0^\infty f_\alpha(v)\, \nu_\alpha(v)\, v^4\, dv \right\}^{-1}, \quad \alpha = d, t; \tag{7}$$

$$Q_\alpha = 2\pi m_\alpha p_\alpha \int_0^\infty F_{0\alpha}(v - v_{0\alpha})\, v^4\, dv, \quad \alpha = d, t; \tag{8}$$

$$Q_{\alpha\beta} = 64\pi^3 e_\alpha^2 e_\beta^2 L \left\{ \frac{1}{m_\beta} \int_0^\infty f_\alpha(v)\, v \left(\int_0^v f_\beta(w)\, w^2\, dw \right) dv - \frac{1}{m_\alpha} \int_0^\infty f_\beta(w)\, w \times \right.$$

$$\left. \times \left(\int_0^w f_\alpha(v)\, v^2\, dv \right) dw \right\}. \tag{9}$$

The particle lifetimes $\tau_{N,\alpha}$ and $\tau_{N,t}$ characterize the losses of deuterons and tritons by various processes, e.g., charge redistribution, instabilities, etc. Therefore $\tau_{N,d}$ and $\tau_{N,t}$ can be considered parameters of the apparatus.

Let us consider the case in which N_d and N_t, $\tau_{N,d}$ and $\tau_{N,t}$ as well as the temperature of the electrons in the tokamak reactor, have values corresponding to reactor conditions [8]. The intensity of the sources is determined from Eq. (4).

It is a well-known fact that the lifetime of the particles with energy is several times smaller than the corpuscular lifetime (particles with high energies can be retained to a lesser degree). This can be phenomenologically brought into account by modeling the losses with the aid of an increasing function of the velocity. We consider energy losses of the type:

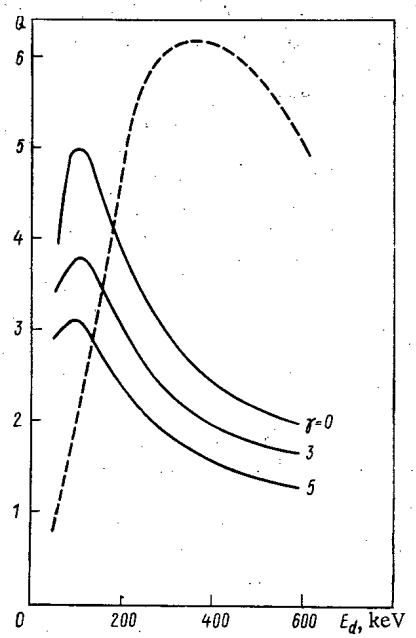

Fig. 3. Dependence of the gain Q of the reactor upon the energy of the injected deuterons at a triton injection energy E_t = 40 keV; various γ values. Electron temperature T_e = 15 keV.

$$\nu_\alpha(v) = \nu_{0\alpha} \exp\left\{\gamma \frac{v}{v_{0\alpha}}\right\}, \quad \alpha = d, t, \tag{10}$$

where ν_{0d}, ν_{0t}, and γ denote certain numerical parameters. The degree to which the functions of Eq. (10) increase determines γ and therefore characterizes the difference between the lifetime of the particles with energy and the corpuscular lifetime. By appropriate selection of this parameter one can reach the necessary relation between the lifetime with energy and the corpuscular energy and, in particular, one can obtain the ratio $\tau_{N,\alpha}/\tau_{E,\alpha} \cong 3$ observed in the majority of experiments on the tokamak reactor. We note that $\gamma = 0$ corresponds to the limit at which the lifetime with energy is equal to the corpuscular lifetime: $\tau_{N,\alpha} = \tau_{E,\alpha}$, with α = d, t. The parameters ν_{0d} and ν_{0t} are selected so that the lifetime (6) of the particles in the stationary state assumes a predetermined value, i.e., so that the following relations are satisfied:

$$4\pi v_{0\alpha} \int_0^\infty f_\alpha(v) \exp\left\{\gamma \frac{v}{v_{0\alpha}}\right\} v^2 dv = \frac{N_\alpha}{\tau_{N,\alpha}}, \alpha = d, t.$$

Since the relaxation time of the electrons is smaller than that of the ions, a Maxwell distribution is used for the electrons. Since the plasma is quasi-neutral, the electron density is $N_e = N_d + N_t$.

Equation system (1) is numerically solved with the method of settling [9]. The efficiency of the thermonuclear reactor depends upon the ratio of the power of thermonuclear reactions to the injected power:

$$Q = qE_{thn} / \sum_{\alpha=d,t} p_\alpha E_\alpha,$$

where E_{thn} = 17.6 MeV denotes the energy released in the thermonuclear reaction D + T = ^{4}He + n; the DD reaction with its small cross section was disregarded; $\sum_{\alpha=d,t} p_\alpha E_\alpha$ denotes the injected power;

$$q = N_d N_t \langle \sigma v \rangle = \int dv_d \int dv_t |v_d - v_t| \sigma(|v_d - v_t|) f_d(v_d) f_t(v_t) = 8\pi^2 \int_0^\infty f_t(v_t) v_t dv_t \int_0^\infty f_d(v_d) v_d dv_d \int_{|v_d - v_t|}^{v_d + v_t} \sigma(u) u^2 du$$

denotes the average number of fusion reactions per cm^3 of the plasma per second; $u = v_d - v_t$ denotes the relative velocity of the deuterons and tritons; $\sigma(u)$ denotes the effective cross section of the DT reaction at fixed tritium.

We used in the present work the experimental $\sigma(u)$ values of Table 1 [10].

Results of Calculations. The distribution functions which were obtained by the numerical solution of Eq. (1) for deuterons and tritons allowed the determination of various characteristics of the thermonuclear reactor with intense injection of deuterons and tritons. We could determine the temperature of each type of ions (Eq. (3)), the rate of energy transfer from one type of particles to another (Eq. (9)), the lifetime of the ions with energy (Eq. (7)), the gain Q of the reactor and its dependence upon the lifetime of the ions (Eq. 6)), the temperature of the electrons, and the parameter γ.

The results of the calculations of various characteristics of the reactor, which correspond to the electron temperatures 10 and 15 keV for $\tau_{N,d} = \tau_{N,t} = 1.2$ and 2 and for $\gamma = 0, 1, 3$, and 5 are listed in Tables 2 and 3. In these calculations the energy of the injected ions was assumed as 200 keV for deuterium and 40 keV for tritium. The results of the calculations show that when γ decreases, i.e., when the lifetime of the particles with energy increases, Q increases. The efficiency in terms of energy can be increased in the reactor by increasing the lifetime of the particles or by increasing the temperature of the electrons.

Figures 1 and 2 show the distribution functions of the deuterons and tritons and the ratio of these distributions to the corresponding Maxwell distributions. The distribution functions were normalized as follows:

$$4\pi \int_0^\infty \hat{f}_\alpha(x)\, x^2\, dx = N_\alpha \cdot 10^{-13}, \quad \alpha = d,\ t.$$

It follows from Fig. 2 that the maximum of each of the ratios $\hat{f}_\alpha(x)/\hat{f}_{M\alpha}(x)$ is reached at a velocity $v_{0\alpha}$ which corresponds to the injection energy E_α, i.e., for $x = 1$ in the case of deuterium and for $x = \sqrt{m_d E_t / m_t E_d} \approx 0.37$ in the case of tritium.

Figure 3 shows the dependence of the reactor gain Q upon the energy of the injected deuterons for various γ values. The maximum of Q is reached at $E_d \approx 100$ keV, which approximately corresponds to the maximum of the cross section of the DT reaction and which several times exceeds the maximum Q values determined in [4]. The dashed line of the same figure indicates the dependence of Q upon the energy of the injected deuterons for the two-component reactor scheme at $T_e = 15$ keV [3]. This curve differs sharply from the calculated curves for the following reasons. It was assumed in [3] that the deuterons participate in the fusion reactions only during the time in which they are slowed down, whereas, in our model, the hot deuterons and tritons react during their entire lifetime; therefore the dependence of Q upon the energy resembles the dependence of the cross section of the DT reaction upon the deuteron energy. In [3] we used the well-known approximation formula of Artsimovich [11] for the cross sections $\sigma(u)$. At high velocities the cross sections which are calculated for the DT reaction with this formula are approximately two times greater than the cross section values used in the present work. Furthermore, $E_{thn} = 22.4$ MeV [3], i.e., the energy (4.8 MeV) of the capture by ^{6}Li, which is part of the blanket, was taken into consideration.

Thus, the analysis of the efficiency in terms of energy of a thermonuclear reactor with intense injection of deuterons and tritons indicates that it is possible to obtain a positive yield of energy from such a system.

The author is indebted to I. N. Golovin for formulating the problem and to Yu. N. Dnestrovskii and D. P. Kostomarov for valuable discussions.

LITERATURE CITED

1. L. A. Artsimovich, Usp. Fiz. Nauk, 91, 365 (1967).
2. J. Dawson, H. Furth, and F. Tenny, Phys. Rev., Lett., 26, 1156 (1971).
3. V. I. Pistunovich, At. Energ., 35, No. 1, 11 (1973).
4. J. Cordy and W. Core, Nucl. Fusion, 15, 710 (1975).
5. D. Callen et al., in: Proc. IAEA Intern. Conf. on Plasma Physics and Nucl. Fusion Research, Tokyo, CN-33/A16-3 (1974).
6. J. Cordy and M. Houghton, Nucl. Fusion, 13, 215 (1973).
7. N. V. Grishanov et al., Fiz. Plazmy, 2, 260 (1976).
8. I. N. Golovin, At. Energ., 39, No. 6, 379 (1975).
9. A. A. Samarskii, Introduction to the Theory of Difference Schemes [in Russian], Nauka, Moscow (1971), p. 450.
10. Report ORNL3113 (1971).
11. L. A. Artsimovich, Controlled Thermonuclear Reactions [in Russian], Fizmatgiz, Moscow (1963), p. 12.

THE HIGH-CURRENT ELECTRON ACCELERATOR IMPUL'S

L. N. Kazanskii, A. A. Kolomenskii, G. O. Meskhi, and B. N. Yablokov

UDC 621.384.659

The accelerator Impul's, which is of the first generation of high-current electron accelerators, was designed and built in the Laboratory of Problems of New Accelerators of the Physics Institute of the Academy of Sciences in 1969-1971 [1]. In 1973 a second block was added to the accelerator and two-beam operation was used on it for the first time in the Soviet Union. This made it possible to increase the efficiency of the accelerator utilization and to perform in parallel different experiments with two independent beams [2].

At the present time the accelerator Impul's consists of a common pulse-voltage generator in air, the associated equipment, and two identical cylindrical blocks. Each block comprises a double pulse-shaping line, a transforming line, and an electron gun (Fig. 1). The transition from one single-beam experiment to another requires only a few minutes and is reduced to changing the connections between the blocks and the pulse voltage generator. The two blocks are connected to the pulse voltage generator for synchronous generation of two beams.

The pulse-shaping lines which were used for the first time on the accelerator and increase the voltage, the glycerin ($\varepsilon = 44$) used for the insulation of the system comprising the double pulse-shaping line and the transforming line, the uncontrolled multi-spark gap, the 30-Ω junction between the glycerin and the vacuum, etc. required trial runs. We describe in the present article the design and its testing in the course of long accelerator operation.

Selection of the Parameters and Design of the Main Accelerator Components

The accelerator Impul's was designed for the generation of single electron beam pulses with a duration of 30-40 nsec and the parameters 1 kJ, 1 MeV, and 35 kA at the smallest possible dimensions of the apparatus.

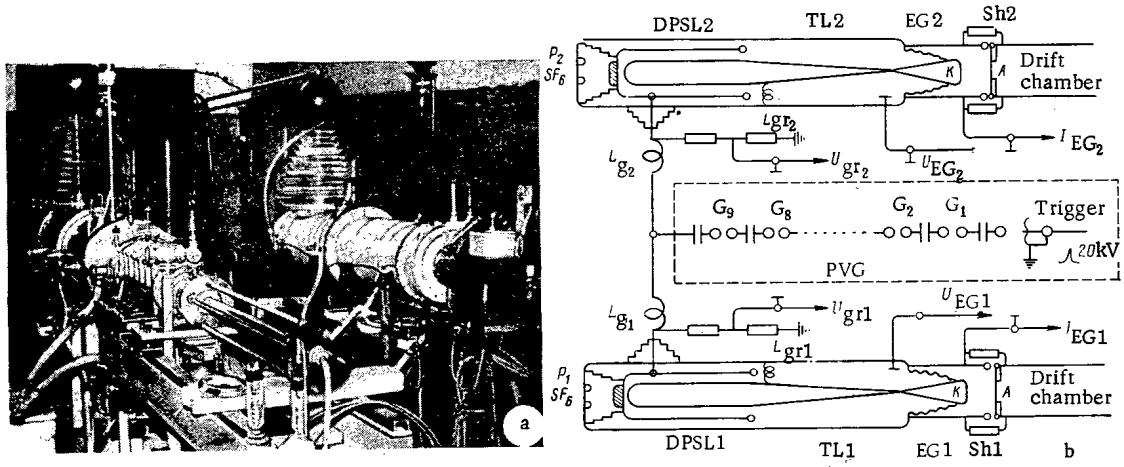

Fig. 1. a) Overall view of the accelerator Impul's and b) its structural scheme. PVG) Pulse voltage generator; EG1, EG2) electron guns; DPSL1, DPSL2) double pulse-shaping lines; G_1-G_9) gaps; Sh1, Sh2) shunts; TL1, TL2) transforming lines. Subscripts: g) gap; gr) ground.

Translated from Atomnaya Énergiya, Vol. 42, No. 2, pp. 113-119, February, 1977. Original article submitted June 4, 1976.

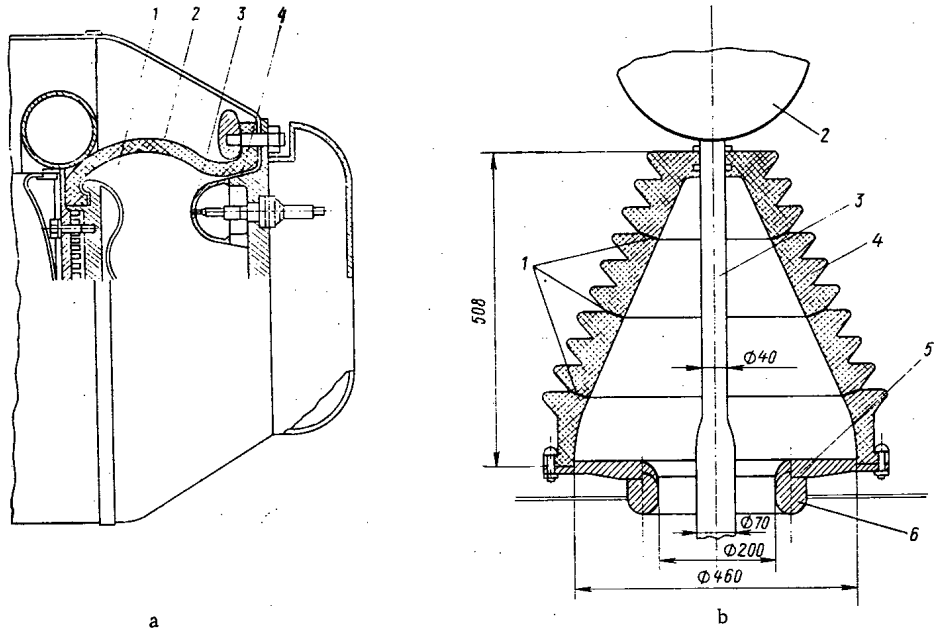

Fig. 2. a) Spark gap of the double pulse-shaping line: 1) high-voltage electrode; 2) housing; 3, 4) grounded electrode and igniting electrode, respectively. b) High-voltage input lead to the double pulse-shaping line: 1) adhesive junctions; 2) sphere; 3) high-voltage rod; 4) insulator; 5) supporting disk; 6) guard ring in the housing of the double pulse-shaping line.

TABLE 1. Dependence of the Ratio of the Lengths of the Transforming Line and the Pulse-Shaping Line upon the Transformation Coefficient

K_{tr}	Z_{out}/Z_{in}	l_{tl}/l_{dsl}	K_{tr}	Z_{out}/Z_{in}	l_{tl}/l_{dsl}
1,2	1,44	0,33	1,8	3,24	3,5
1,3	1,7	0,69	2,0	4,0	4,8
1,4	1,96	1,1	2,5	6,22	8,2
1,6	2,58	2,2	3,0	9,0	12,0

Taking into consideration the volt-second dependency of the electrical breakdown strength of the dielectric materials ($Et^{1/3} \approx$ const for $t \leq 1\mu$sec), it was decided to increase the voltage in the transfer of energy to the electron guns; the accelerator circuit comprising the pulse voltage generator, the double pulse-shaping line, the transforming line, and the electron guns were accordingly chosen.

Transforming Line. The transformation coefficient of the transforming line is limited by the tolerable increase in the length of the apparatus at a given distortion $\Delta U/U$ of the pulse shape. When both the double pulse-shaping line and the transforming line are made of the same dielectric material and when $\Delta U/U = 0.1$, the ratio of the lengths of the lines is given by the tabulated values. We selected $l_{tl} = l_{dsl}$ and $K_{tr} = 1.4$ for the Impul's. The transforming line was given the form of a coaxial line with a conical central electrode having a diameter of 90 mm at the input and of 15 mm at the output. The outer electrode had a diameter of 410 mm, and the transforming line a length of 850 mm. The wave impedance changes from 14 to 30 Ω. The measured distortion of the top of a 35 nsec pulse does not exceed 10%.

Double Pulse-Shaping Line. The total capacity of the double pulse-shaping line with a safety margin of 25% is obtained with the formula $C_{dsl} = 1.25(2W/U_{eg}^2)K_{tr}$ and is approximately 5 nF, where W denotes the given energy in the beam and U_{eg}, the voltage at the gun; the required charging voltage is $U_{dsl} = 700$ kV. A wave impedance of 14 Ω is obtained ($Z_{dsl} = C_{dsl}/\tau_p$); the best impedance matching is obtained with identical Z values, with $Z = 0.5$, $Z_{dsl} = 7$ Ω.

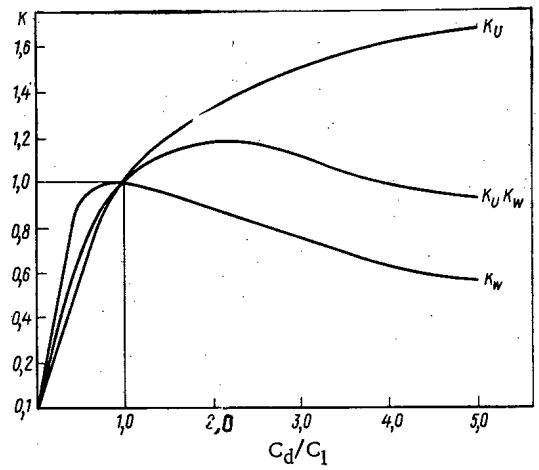

Fig. 3. Dependence of K_W, K_U, and $K_U K_W$ upon C_d/C_l.

The selection of the parameters of the double pulse-shaping line sets rigorous requirements to the switching time of the spark gap:

$$t_s \approx 2.2\,[\tau_R^2 + (I_g/Z)^2]^{1/2} \leqslant 0.3\tau_p, \tag{1}$$

where L_g denotes the inductance of the spark gap and τ_R denotes the time constant within which the resistance of the sparks decreases. Assuming that the contributions of the two components are equal, we obtain the following conditions for a current of ~100 kA: $L_g \leq 20$ nH and $\tau_R \leq 3$ nsec; these values can be obtained only with multi-spark operation of the spark gaps.

When the wave impedances Z of the double pulse-shaping lines are fixed, the condition of maximum energy storage can be used to determine the optimum ratio α_{opt} of the diameters of the electrodes forming the line and the optimum dielectric constant ε_{opt} [3]. It is assumed that the liquid dielectrics with various ε values have the same dielectric breakdown strength values:

$$W/V = \frac{60}{\pi c}\frac{E^2}{Z^2}\frac{\ln^3\alpha}{\alpha^4} = \text{const}\,\frac{\ln^3\alpha}{\alpha^4}, \tag{2}$$

where V denotes the volume of the double pulse-shaping line and c, the velocity of light. The maximum of the specific energy capacity is reached at $\alpha_{opt} = 2.12$, whereas the dielectric constant which corresponds to α_{opt} and Z is $\varepsilon_{opt} = [(60/Z)\ln\alpha_{opt}]^2 = 2000/Z^2$. For Z = 7 Ω, we have $\varepsilon_{opt} = 42$, and this led to the selection of glycerin ($\varepsilon = 44$) as the dielectric.

We also took into consideration that the glycerin does not require a purification system and special materials and that satisfactory relations are obtained between the lengths and diameters of the double pulse-shaping line and the transforming line. The maximum field strength in the double pulse-shaping line was assumed as 200 kV/cm in the operation; accordingly, the following diameters of the coaxial electrodes of the double pulse-shaping line were assumed: central diameter 90 mm, average diameter 190 mm, and external diameter 410 mm. The length of the double pulse-shaping line was $l_{dsl} = \tau_p c/2\varepsilon^{0.5} \approx 850$ mm. The central electrode of the inner line of the double pulse-shaping line was grounded through an inductance $L_{gr} = 3.5$ μH whose impedance at the discharge frequency is much smaller than the impedance of the pulse voltage generator and, in the nanosecond range, much greater than the output resistance of the double pulse-shaping line. The inductance was inserted into the initial portion of the transforming line and was a cylindrical, single-layer coil with an average diameter of 30 mm, the coil wound from 2 mm copper wire.

Spark Gap of the Double Pulse-Shaping Line (Fig. 2a). The spark gap was inserted into the external line and upon breakdown automatically cuts off the pulse voltage generator from the double pulse-shaping line. This position of the spark gap is advantageous also for controlling its ignition. The spark gap was mounted in a barrel-shaped Plexiglas insulator with a diameter of about 250 mm and a height of about 250 mm and attached to the face of the double pulse-shaping line. The anode of the spark gap is a truncated sphere (radius and diameter ~180 and 150 mm, respectively); the anode is made from 2-mm-thick aluminum. The grounded cathode consists of 6 rods with a diameter of 30 mm and hemispherical roundings; the rods are arranged on a circle with a diameter of 120 mm. The upper rod sections are made from stainless steel. The spark gap was filled with the inert gas SF_6 to a pressure of 150-400 kPa.

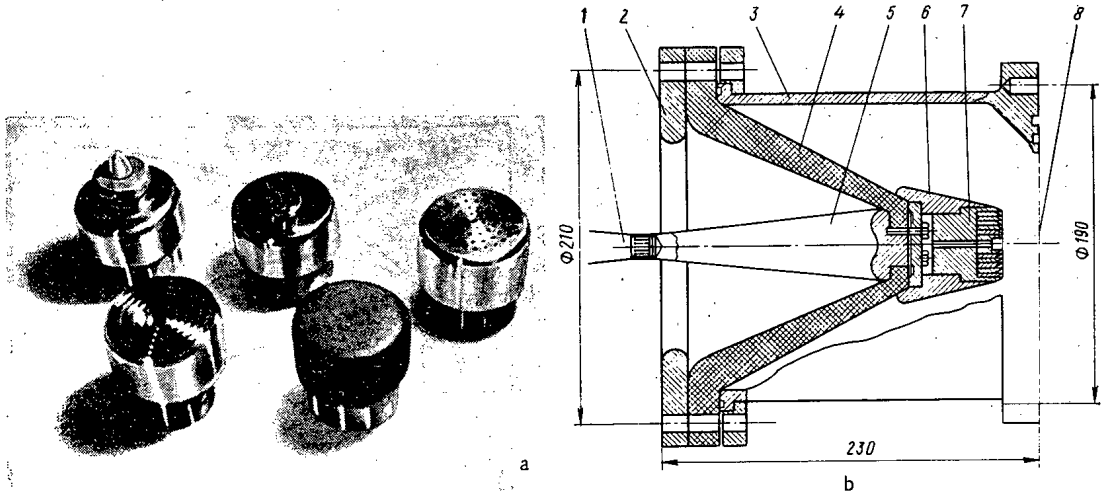

Fig. 4. a) Overall view of the cathodes used and b) schematic sketch of the gun: 1) internal electrode of the transforming line; 2) ring acted as a diaphragm; 3) jacket; 4) high-voltage insulator; 5) matching cone; 6) cathode holder; 7) cathode; 8) anode.

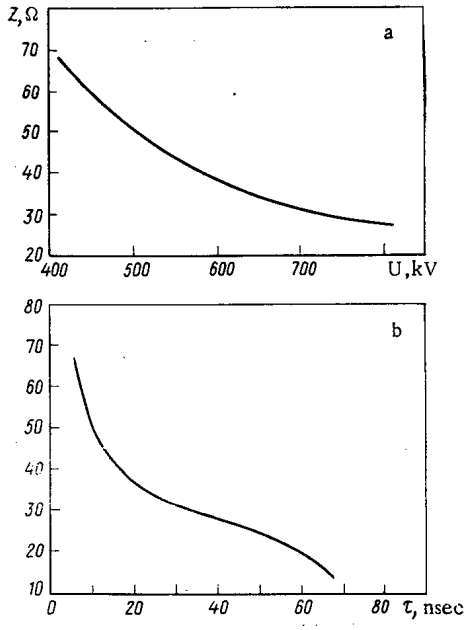

Fig. 5. Dependence of the impedance of the gun upon the voltage in the case a) of fixed anode–cathode distance and b) during a high-voltage pulse.

Pulse Voltage Generator. The use of glycerin with the small specific resistivity $\rho \geq 10^6\ \Omega \cdot$cm limits the line's discharge time. The energy losses occurring upon the discharge of the double pulse-shaping line with a voltage of $0.5U_{max}(1 - \cos\omega t)$ and the switching at the maximum of the voltage are $\Delta W/W \approx 2.6 \cdot 10^{13}/\omega\varepsilon\rho$. When we tolerate an energy loss of at most 10%, we obtain for glycerin with $\varepsilon = 44$ and $\rho \geq 2 \cdot 10^6\ \Omega \cdot$cm a charging time $t_{ch} = \pi/\omega$ of less than 1 μsec for the double pulse-shaping line. The discharge capacity C_d of the voltage pulse generator should be selected so that the maximum energy is transferred to the pulse-shaping line. When the losses are disregarded, we have

$$W_{dsl} = [C_d C_{dsl}/(C_d + C_{dsl})^2]\, W_g = K_W W_g, \qquad (3)$$

where W_g denotes the energy stored by the pulse voltage generator. The voltage at the double pulse-shaping line should be greater than the discharge voltage of the pulse generator voltage. Based on these considerations, the ratio C_d/C_{dsl} should be selected near the maximum of $K_W K_U$, where $K_U = U_{dsl}/U_d$ (Fig. 3).

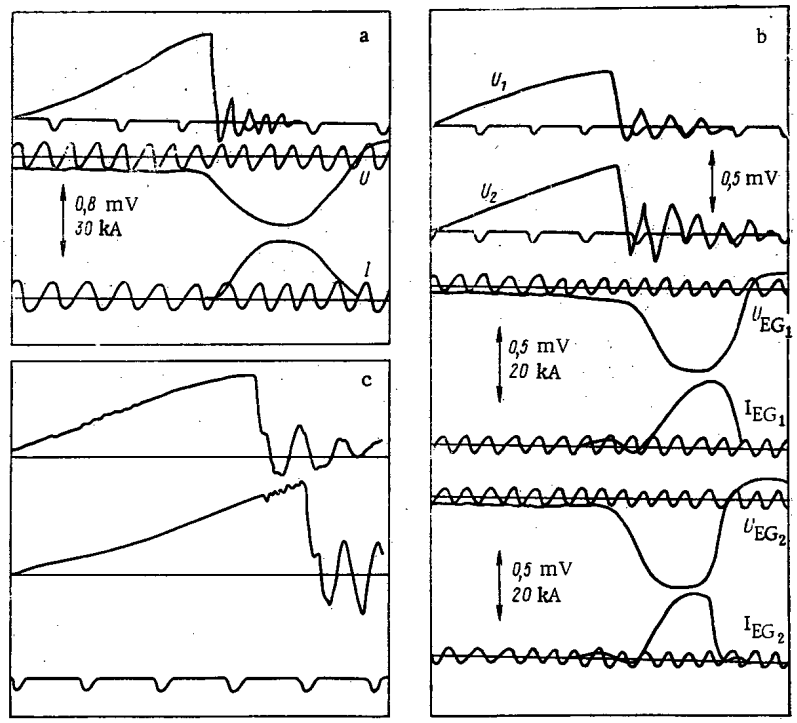

Fig. 6. Oscillograms of the charging voltage, the voltage and the current of the electron gun in: a) single-beam and b) double-beam operation of the accelerator; c) oscillograms of the charging voltages of the two double pulse-shaping lines in the case of beams shifting in the course of time. Time marks of 200 nsec at the charging voltages; calibrating sinusoidal voltage of 100 MHz.

We assumed for one double pulse-shaping line $C_d = 2C_{dsl}$; the minimum discharge voltage of the pulse voltage generator is obtained from the relation $U_d = U_g/[\exp(-\pi/2Q)]K_U$, where $Q \approx 15$ denotes the Q factor of the charging circuit (~600 kV). The inductance of the charging circuit must be less than 20 μH.

The pulse voltage generator of the accelerator Impul's comprises four standard GIN-400-0.06/5 generators which are connected in parallel and in series. Identical stages of the two columns (two GIN-400 generators in each column) are electrically connected to the common lines of the switching spark gaps which are mounted in a common vinyl plastic tube with a diameter of 110 mm and which are operated in a nitrogen atmosphere under a pressure of 100-500 kPa. By changing the pressure, one can adjust the output voltage of the pulse voltage generator during operation. The first spark gap of the high-voltage generator is a trigatron with a separately adjustable nitrogen pressure. The shock-load capacity of the pulse voltage generator is 12 nF, its inductance is 5 μH, the length of a single-period resonance discharge of the double pulse-shaping line is about 0.65 μsec, and the measured K_g value is 1.3. The charging voltage is applied to the double pulse-shaping line through a conical Plexiglas insulator (see Fig. 2b).

Electron Gun. The dimensions of the guns of the accelerator Impul's were selected so that a convenient attachment to the drift chamber was possible and that a magnetic field could be applied (length 250 mm, diameter ~180 mm for the guns). The dimensions of the electron guns limited their electric breakdown strength ($U_{eg\,max} \leqslant 850$ kV), but to date we have not used electron guns of large dimensions. The transition from the medium with a high ε value necessitates the conical shape of the insulator and precludes gradient rings (Fig. 4a) [4]. The high-voltage pulse which is applied to the electron gun from the transforming line passes through a three-layer coaxial line with a constant wave impedance; the line is formed by the jacket, the insulator, and the transition cone. Titanium foil with a thickness of 20-50 μ or a stainless steel net are used as the anode. During operation, the vacuum in the gun is at least $(1-2)\cdot 10^{-5}$ mm Hg. The cathode holder is designed so that the anode–cathode gap can be changed between 0.5 and 2.5 cm and that the impedance of the gun can be appropriately selected.

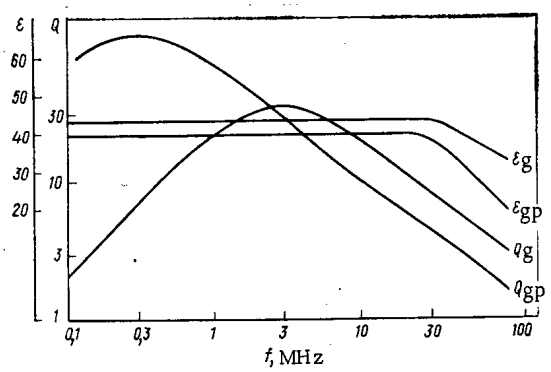

Fig. 7. High-frequency properties of the glycerin: g) 94% glycerin; gp) glycerin of brand "p" (pure); $\rho = 1.7 \cdot 10^6$ and $60 \cdot 10^6$ Ω · cm, respectively.

Various cathode configurations were tested: single-needle cathodes, multi-needle cathodes, and a cathode with a flat emitting surface and inlaid dielectric (see Fig. 4b). Presently cathodes with a diameter of 44 mm made from smooth graphite or stainless steel are used; the cathodes have seven concentric grooves with a spacing of 3 mm. The gun impedance is ~30 Ω at an anode–cathode distance of 10-17 mm and changes approximately like $U^{-1/2}$ when the voltage is increased (see Fig. 5a). The change of the gun impedance during a high-voltage pulse is shown in Fig. 5b. At a voltage of 700-800 kV at the gun, the electric field strength on the surface of the cathode holder reaches $(3\text{-}4) \cdot 10^5$ V/cm, which causes emission from the lateral surface and subsequent breakdown over the surface.

Conditions of Operation of the Accelerator Impul's

Single-Beam Operation. In single-beam operation the accelerator delivers a beam with a maximum energy of about 800 keV, a current of up to 30 kA, a pulse duration of ~40 nsec, and an energy of about 700 J (Fig. 6). The voltage and current pulses have a leading edge of ~18 nsec, which corresponds to the distortion in the spark gap, in glycerin, and at the input of the electron gun. A sharp cut, which is caused by flashover of the insulator of the electron gun, is frequently observed on the top or at the leading edge of the pulse. Usually the accelerator is operated with up to 700 keV and 20 kA; the beam at the anode is relatively homogeneous and has a diameter of 3-5 cm. When a truncated Teflon cone (height 12 mm and diameter 5/12 mm) is placed at the center of the cathode, the beam is reduced to a width of a few millimeters.

Two-Beam Operation. In two-beam operation the two double pulse-shaping lines of the Impul's are charged in parallel and two beams are generated in synchronism.

We obtain for the amplitude of the charging voltage of each of the n pulse-shaping lines having the capacity C_l with an accuracy sufficing for practical applications:

$$U_n/U_g = [2C_g/(C_g + nC_l)] \exp(-\pi/2Q), \quad (4)$$

where U_g and C_g denote the voltage and the capacity of the pulse voltage generator; and Q denotes the Q factor of the charging circuit. In the case of the accelerator Impul's, we have $C_{dsl} = 0.5C_g$ in single-beam operation and $nC_{dsl} \approx C_g$ in double-beam operation, with $Q \approx 15$. According to Eq. (4), at these relations of the capacitances, the parameters of each of the two synchronous beams are reduced to ~80% of the accelerating voltage and to ~60% of the stored energy of single-beam operation.

In double-beam operation, the switching spark gaps must be simultaneously triggered or the voltage of one of the spark gaps must be slightly reduced when the other is prematurely triggered. Therefore, each of the lines is connected to the pulse voltage generator through an additional decoupling inductance $L_{add} = 2L_0$, where L_0 denotes the inductance of the pulse voltage generator. The possibility of simultaneously generating two beams is influenced by the stability of operation of the spark gaps of the double pulse-shaping line. In the accelerator Impul's, in which uncontrolled spark gaps are used, particular risks were encountered and experimentally verified. It turned out that the mean-square spread of the triggering of the spark gaps of the double pulse-shaping lines does not exceed 10 nsec, provided that the pressure in each of the pulse-shaping lines is individually adjusted with an accuracy of about 0.02 mm Hg.

When the two beams are simultaneously generated, the voltage at the guns reaches 700 kV, the current 20 kA, and the energy about 400 J in each beam. Oscillograms, which illustrate the two-beam operation of the accelerator, are shown in Fig. 6b. The accuracy of the beam synchronization was better than 10 nsec. In the case of external mismatching of the pressures in the spark gaps, the pulses can appear shifted on the time scale by about 100 nsec and with a stability of ±12 nsec; it follows from the oscillograms of Fig. 6c that the triggering of the spark gap of one of the double pulse-shaping lines does not sharply modify the voltage of the other pulse-shaping line.

Result of Investigations and Experience in the Operation

The experience gathered in the operation of the accelerators has shown that the voltage pulse generator provides only a small range of control (15-20%). The reason is that there is no light guide between the spark gaps, that the surge level in the first stages of the GIN-400 generator is low (~40%), and that the design has shortcomings which preclude the accurate adjustment of the distances between the electrodes of the spark gaps (spread ±10%).

Owing to the internal charging inductance (L_{gr}) in the double pulse-shaping lines, there exist voltage differences between the pulse-shaping lines and the voltage difference is applied to the electron gun. Investigations of the influence of L_{gr} upon the amplitude of the voltage before the pulse and upon the energy losses during the main pulse have shown that good results obviously cannot be obtained when the inductances are placed in a medium with a large ε value. Acceptable results (amplitude of the voltage before the pulse $\leqslant$10% and energy losses $\leqslant$20%) can be obtained in our case, because an additional inductance of 12 μH was inserted between the voltage pulse generator and the double pulse-shaping line.

When the accelerator Impul's was built, the high-voltage and high-frequency properties of glycerin were investigated (Fig. 7). The drop of ε and Q at frequencies exceeding 30 MHz limits the curvature of the pulse edges to values $\geqslant$10 nsec. But when pulses with an edge length of 10-15 nsec are shaped, glycerin can be used. The high-voltage properties of glycerin are appropriately described by the formula

$$E_{acc} = 0.35 t_{eff}^{1/3} S_{eff}^{1/10} \text{ (MV/cm)}, \quad (5)$$

where t_{eff} and S_{eff} denote the effective time (μsec) and area (cm^2), respectively.

Glycerin proved appropriate as a dielectric but when it was filled in, the lines had to be evacuated and the glycerin heated to 50-60°C. In our apparatus, the glycerin kept its insulating characteristics and high-frequency characteristics for two to three years even after several breakdowns had occurred in it.

The form of the electrodes of the switching spark gap of a double pulse-shaping line guarantees that two or three sparks burn in each discharge without ignition. The accuracy of triggering is ±10 nsec. The overvoltage reaches 1.6-1.8 in the spark gap at the time of the breakdown. Switching currents up to 100 kA at a voltage of 700 kV occur within 8-10 nsec in a 2.2-cm gap. These results are in good agreement with the estimated inductance and resistance of the two sparks [5, 6].

The accelerator "Impul's" proved to be suitable for experimental work and was rather reliable even in prolonged use. The total number of discharges made in the accelerator reaches several ten thousand. Basically suitable proved the measures taken in building the accelerator, e.g., the selection of the system comprising the pulse voltage generator, the double pulse-shaping line, and the transforming line, the coaxial form of the lines, the multi-spark gaps, and the use of glycerin in a small, compact apparatus. Particularly important is the great advantage obtained by using the accelerator in double-beam operation.

The authors thank A. N. Lebedev, D. D. Krasil'nikov, V. B. Sidorov, O. I. Saksonov, V. T. Eremichev, S. I. Vlasenko, and A. V. Serov for their great help and support in building the accelerator and in putting it into operation.

LITERATURE CITED

1. L. N. Kazanskii et al., Preprint JINR D-9-6707 [in Russian], Dubna (1972), p. 161.
2. L. N. Kazanskii, A. A. Kolomenskii, and B. N. Yablokov, in: Trans. Fourth All-Union Conference on Accelerators of Charged Particles [in Russian], Vol. 1, Nauka, Moscow (1975), p. 310.
3. L. N. Kazanskii and B. N. Yablokov, in: Trans. Second All-Union Conference on Accelerators of Charged Particles [in Russian], Vol. 1, Nauka, Moscow (1972), p. 98.

4. G. O. Meskhi and B. N. Yablokov, in: Trans. Second All-Union Conference on Accelerators of Charged Particles Vol. 1, Nauka, Moscow (1972), p. 90.
5. S. I. Barannik, S. B. Vasserman, and A. N. Lukin, Zh. Tekh. Fiz., 44, No. 11, 2352 (1974).
6. W. Pfeiffer, Elektrotech. Z. A., 95, No. 8, 405 (1974).

INFORMATION FOR THE AUTHORS

The articles submitted to the journal Atomnaya Energiya must be presented in very concise, brief form. One must avoid repetitions of tabulated data and graphs and omit the simultaneous presentation of numerical results in the form of tables and graphs.

Reviews normally must not exceed 20-22 pages; original articles, 10-12 pages; abstracts of deposited articles, 2 pages; and letters to the editors, 5 pages of typed text (including figures with legends, tables, and reference citations).

In preparing manuscripts, the authors must be guided by the following rules:

1. The texts (which must necessarily comprise the first of the typewritten copies) and the illustrated papers must be presented in four copies in final form for printing. The text must be written with double spacing and with 28-29 lines per page; the margins must not be narrower than 4 cm; handwritten inserts cannot be accepted.

2. The text (writing of formulas, Greek and Latin letters, lower-case letters and capital letters, abbreviations of words, etc.) must conform to the usual rules adopted in scientific and technical journals. Letters used for the notation which are hard to discern in manuscripts and corresponding must be explained on the margins.

3. The units of all physics quantities must be indicated in the International System.

4. Tables appended to the test must be given numbers in the order of their appearance; each table must have a title.

5. Drawings are to be made with black Indian ink on 15 × 20-cm paper; photographs must have sufficient contrast and a size of 12 × 18 cm.

6. Legends to figures must be appended on a separate sheet. The text must refer to the drawings.

7. The cited literature is stated at the end of the paper in an overall list which has to indicate;

a) in the case of journal articles, the name and the initials of the authors, the name of the journal, the year, and the numbers of the volume, the edition, and the page;

b) in the case of books, the name and the initials of the authors, the full title of the book, the place of its edition, the editorial, and the year of the edition; in the case of foreign books, also information pertaining to its Russian translation must be indicated;

c) in the case of articles of a collection, the name and the initials of the authors of the article, the title of the collection, the initials and names of the compiler or editor of the collection, the portion thereof, the edition, the place of the edition, the editorial, the year, and the page.

No reference must be made to unpublished work.

8. Articles, reviews, and letters to the editor must be accompanied by abstracts which are to be compiled according to the rules of the abstracting journals; the goal and the results of the work must be clearly stated. Furthermore, abstracts of articles and reviews must be translated into English (with the translation strictly corresponding to the Russian abstract).

Translated from Atomnaya Énergiya, Vol. 42, No. 2, p. 119, February, 1977.

9. The titles of all papers submitted to the editor (articles, reviews, deposited articles, reviews, deposited articles, and letters to the editor) must be translated into English and both the name and the initials of the authors must be transliterated into English.

10. The texts and the figures must be signed by all authors. The exact address, the telephone number, the name, the full name, and the patronymic of the authors mjst be indicated.

The editorial office sends to the author only one corrected copy which he must return within the shortest possible time.

Manuscripts which do not satisfy the above requirements will be ignored. Rejected articles will not be returned.

ESTABLISHING PERMISSIBLE DOSES ON THE BASIS OF BIOLOGICAL RISK

V. G. Denisenko, U. Ya. Margulis, and A. I. Klemin

UDC 539.1.01/539.1.04

In planning the development of nuclear energy, and in the principal use of radioactive materials and sources of ionizing radiation, it is important to estimate the possible effect of radiation on the population and the surrounding environment, in order to produce definite requirements as to the reliability and positioning of nuclear equipment. In normal use, radiation sources may produce only small doses. To estimate the effects of such small doses, according to the recommendations of the International Commission on Radiological Protection (ICRP), data on the long-term effects of comparatively large doses (which can be reliably identified) can be extrapolated to the region of small doses, assuming a linear relation between the radiation dose and the biological effect. Extrapolation on the assumption that there is no threshold in the effect of radiation loads to an overestimate of the probable risk associated with small doses [1-3]. Because of the many imponderables involved in the genesis of long-term effects, it is difficult and sometimes even impossible to relate effects to previous irradiation. Therefore, the long-term effects of small doses of radiation can only be estimated by statistical means, determining the total yield of injuries in a large population.

To ensure radiation safety, it is necessary to create conditions such that the incidence of possible injuries in the population is at a low level, not posing a danger to society. But what number of injuries may be regarded as justified This problem is not purely scientific but also social. Without doubt, the criteria will be different at each stage of society. The chosen criterion might be the number of injuries in the safest branches of industry (e.g., dressmaking or light industry) or due to natural causes (damage by meteorite shower, lightning, etc.). One proposed approach to establishing such a norm is to make a quantitative comparison of the incidence of a certain biological effect in conditions where radiation has been present and absent (apart from ordinary background radiation). In this case it seems more correct to apply the condition of no observable effect, according to which the number of injuries resulting from the use of atomic energy must not exceed the random variations of similar injuries, due to natural causes; in particular, this condition is discussed in [4].

According to this condition, the "acceptable" level of radiation for any population of N humans is that at which the number of radiational injuries cannot be isolated by statistical analysis of a sequence of values obtained at different times, characterizing the dynamics of the same kind of natural morbidity. As a rule, the considered population is part of some larger population (e.g., a whole state), numbering N_0 people. At time t, the larger population may be represented by some set of N_0/N population of equal size, and hence it is possible to consider distributions of two types.

Translated from Atomnaya Énergiya, Vol. 42, No. 2, pp. 120-122, February, 1977. Original article submitted October 8, 1976.

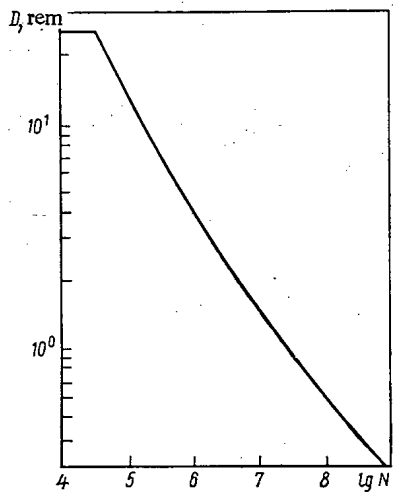

Fig. 1. Dependence of limiting dose of external γ radiation on population size N.

1. Denoting by i the number of the considered population in the indicated set (i = 1, 2, ..., N_0/N) and by f(i, N, t) the frequency of morbidity characterizing the i-th population of N people at time t, it is possible to consider the distribution of the frequency f over the N_0/N equal-sized populations.

We denote the arithmetic mean of this distribution by $\Phi(N, t)$ and the standard deviation by $\sigma_\Phi(N, t)$.

2. For each population i, the frequency f may be used to construct a sequence of values obtained at different times characterizing the evolution of morbidity for the given population. Assuming a random variation of f with time, we obtain some distribution over time; we denote the arithmetic mean of the distribution by $\Phi(i, N)$ and the standard deviation by $\sigma_\Phi(i, N)$.

Note that $\sigma_\Phi(i, N)$ is used to determine the norm. If there is a linear dependence between the radiation dose D of the critical organ and the effect of the radiation, then the initial condition leads to the requirement that

$$CDN \leqslant \sigma_\Phi(i, N), \tag{1}$$

where C is a constant.

To derive a practically useful formula, we assume that in all the populations of equal size N the means and standard deviations are the same

$$\begin{gathered}(\partial/\partial i)\,\Phi(i, N)\,(\partial/\partial i)\,\Phi(i, N) = 0; \\ \partial/\partial i \sigma_\Phi(i, N) = 0.\end{gathered} \tag{2}$$

By definition

$$f(N_0, t) = \sum_{i=1}^{N_0/N} f(i, N, t) = (N_0/N)\,\Phi(N, t). \tag{3}$$

If $\Phi(N_0) = (1/n) \sum_{i=1}^{n} f(N_0, t)$, then according to Eqs. (2) and (3)

$$\Phi(N_0) = (1/n) \sum \sum_i f(i, N, t) = (N_0/N)\,\Phi(i, N) = (N_0/N)\,\Phi(N), \tag{4}$$

where n is the number of instants at which values are taken.

By the definition of the standard deviation

$$n\sigma_\Phi^2(i, N) = n\sigma_\Phi^2(N) = \sum_{i=1}^{n} [f(i, N, t) - \Phi(N)]^2. \tag{5}$$

Denoting by $\xi(i, N, t)$ the difference $f(i, N, t) - \Phi(N, t)$, Eq. (5) may be written in the form

$$n\sigma_\Phi^2(N) = \sum_t [\Phi(N, t) - \Phi(N)]^2 + 2 \sum_t [\Phi(N, t) - \Phi(N)]\,\xi + \sum_t \xi^2. \tag{6}$$

It is not difficult to see that the first sum in Eq. (6) is equal to $n[(N/N_0)\sigma_\Phi(N_0)]$; this is obvious on introducing the expressions for $\Phi(N, t)$ and $\Phi(N)$ in Eqs. (3) and (4).

We denote the second and third terms in the right-hand side of Eq. (6) by X_2 and X_3, respectively. From Eq. (2) it follows that

$$\sum_{i=1}^{m}(X_2+X_3)=m(X_2+X_3). \tag{7}$$

On taking into account the properties of $\xi(i, N, t)$, we obtain $(1/m)\sum_i X_2 = 0$. The sum $(1/m)\sum_i X_3$ takes the form

$$(1/m)\sum_i X_3=(1/m)\sum_i\sum_t \xi^2=\sum_t \sigma_\Phi^2(N, t). \tag{8}$$

Therefore $X_2 + X_3 = \sum_t \sigma_\Phi^2(N, t)$. Finally, we obtain

$$n\sigma_\Phi^2(N)=n[(N/N_0)\,\sigma_\Phi(N_0)]^2+\sum_t\sigma_\Phi^2(N, t). \tag{9}$$

From Eqs. (1) and (9), we obtain an equation which can be used to determine a limiting maximum dose on the population

$$D\leqslant C^{-1}\left\{\left[\frac{\sigma_\Phi(N_0)}{N_0}\right]^2+\frac{1}{N^2n}\sum_t\sigma_\Phi^2(N, t)\right\}^{1/2}. \tag{10}$$

If the frequency f is sufficiently small, then in accordance with the properties of the Poisson distribution $\sigma_\Phi^2(N, t) = \Phi(N, t)$ and the sum in Eq. (9) is $(N/N_0)\Phi(N_0)n$; hence Eq. (10) takes the form

$$D\leqslant C^{-1}\left\{\left[\frac{\sigma_\Phi(N_0)}{N_0}\right]^2+\frac{\Phi(N_0)}{NN_0}\right\}^{1/2}. \tag{11}$$

As an example, we consider the norm given by Eq. (11) in the case of external γ irradiation of the whole organism; the injury chosen is leukemia, since it leads to a fatal outcome in 100% of cases. Moreover, of all the relevant injuries, leukemia has the lowest probability of natural incidence. In accordance with [4], we set $C = 1.5\cdot10^{-6}$ (injuries/yr)/(person · rem). In the calculation we use data on the natural frequency of malignant neoplasms in a population of $N = 10^5$ people in the USSR taken from [5]

1961	139.3	1965	166.2
1962	147.2	1966	171.6
1963	151.6	1967	172.0
1964	167.2		

Applying the last-squares method to this series gives a standard deviation of 0.8 injuries/yr. Since the probability of mortality is 4.3% of the total sum [5], the results for leukemia are characterized by a standard deviation of $3.4\cdot10^{-2}$ injuries/yr. Since this frequency is insignificant, Eq. (11) is used, and $\Phi(N_0)$ is found by averaging the data taking into account the incidence of leukemia. Finally, the formula obtained is

$$D\leqslant 6\cdot10^5[1.1\cdot10^{-13}+N^{-1}6.5\cdot10^{-5}]^{1/2}. \tag{12}$$

From Eq. (12) it is evident that the permissible dose, decreasing with increase in the size of the population, tends to some limiting value equal to 0.2 rem in the considered case.

The curve for D(N) in Fig. 1 for N between 10^4 and 10^9 shows that, as N decreases, D increases and may reach a value at which, in addition to the long-term consequences, short-term effects of the radiation appear. Therefore, if the radiation is to satisfy the condition of no observable effect, a reasonable upper limit must be imposed on D. The available material, obtained from experiments on animals and by the analysis of data on the state of health of persons exposed to radiation, shows that no change in the state of health of a human being can be observed after a single irradiation of the whole body in doses up to 25 rem. This value can be accepted as a reasonable upper limit on the dose.

The present estimate shows, in particular, that for the currently permitted maximum dose of 0.5 rem/yr for individuals in the population, the condition of no observable effect will be satisfied for $N \sim 10^8$. In other words, if ~40% of the population of the USSR are exposed to the maximum permitted individual dose, the number of possible long-term effects due to radiation will be undetectable against the fluctuating background of analogous effects due to natural causes.

However, it should be pointed out that this analysis does not exhaust the complexities of establishing a safety norm on the basis of the concept of biological risk. The procedures for establishing a norm must be based on statistical principles and determined only after a detailed investigation of other aspects, including, in particular, the role of geographical factors, the type of radiation, the selection of the monitored injuries, etc.

LITERATURE CITED

1. V. P. Shamov (editor), Radiation Protection, ICRP Recommendations [Russian translation], Atomizdat, Moscow (1967).
2. Papers of the UN Committee on the Effect of Atomic Radiation (1962 and 1965) [Russian translation], UN Documents (1962, 1965).
3. A. A. Letavet et al., At. Energ., 28, No. 3, 225 (1970).
4. Yu. I. Moskalev et al., The Concept of the Biological Risk of the Effect of Ionizing Radiation [in Russian], Atomizdat, Moscow (1973).
5. Morbidity and Mortality Rates of USSR Population due to Malignant Neoplasma [in Russian], Meditsina, Moscow (1970).

DEPOSITED ARTICLES

EFFECT OF INSULATOR SPACE CHARGE ON DIRECT-CHARGE-DETECTOR CURRENT

A. A. Kostritsa and L. V. Chekushina

UDC 537.533.7+621.039.564.2

The field created by a space charge of electrons arising in an insulator separating the emitter and collector of a direct-charge detector (DCD) is considered.

For plane electrode geometry, the potential difference between the electrodes, which discharges the peak of the potential barrier at the dielectric edge, is

$$U \approx l^2 \sqrt{eS/2\varepsilon b\lambda_2}.$$

Here l is the insulator thickness; λ_2 is the electron free-path length; ε is the dielectric permeability; e is the electron charge; S is the number of electrons leaving unit area of the emitter in unit time. The electron mobility b is assumed to be independent of the electric field strength.

For cylindrical geometry

$$U\sqrt{\frac{3\varepsilon b}{eQr_k^3}} = \frac{2k-5}{3}\sqrt{2k+1} - \ln\frac{\sqrt{2k+1}-1}{\sqrt{2k+1}+1} + 0.415,$$

where $k = r_e/r_c$; $Q = Sr_e/\lambda_2 - r_e$; r_e is the emitter radius; r_c is the collector radius; the electron density is proportional to $1/r$.

From an investigation of the volt–ampere characteristics for a DCD with a rhodium emitter taken in the active zone of a water-moderated reactor, the change in current due to the effect of the space charge was determined.

Original article submitted August 12, 1975.

CALCULATION OF THE ENERGY SPECTRA OF γ QUANTA BY THE YVON–MERTEN METHOD

V. S. Galishev

UDC 539.121.72.75

The papers [1, 2] studied the influence of successive approximations in the Yvon–Merten method on the energy spectra of γ quanta reflected and transmitted by a layer. The results of the calculations for the function $\Psi_0(X, E)$ of the energy flux of scattered γ rays of energy E at a distance X from the source are shown in Figs. 1a and b for a gamma source with an initial energy of 1 MeV and for the case of normal incidence of the radiation on a layer of water of a thickness equal to double the mean free path. It is seen that the reflection spectra calculated in the $2P_1$ and $2P_2$ approximations almost coincide with each other over the entire energy range studied but differ significantly from the spectrum obtained in the $2P_0$ approximation. For the transmission spectra, the curves corresponding to the $2P_0$, $2P_1$, and $2P_2$ approximations differ most from each other at an energy equal to the source energy. However, as the energy of the scattered γ quanta decreases, the results corresponding to the $2P_1$ and $2P_2$ approximations approach each other, although as before they still differ significantly from what the $2P_0$ approximation gives.

Translated from Atomnaya Énergiya, Vol. 42, No. 2, pp. 123-127, February, 1977.

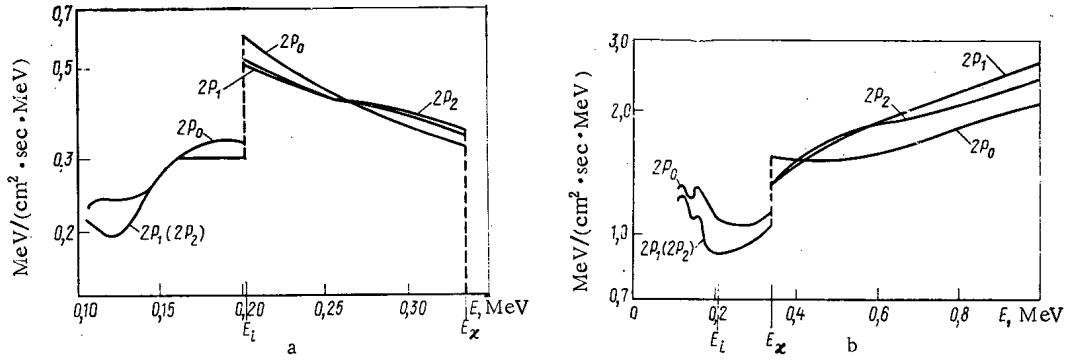

Fig. 1. Reflection and transmission spectra for γ quanta in $2P_0$, $2P_1$, and $2P_2$ approximations by Yvon–Merten method.

Therefore, if the $2P_1$ approximation can be used to calculate reflection spectra, the $2P_3$ approximation must evidently be taken into account for transmission spectra.

LITERATURE CITED

1. S. Gerstel, Dissertation, Technische Hochschule, Karlsruhe (1967).
2. S. Gerstel, Ein ALCOL-Programm zur Berechnung von Energiespektren gestreuter Gammastrahlen in einer ebenen Abschirm-Schicht, BMWF-FB K 69-43 (1969).

Original article submitted January 27, 1976.

PROPAGATION OF γ RAYS IN SYSTEM OF PLANE INFINITE LAYERS

I. SPACE-ENERGY DISTRIBUTION OF SECONDARY ELECTRONS

I. R. Entinzon, O. P. Verkhgradskii, and A. M. Kabakchi

UDC 541.15-185+539.166.9:535.3

During the irradiation of a substance with γ rays a stationary space–energy distribution of photons and generated electrons is established. In the present paper a method is developed for determining the distribution function of electrons generated in the irradiated substances.

Suppose that the irradiated substance with an established space–energy distribution of photons is surrounded by a vacuum, i.e., that the photon distribution function outside the irradiated substance is zero. This assumption introduces an error in the sought radiation field of the generated electrons but it is not significant inside the substance, where electronic equilibrium is ensured. Therefore, we shall consider the region of electronic equilibrium.

The incoming photon spectrum is used to calculate the initial concentration of electrons produced by Compton scattering and the photoelectric effect (pair formation is not taken into account since it is insignificant in the energy range under consideration).

The initial electron concentration enters into the calculations of the kerma and the radiation field of the secondary electrons. Comparison of the kerma and the absorbed dose allows the fraction of secondary-electron energy lost to bremsstrahlung in the material to be evaluated.

Calculation of the distribution function of secondary electrons with respect to energy and coordinates, i.e., the electron radiation field, is carried out by the successive collision method together with the method of continuous retardation. The motion of electrons in the substance, on the one hand, reflects continuous retardation and, on the other hand, is represented as a chain of successive "collisions."

A computational program based on the input algorithmic language ALGOL was written for calculating the distribution function and its derivative quantities. The calculations were performed on a BÉSM-6 computer for four irradiated materials: cellulose triacetate, aluminum, copper, and lead.

The composition of the electron radiation in the materials is compared with different atomic numbers.

The Bragg–Gray relation is used to compare the experimental value obtained for the absorbed dose with the calculated value. The experimental and theoretical data are in good agreement for light materials. The experiments was carried out on the γ radiation facility UKP-100000 of the L. V. Pisarzhevskii Institute of Physical Chemistry, Academy of Sciences of the Ukrainian SSR. The calculations were performed for a model of this facility.

Original article submitted February 4, 1976.

POTENTIOSTATIC AND PULSED-POTENTIOSTATIC ELECTRODEPOSITION OF URANIUM ON LIQUID ZINC WITH AN ANODE LAYER

S. L. Gol'dshtein, S. M. Zakhar'yash, D. F. Rakipov, and S. P. Raspopin

UDC 541.135+669.5.822

The authors investigated the potentiostatic and pulsed-potentiostatic electrodeposition of uranium from a KCl–NaCl fused electrolyte (4.3 wt. % UCl_3) on a zinc cathode layer ($m_k \approx 1$ and 5 g, $S_k \approx 0.75$ and 1.68 cm^2, respectively) at 700°C with an anode layer in an argon atmosphere. The reference electrode was a chloride half-cell.

The range of potentials (2.30-2.37 V) of optimal potentiostatization was determined rapidly by potentiodynamic measurements (~0.2 V/sec).

Potentiostatic electrolysis with replacement and subsequent chemical analysis of the cathode for every value of φ_z made it possible not only to verify but also to identify the characteristic ranges with concrete electrochemical processes. Thus, when $\varphi_z < -2.20$ V it is possible to reduce electropositive impurities (corroded zinc). In the operating potential range (2.25-2.37 V) it becomes possible to produce precision zinc–uranium alloys closely conforming to the "potential-composition" thermodynamic function. The decrease in the deposition of uranium when $\varphi_z < -2.37$ V is associated with the flow of a competitive discharge of alkali metal ions.

On the basis of the results of analysis of the potentiostatic curves of current decay, plotted for various heights l of the cathode layer (the temperature gradient with respect to height was 1°C/cm), it was assumed that the mode of mass transfer of uranium in zinc changed. It was established that with a cathode of small dimensions the molecular (atomic) mechanism prevails, and when $l > 10$ mm the effect of convection must be taken into account.

The process of deposition of uranium on liquid zinc is intensified by the pulsed-potentiostatic mode (pulsation frequency 0.5 Hz, pulse ratio 1.1) allowed an improvement to be made in the principal technological indices (current efficiency 94% as compared to 80% in "ordinary" potentiostatization).

Original article submitted February 20, 1976.

OPTIMIZATION OF SHIELDING CONTAINERS FOR ISOTOPIC NEUTRON SOURCES

Yu. N. Kazachenkov, A. P. Suvorov, and R. P. Fedorenko

UDC 621.039.78

Optimal variants of a one-dimensional heterogeneous spherical shield are determined in the present paper. The method of successive approximations was used along with the linear theory of small perturbations to obtain optimal shield compositions. Account was taken of various constraints on the problem parameters and functionals by employing the principles of the nonclassical calculus of variations. The propagation of neutrons was described in the five-group P_1 approximation. Attenuation of γ rays from the source was described in the four-group approximation by an exponential kernel with a geometric power-law build-up factor. Secondary γ rays were similarly calculated. This method was used in [1] to calculate one-dimensional shield compositions.

Heterogeneous sheilds of iron, lead, paraffin, and boron carbide were investigated; in almost all cases, these materials had boron carbide (no more than 5 vol. %) added to them. The outside layer consisted of 1 cm of iron (for strength),which at the same time also served as a shield (primarily for γ rays).

Variants of shields were found with minimum mass for a given dose on the container surface D = 10; and 200 mR/h in the second and third transport category, respectively, for californium and (α, n) neutron sources with a yield of 10^9 to $5 \cdot 10$ neutrons/sec. The spectra of the isotopic neutron sources were taken from [2, 3]. It was established that the mass of the optimal containers can, at times, be several times smaller than that of nonoptimal ones.

A characteristic feature of all optimal compositions is that, in the first place, the internal layer should be a heavy component, Pb or Fe, and a light component, CH_2, should be next. If the first layer is lead and not iron, there is a significant gain in mass. The ratio of the heavy component to the light component rose sharply in comparison with the results obtained for a one-dimensional shield [1]. This is explained by the fact that in the present paper the calculation was carried out for a spherical geometry whereas in [1] it was for a plane geometry.

The addition of a small quantity of B_4C has little effect on the minimum mass. This was verified by calculation when each layer, apart from the outside layer, consisted of a homogeneous mixture of Pb, Fe, B_4C, and CH_2. In this case as well the chemical composition of the layers and their alternation for optimal composition did not change so that the composition $Pb-CH_2-Fe$ (1 cm) may be considered to be the most optimal.

LITERATURE CITED

1. A. P. Suvorov and R. P. Fedorenko, in: Problems of the Physics of Reactor Shielding [in Russian], No. 3, Atomizdat,(1969), p. 6.
2. N. D. Tyufyakov et al., in: Radiation Techniques [in Russian], No. 5, Atomizdat, Moscow (1970), p. 90.
3. N. D. Tyufyakov et al., in: Applied Nuclear Spectroscopy [in Russian], No. 1, Atomizdat, Moscow (1970), p. 24.

Original article submitted April 5, 1976.

OPTIMAL OPERATION FOR RESEARCH REACTORS

A. S. Gerasimov

UDC 621.039.514.25

The paper considers the problem of optimizing the cyclical operation of a research reactor with account for xenon poisoning. Each period lasted 24 h and for a time τ at the beginning of the period the reactor power U(t) was zero (planned shutdown). For the rest of the time (operation) U(t) is a function of time and the xenon concentration should not exceed a set value associated with the reactivity reserve for poisoning. The power should be varied during the operation so that the total energy release in a cycle is maximum.

The Pontyragin maximum principle was used to solve the problem. A characteristic feature of the given problem in comparison with other treatments of xenon optimization problems is that the cyclical operation of the reactor is optimized. As a result, the state of the reactor at the beginning of the operation is essentially steady-state and, moreover, there is a connection between the final and initial state of the operation (feedback) which leads to specific transversality conditions for the adjoint functions.

Depending on the concrete properties of the reactor, the period T, and the shutdown time τ, the optimal operation is only three-phase,

$$U(t)=U_{\max},\quad \tau\leqslant t\leqslant t_1;\quad U(t)=U_{\mathrm{cl}}(t),$$
$$t_1\leqslant t\leqslant t_2;$$
$$U(t)=U_{\max},\quad t_2\leqslant t\leqslant T,$$

or four-phase,

$$U(t)=U_{\max},\quad \tau\leqslant t\leqslant t_1;\quad U(t)=U_{\mathrm{cl}}(t),\quad t_1\leqslant t\leqslant t_2;$$
$$U(t)=U_R(t),\quad t_2\leqslant t\leqslant t_3;\quad U(t)=U_{\max},\quad t_3\leqslant t\leqslant T,$$

where U_{max} is the maximum power, U_{cl} is the power corresponding to so-called classical operation, and U_R is the power at which the xenon concentration is the maximum allowed. Three-phase operation is realized in cases when the length of the operation $T-\tau$ is relatively short and the xenon characteristics do not reach the limit. Four-phase mode is optimal for long operations. As numerical calculation for concrete samples shows, the energy release in optimal operation is typically double that in simple cyclical operation without optimization.

Original article submitted June 21, 1976.

CONDITIONS OF ELECTRONIC EQUILIBRIUM DURING IN-PILE IRRADIATION OF HETEROGENEOUS OBJECTS

B. A. Briskman, V. P. Savina,
L. V. Popova, and V. D. Bondarev

UDC 621.039.51

The purpose of the present paper is to investigate the redistribution of the absorbed energy of γ rays from reactor radiation because of transport by knock-out electrons in a system consisting of several elements. The computational model considered was a system of three coaxial infinite cylinders. The external cylinder (d_{ext} = 33 mm, δ = 2.5 mm) was made of aluminum, the solid internal cylinder (d = 5 mm) was made of magnesium. The middle cylinder (d_{ext} = 16 mm, δ = 1 mm) was made of Zn, Zr, Sn, and Pb. The calculations were carried out for three types of reactor γ-ray spectrum, obtained by the Monte Carlo technique for a light-water reactor in the reflector ($\Phi_{\gamma 1}$ and $\Phi_{\gamma 2}$) and in the active zone ($\Phi_{\gamma 3}$). The redistribution of the γ-ray energy in a system of n elements was calculated by the formula

TABLE 1. Values of K for Different Sets of Coaxial Cylinders

System	Spectrum	$\bar{E}_l \approx 1/2\,\bar{E}_\gamma$	Knockout electron spectrum allowed for	K_{expt}
Al—Zn—Mg	Φ_{γ_1}	0,990	0,980	0,98
	Φ_{γ_2}	0,988	0,976	—
	Φ_{γ_3}	1,02	1,03	1,05
Al—Zr—Mg	Φ_{γ_1}	0,940	0,888	0,93
	Φ_{γ_2}	0,960	0,920	—
	Φ_{γ_3}	0,997	0,983	1,00
Al—Sn—Mg	Φ_{γ_1}	0,916	0,954	0,96
	Φ_{γ_2}	0,932	0,951	—
	Φ_{γ_3}	0,967	1,003	1,00
Al—Pb—Mg	Φ_{γ_1}	0,878	0,874	0,91
	Φ_{γ_2}	0,897	0,851	—
	Φ_{γ_3}	0,929	0,872	0,94

$$G_m P_m = \sum_i P_{\gamma_{im}} \left(1 - \sum_n F_{im}\varphi_{mn}\right) G_m + \sum_n \sum_i P_{\gamma_{in}} \varphi_{nm} F_{in} G_n,$$

where $G_{m,n}P\nu_{im,n}$ is the absorbed energy in the m-th and n-th elements from the i-th group of the γ-ray energy spectrum corresponding to the condition of electronic equilibrium in the system; G_mP_m is absorbed energy in the m-th element corresponding to the final distribution; $G_{m,n}$ is the mass of the element at a height of 1 cm, the index n referring to elements of a system mixed with m elements; and $F_{m,n}$ is the fraction of absorbed energy P_γ removed from each of the system by electrons. The exposure factors φ_{mn} and φ_{nm} were used to calculate it [1].

One of the basic conditions for employing the technique presented above is that of reliably determining the mean electron energy $\bar{E}_e$ of electrons knocked out by γ rays with an energy of $\bar{E}_\gamma$.

Two series of calculations were made: using the approximate relation $\bar{E}_l \approx 1/2\bar{E}_\gamma$ and using secondary-electron spectra calculated by the Monte Carlo technique for the initial γ-ray spectra. As a characteristic measure of the deviation from the condition of electronic equilibrium we chose the value $K = K_2/K_1$, where K_1 is the ratio of the power of the absorbed dose of γ rays for the middle and internal cylinders under conditions of electronic equilibrium, and K_2 is the analogous ratio with allowance for the redistribution of the γ-ray energy because of knock-out electrons (Table 1).

The γ-ray spectra are arranged in Table 1 in order of increasing hardness. The experimental verification was carried out with a calorimetric spectrometer [2]. For all systems, as the hardness of the γ-ray spectrum increases, the deviation from the condition of electronic equilibrium decreases. The greater the Z of the material of the middle cylinder, the greater the deviation from the condition of electronic equilibrium reaching 12%; this must be taken into account when evaluating the error of the radiation detectors and when transferring the dose from the detector to the irradiated object.

It has been established that the γ-ray energy is redistributed by the resulting energy transfer by electrons knocked out of the materials with a high atomic number to materials with a low atomic number. Photoelectrons make an overwhelming contribution to this transfer.

LITERATURE CITED

1. R. Richards and B. Rubin, Nucleonics, 6, 42 (1950).
2. B. A. Briskman et al., At. Energ., 41, 325 (1976).

Original article submitted April 14, 1976.

ERRATA

In the paper by Yu. P. Abolmasov, "Tritium content in liquid media and in air of working locations of nuclear power stations," 41, No. 3, 845 (1976), line 1 of Table 1 should read "Q, μCi/liter."

LETTERS

CONDITIONS FOR PRODUCING NONUNIFORM FIELDS IN NUCLEAR REACTORS

A. M. Zagrebaev and V. I. Naumov

UDC 621.039.51

Consideration is being given to the possibility of zone variation of power in high-power reactors of the RBMK type; this could be used in operation at partial load, in transient operating conditions, during fuel recharging, in some accident situations, etc. [1]. From technical considerations it might be desirable for the transition region between zones of different power to be a minimum. A simple evaluation of the dimensions of the transition region under concrete specified conditions can be obtained in the one-dimensional one-group approximation for a homogenized reactor. Suppose that a reactor with uniform breeding properties contains two zones, in which the neutron flux density is kept at different levels φ_0 and $\alpha\varphi_0$ (where $\alpha < 1$) by control systems, and a transition region between them. The distribution of the neutron flux densities is uniform in the zones. The equation for the neutron flux density in the transition region is of the form

$$d^2\varphi/dx^2 + \varkappa^2\varphi(x) + u(x)\varphi(x) = 0 \tag{1}$$

with the boundary conditions

$$\varphi(0) = \varphi_0; \quad \varphi'(0) = 0; \quad \varphi(H) = \alpha\varphi_0; \quad \varphi'(H) = 0, \tag{2}$$

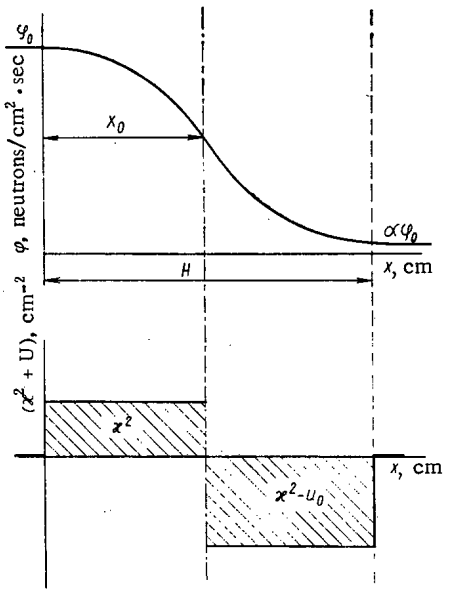

Fig. 1

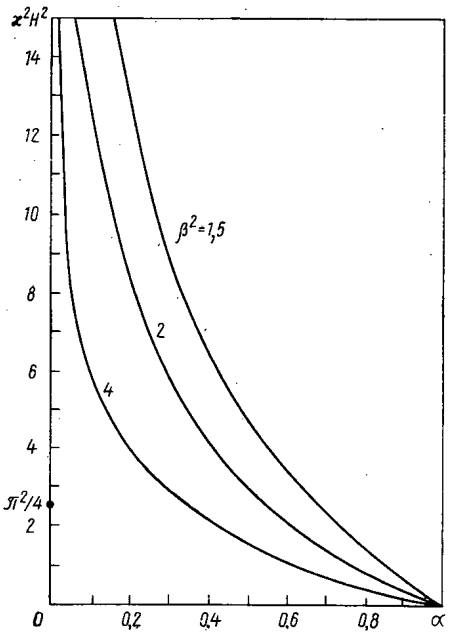

Fig. 2

Fig. 1. Distribution of neutron flux density and control in the transition angle.

Fig. 2. The excess multiplication factor in the transition region vs the drop in neutron flux density at various values of β^2.

Translated from Atomnaya Énergiya, Vol. 42, No. 2, pp. 128-129, February, 1977. Original article submitted February 20, 1976.

where u(x) is the function (control) being varied, such as a quantity proportional to the variable macroscopic cross section for absorption introduced during control and $\varkappa^2$ is the material parameter.

The introduction of control is assumed not to change the diffusion coefficient. The size H of the transition region is minimized with the following constraints on the equation:

$$-u_0 \leqslant u(x) \leqslant 0.$$

Applying the Pontryagin maximum principle [2], we can show that in the given problem, which belongs to the class of problems in speed of response, the optimal types of control are those which lie on the boundary of the region of allowable controls, and the composition of two subregions with controls u = 0 and $u = -u_0$ (Fig. 1) is optimal. Then Eq. (1) for the first and second subregion, respectively, is of the form

$$d^2\varphi_1/dx^2 + \varkappa^2\varphi_1 = 0; \tag{3}$$

$$d^2\varphi_2/dx^2 + \varkappa^2\varphi_2 - u_0\varphi_2 = 0. \tag{4}$$

The "joining" conditions for the neutron flux density and the neutron current density at the subregion boundary are

$$\varphi_1(x_0) = \varphi_2(x_0); \tag{5}$$

$$\varphi_1'|_{x=x_0} = \varphi_2'|_{x=x_0}. \tag{6}$$

Solving Eqs. (3) and (4) with conditions (2), (5), and (6), we get an expression for the minimum dimension of the transition region:

$$H = \varkappa^{-1}\{\arcsin\beta^{-1}[(\beta^2-1)(1-\alpha^2)]^{1/2} + (\beta^2-1)^{-1/2}\operatorname{arsh}(\alpha\beta)^{-1}(1-\alpha^2)^{1/2}\},$$

where $\beta^2 = u_0\varkappa^{-2} > 1$ is the maximum control expressed in units of the material parameter. Hence, the excess multiplication factor necessary for producing such a region

$$\Delta k = k_\infty - 1 = (H/M)^{-2}\{\arcsin\beta^{-1}[(\beta^2-1)(1-\alpha^2)]^{1/2} + (\beta^2-1)^{-1/2}\operatorname{arsh}[(1-\alpha)^{1/2}/\alpha\beta]\}^2,$$

where H/M is the dimension of the transition region, expressed in migration lengths. Figure 2 plots the dependence of $\varkappa^2H^2 = \Delta k\,(H/M)^2$ on the ratio of fluxes at the boundaries of the transition region α with maximum control β^2. It is seen from Fig. 2 that to produce a transition region of a specified size it is necessary to have an excess multiplication factor and the greater the planned power loss at the boundaries of the transition and the smaller the region size, the greater that factor should be. From physical considerations it is clear that the maximum drop $\alpha = 0$ is possible only with an infinitely large β^2, and with $\varkappa^2H^2 = \pi^2/4$.

Let us evaluate the excess multiplication coefficient required for creating zones with different power levels in a concrete example. Let us determine the excess multiplication factor required for producing zones with powers differing by 50% ($\alpha = 0.5$) at a given value of the maximum control ($\beta^2 = 2$) and given transition region size ($H/M \geq 10$). It is seen from Fig. 2 that in this case $\varkappa^2H^2 \approx 3$ or $k_\infty - 1 \approx 3(H/M)^{-2} = 0.03$.

Thus, to vary the power of the zones within given limits it is necessary to have an excess multiplication factor corresponding to $\Delta k = 3\%$ in the transition region. With these conditions for creating a large power drop, say, a 90% drop (i.e., $\alpha = 0.1$), we must have $\Delta k = 12\%$.

The authors wish to thank L. N. Yurovii and V. I. Savander for a useful discussion and comments.

LITERATURE CITED

1. N. A. Dollezhal' et al., in: Experience in Operating Atomic Power Plants and Further Development of the Atomic Power Industry [in Russian], Vol. II, Izd. FÉI (1974), p. 233.
2. A. F. Rudik, Nuclear Reactors and the Pontryagin Maximum Principle [in Russian], Atomizdat, Moscow (1971).

STATISTICAL REGULARIZATION METHOD FOR ESTABLISHING FAST-NEUTRON ENERGY SPECTRA ACCORDING TO READING OF ACTIVATION THRESHOLD DETECTORS

V. E. Aleinikov, V. P. Bamblevskii, and M. M. Komochkov

UDC 539.125.164

Establishing fast-neutron spectra (E) according to the results of radioactivity measurements by threshold detectors [1, 2] reduces to solving Fredholm integral equations of the first kind:

$$A_j + \varepsilon_j = \int_0^\infty \varphi(E)\,\sigma_j(E)\,dE, \qquad j = 1, 2, \ldots, n,$$

where A_j is the rate of activation of the j-th threshold detector, per isotope nucleus; σ_j is the cross section for the activation of the j-th threshold detector; ε_j is the total error due primarily to errors in determining the absolute activity and the activation cross sections for the j-th threshold detector; E is the neutron energy; and n is the number of threshold detectors.

In the methods hitherto used to determine $\varphi(E)$ with threshold detectors (e.g., [1, 2]) the equation given above (in which ε_j is zero, i.e., A_j is used to be an exact quantity) is solved. These methods are based, as a rule, on highly artificial a priori information about the form of the spectrum sought and, therefore, have a limited range of application and, moreover, the solution is often oscillatory. The concept of the random character of measured quantities within a general approach to the solution of incorrect problems, developed by A. N. Tikhonov [3], led to the so-called method of statistical regularization [4-7] (MSR). The principal advantages of this method are: the natural character of the a priori information, related to the statistical nature of the measured quantities and the smoothness of the solution sought, the possibility of determining the error of establishing the desired function, and rigorous mathematical proof.

The purpose of the present paper is to verify the effectiveness of employing MSR to establish neutron spectra according to the readings of threshold detectors as well as to measure the spectrum of fast neutrons in the beam of the IBR-30 reactor.

In establishing the spectra, use was made of a program written in FORTRAN which did not essentially differ from the program given in [8]. The calculations were performed on an SDS-6200 computer. The machine computation time for establishing one spectrum depends on the number of detectors; this time was 2 and 7 sec for establishing a spectrum with four and nine detectors, respectively.

TABLE 1. Set of Threshold Reactions Used

№	Reaction	№	Reaction
1	$^{27}Al\,(n, \alpha)\,^{24}Na$	7	$^{59}Co\,(n, \alpha)\,^{56}Mn$
2	$^{24}Mg\,(n, p)\,^{24}Na$	8	$^{31}P\,(n, p)\,^{31}Si$
3	$^{58}Ni\,(n, p)\,^{58}Co$	9	$^{27}Al\,(n, p)\,^{27}Mg$
4	$^{115}In\,(n, n')\,^{115m}In$	10	$^{54}Fe\,(n, p)\,^{54}Mn$
5	$^{32}S\,(n, p)\,^{32}P$	11	$^{56}Fe\,(n, p)\,^{56}Mn$
6	$^{127}I\,(n, 2n)\,^{126}T$		

Translated from Atomnaya Énergiya, Vol. 42, No. 2, pp. 129-131, February, 1977. Original article submitted March 29, 1976.

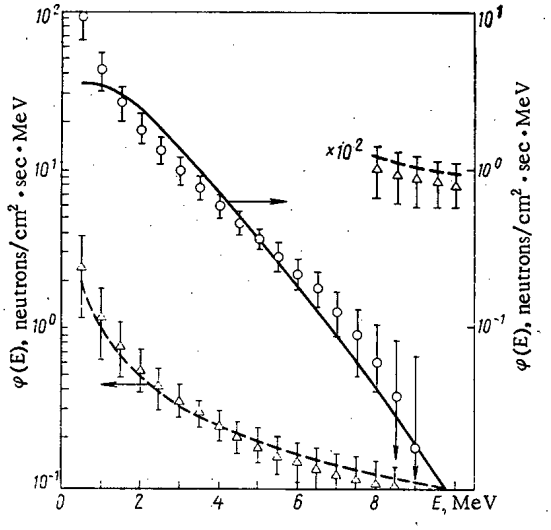

Fig. 1

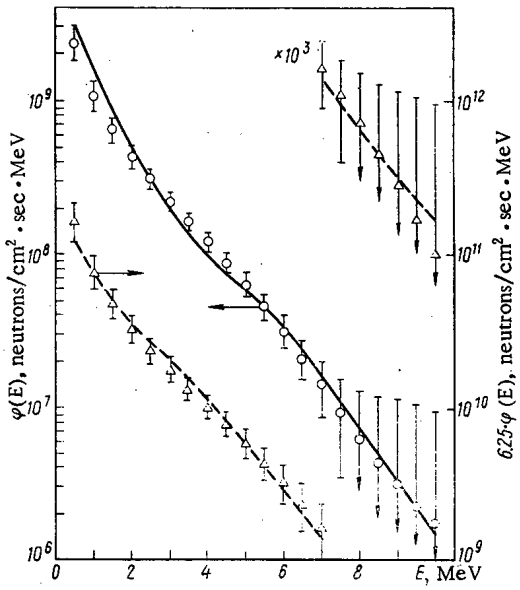

Fig. 2

Fig. 1. Results of establishing test spectra according to reactions 1-4 (see Table 1): ----) spectrum 1/E; ——) fission-neutron spectrum; ○ and △) spectra established by MSR.

Fig. 2. Energy spectra of neutrons from reactors: ——) BR-5 [11], ----) APFA-III [12]; ○ and △) MSR, reactions 1-5; 8-11, and 1-4, respectively.

Control calculations were carried out to check the program and the applicability of MSR in establishing neutron spectra with threshold detectors. In these calculations the activation rate A_j was calculated from given (test) spectra and known activation cross sections, the error ε_j was assigned, and the equation given above was solved. The functions $\varphi(E)$ so established were compared with the test functions. Test spectra, and later actual spectra, were established in the energy range 0.5-10 MeV with a uniform subdivision of 0.5 MeV. The data on the activation cross section were taken from [9]. The following functions were considered as test spectra: $\varphi(E) = \text{const}$; $\varphi(E) = 1 - 0.057\,E$; $\varphi(E) = \exp(-0.511E)$; and $\varphi(E) = 1/E$. The fission-neutron spectrum determined by the Cranberg formula [10] is of the form $\varphi(E) = 0.4527\ \mathrm{sh}\sqrt{2.29E}\ \exp(-0.965\,E)$.

The number of detectors varied from four to ten; the threshold reactions and their numbering are listed in Table 1. The error was varied in random fashion over the interval

$$6\% \leqslant \frac{\varepsilon_j}{A_j}\,100\% \leqslant 21\% \quad \text{and} \quad \left(\overline{\frac{\varepsilon_j}{A_j}\,100\%}\right) = 12\%.$$

Analysis of the results shows that, within the limits of error, the spectra established coincide with the test spectra practically over the entire energy interval. Some results of control calculations are given in Fig. 1. It can be concluded that when 5-6 threshold reactions are employed, the method of statistical regularization enables fast-neutron spectra to be established quite reliably. Increasing the number of detectors does not always significantly improve the results and may lead to only a slight decrease in the error. Proper evaluation of the error ε_j in the equation employed seems to be essential. To establish neutron spectra more reliably in the energy range from tenths of a MeV to 1 MeV, in addition to ^{115}In(n, n') use must be made of other reactions with a low energy threshold, such as ^{103}R(n, n') and ^{237}Np(n, f).

To compare MSR with other methods, actual spectra were established (Fig. 2) in accordance with the experimental data of [11, 12]. It should be noted that a set of 14 and 12 threshold detectors, respectively, was used in the papers cited.

Figure 3 presents the fast-neutron spectrum of the IBR-30 reactor [13]. Comparison of the integrated energy densities of the neutron fluxes in the intervals 1.4-2.8 and 2.8-10 MeV according to the data of the present paper and [13] reveals good agreement. The detectors were irradiated at the 10-m base of IBR-30 beam No. 6 with the following reactor operating mode: power 15 kW, pulse frequency 5 Hz, moderator 40 mm water.

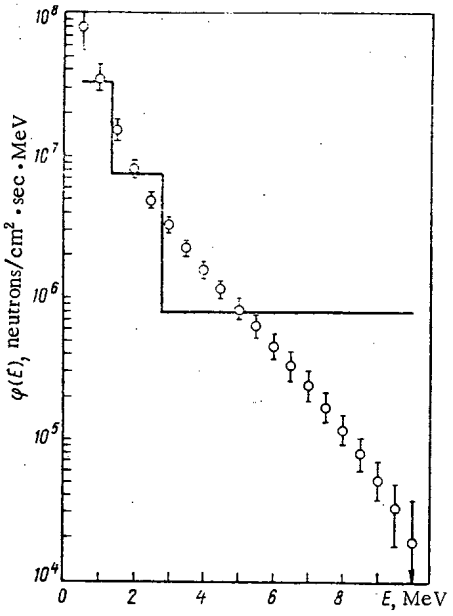

Fig. 3. Energy spectrum of fast neutrons of IBR-30 reactor; ○) spectrum established according to reactions 1-7 by MSR; ——) according to data of [13].

The authors thanks to A. K. Utkin and V. P. Gerdt for their assistance in the work and E. A. Kramer-Ageev and V. S. Troshin for a useful discussion.

LITERATURE CITED

1. S. S. Lomakin, V. I. Petrov, and P. S. Samoilov, Neutron Radiometry by the Activation Method [in Russian], Atomizdat, Moscow (1975).
2. A. A. Lapenas, Measurement of Neutron Spectra by the Activation Method [in Russian], Éinatne, Riga (1975).
3. A. N. Tikhonov, Dokl. Akad. Nauk SSSR, 151, No. 3, 501 (1963).
4. V. F. Turchin, Zh. Vychisl. Mat. Mat. Fiz., 7, No. 6, 1270 (1967).
5. Ibid., 8, No. 1, 230 (1968).
6. V. F. Turchin and V. Z. Nozik, Izv. Akad. Nauk SSSR, Fiz. Atm. Okean., No. 5, 29 (1969).
7. V. F. Turchin et al., Usp. Fiz. Nauk, No. 102, Issue 3, 345 (1970).
8. L. S. Turovtseva, IMP Preprint, Moscow (1975).
9. A. Schett et al., Compilation of Threshold Reaction Cross Sections for Neutron Dosimetry and Other Applications, NDCC, Saclay (1974).
10. L. Cranberg et al., Phys. Rev., 103, 662 (1956).
11. V. V. Bolyatko et al., in: Problems of Dosimetry and Radiation Shielding [in Russian], No. 12, Atomizdat, Moscow (1971), p. 138.
12. W. McElroy et al., Nucl. Sci, and Eng., 48, 51 (1972).
13. V. V. Golikov et al., JINR Report 3-5736, Dubna (1971).

ELECTROCHEMICAL PREPARATION OF SINGLE CRYSTALS OF $^{235}UO_2$

V. O. Kordyukevich, V. I. Kuznetsov, Yu. D. Otstavnov, and N. N. Smirnov

UDC 541.135.3

At the Scientific-Research Institute of Nuclear Physics of Moscow State University, experiments have recently been performed to determine the lifetimes of excited compound nuclei formed in fission reactions $^{238}U + n$ for neutron energies of 1.7-5 MeV [1, 2]. The target was a single crystal of UO_2 with natural uranium-isotope composition, i.e., the experimenters determined the lifetime of the compound nucleus ^{239}U formed by the reaction $U^{238}U_{92} + {}^1n_0$. To study the properties of the compound nucleus ^{236}U they needed a single crystal of UO_2 with maximum possible enrichment with ^{235}U.

There are various methods for obtaining single crystals of UO_2 – sublimation [3], zone melting [4], chemical transport reactions [5], etc. [6-9]. One of the most convenient methods of obtaining the crystalline

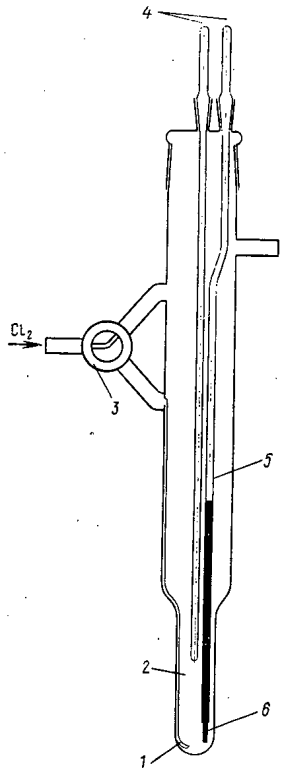

Fig. 1. Quartz electrolytic cell. 1) Tube for for passing chlorine through melt; 2) cathode; 3) tap for switching chlorine supply between chlorination and electrolysis; 4) platinum current leads; 5) anode jacket (Pyrex glass); 6) anode.

Translated from Atomnaya Énergiya, Vol. 42, No. 2, pp. 131-133, February, 1977. Original article submitted April 1, 1976.

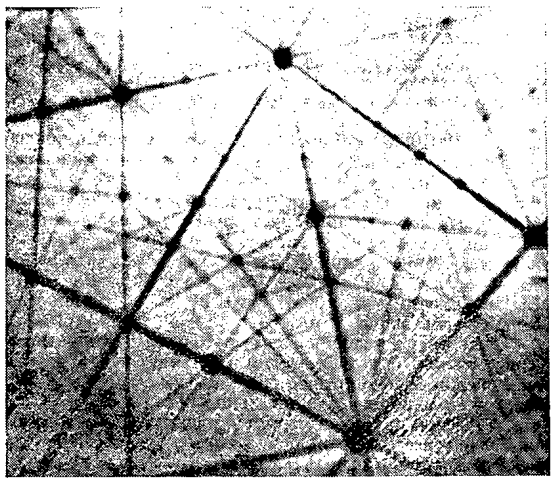

Fig. 2. Part of druse of single crystals of UO_2 (×6).

Fig. 3. Protonogram of single crystal of $^{235}UO_2$ with $E_p = 600$ keV.

dioxide is electrolysis from chloride melts containing uranyl ions [10-12]. This method requires large amounts of uranium (100-200 g in terms of UO_2).

In this article we shall study the electrochemical preparation of UO_2 from small amounts of ^{235}U (25-40 g in terms of UO_2), i.e., in small volumes of fused electrolyte, in conditions involving spatial hindrance to the growing front of the single crystals.

In a physical experiment, the following requirements are imposed on the quality of the crystals: maximum possible structural perfection of the crystal; absence of mosaicity; dimension of perfect crystallographic planes not less than 3 × 3 mm.

Single crystals of UO_2 were obtained by electrolysis on a cathode made of fused uranyl chloride (25 mass %) in $2KCl-PbCl_2$ (replacement of the $PbCl_2$ or lithium chloride leads to marked corrosion of the electrolytic cell). The total volume of melt was about 30 cm^3. The cathode was the end of a platinum wire, 0.5 mm in diameter, fused into glass, and the anode was of spectrally pure graphite.

The electrolytic cell was a specially constructed sealed quartz vessel (Fig. 1), which, without breaking the seal on the system, enabled us to chlorinate the powdered UO_2 (the original raw material of the uranium) to UO_2Cl_2 and to electrolytically produce monocrystalline UO_2.

The cell was heated in an electrical resistance furnace (TEP-1) containing a quartz vessel with fused $LiCl-KCl$ which served as the heating medium for the electrolytic cell. This permitted us to obtain uniform heating of the working surface of the cell. The temperature was kept constant during growth of the single crystals by stabilizing the current through the heating elements. The temperature fluctuations did not exceed 0.1°C/h. The temperature was measured by a Chromel-Alumel thermocouple immersed in the LiCl-KCl melt in a quartz sheath.

Uranyl chloride was obtained directly in the electrolytic cell by passing a current of dry chlorine at 0.5 liters/min through the melt at 650°C for 6-7 h. In the electrolysis mode we kept the melt temperature at 520°C; the excess pressure of chlorine was 500 mm H_2O; and the chlorine flow rate (above the melt) was 0.05 liter/min.

In determining the optimum conditions for electrolytic preparation of single crystals of UO_2, we took account of the following circumstances.

It is known that a factor permitting the formation of high-quality single crystals of UO_2 is that electrolysis shall occur with a low current density, at a high melt temperature, with a large content of uranyl chloride [13]. However, such electrolysis conditions prevent us from obtaining sufficiently large single crystals, because a low current density increases the time of separation of UO_2 so that the uranyl chloride decomposes according to the reaction

$$4UO_2Cl_{2\,melt} \rightleftarrows U_3O_{8\,solid} + UCl_{4\,melt} + 2Cl_{2\,gas},$$

the rate of which increases with temperature and with increasing concentration of uranyl chloride in the melt.

It is also necessary to take account of the interaction of UO_2 with the uranyl chloride melt:

$$2UO_2Cl_{2\,melt} + 2UO_{2\,solid} \rightleftarrows U_3O_{8\,solid} + UCl_{4\,melt},$$

the rate constant of this is quite appreciable above 600°C [14].

Preliminary experiments revealed that control of the cathode potential [15, 16] does not guarantee success in the preparation of high-quality single crystals. It is more effective to conduct the electrolysis with controlled current. For this purpose, in the initial phase of the electrolytic separation of UO_2 we raised the current according to a linear program from zero to 45-50 mA over 7-8 h, and also carried out electrolysis for 45 h. The stabilization system for the direct electrolysis current kept it constant despite large changes in the load resistance.

These initial conditions of the electrolysis current limited the number of single-crystal nuclei. During electrolysis there was a fall in the current density per unit surface area of the growing front of the single crystals, correlated with a decrease in the uranyl chloride concentration in the melt; this was apparently unavoidable when the quantity of the element liberated at the cathode is comparable with the quantity contained in the melt.

The current yield of UO_2 in these electrolysis conditions (5.0 g/A·h) was close to the theoretical value of 5.04 g/A·h, in agreement with the data [16] on the deposition of UO_2 onto the cathode like a metal as a result of direct discharge of the UO_2^{2+} cation at a more positive potential than that of charging of U^{4+} to U^{3+} and its discharge to the metal.

In the separation of UO_2, in which we can neglect the of loss the element in the melt, one of the most important conditions of electrolysis is constancy of the current density at the surface of the crystal growth front. In this case the time dependence of the current will be given by the expression $I = a^3b^3t^2$, where $a = \sqrt[3]{36\pi q^2/d^2}$, where q is the electrochemical equivalent of UO_2 in g/A·h, d is the density of UO_2 in g/cm^3, b is the quantity $B/\sqrt[3]{9}$ where B is the given current density in A/dm^2, and t is the electrolysis time in hours.

Figure 2 is a photograph of part of a druse of single crystals of UO_2 grown at the cathode. We see that the crystals grow preferentially in the crystallographic 100 direction, so that they take the form of a truncated four-sided prism (the side faces are 111 planes and the top is the 100 plane). The individual faces of the crystals are up to 4 × 4 mm in size.

The quality of the crystals and the absence of mosaicity of the structure were determined by protonography with 600-keV protons (Fig. 3). By processing the protonograms we found that the quality of the crystals fully satisfied the requirements of physics experiments.

LITERATURE CITED

1. Yu. Melikov et al., Nucl. Phys., A180, 241 (1970).
2. P. E. Vorotnikov et al., Yad. Fiz., 17, 901 (1973).
3. W. Lierde et al., J. Nucl. Mater., 5, 250 (1962).
4. A. Chapman and W. Clark, J. Am. Ceram. Soc., 48, 494 (1965).
5. K. Naito, N. Kamegashira, and Y. Nomura, J. Cryst. Growth, 8, 219 (1971).
6. S. Nasu, J. Appl. Phys. Jn., 3, 664 (1964).
7. M. Shlechter, J. Nucl. Mater., 28, 228 (1968).
8. T. Sakurai, O. Kamada, and M. Ishigame, J. Crystal Growth, 2, 326 (1968).
9. S. Yajima, H. Furuya, and K. Aoki, Nippon Genshiryoku Gakkaishi, 10, 16 (1968).
10. R. Robins, J. Nucl. Mater., 2, 189 (1960).
11. R. Robins, J. Nucl. Mater., 3, 294 (1961).
12. F. Schott and L. Mudge, J. Nucl. Mater., 9, 245 (1963).
13. A. N. Barabashkin and K. A. Kaliev, At. Energ., 25, No. 3, 193 (1968).
14. M. V. Smirnov, V. E. Komarov, and A. P. Koryushkin, At. Energ., 22, No. 1, 30 (1967).
15. M. V. Smirnov and O. V. Skiba, Tr. Inst. Elektrokhim., Nauk SSSR, Ural. Fil., 4, 3 (1963).
16. Ibid., p. 17.

PRECIPITATION OF MOLYBDENUM DURING EVAPORATION OF NITRATE SOLUTIONS

Yu. P. Zhirnov, E. P. Efremov,
M. I. Zhikharev, and A. N. Efimov

UDC 621.039.733

To reduce the volume of solutions requiring storage or solidification, highly active aqueous nitrate solutions (raffinates) from the extraction treatment of irradiated fuel elements are evaporated [1-3]. It is known [4, 5] that evaporation of nitrate raffinates forms precipitates of poorly soluble substances, and this limits the degree of concentration, forms scale, increases corrosion, and clogs pipes with the precipitates. Thus it is important to investigate the conditions for the formation of precipitates during evaporation.

In this article we give the results of a study of the conditions for precipitation of molybdenum compounds.

It has been suggested [4, 5] that during evaporation of highly active nitrate raffinates, molybdenum is precipitated in the form of the trioxide and cesium phosphomolybdate. Since the exact composition of the precipitatesis unknown, data on the solubilities of various hydrates of molybdenum trioxide [6-9] cannot yet help us to make precise estimates of the behavior of molybdenum during evaporation of raffinates.

In principle, the method of investigation reproduced the process of industrial concentration. The evaporation apparatus (made of quartz glass) was described by us in [10].

Into the apparatus we poured 150 ml of a solution of given* composition and heated it to boiling at atmospheric pressure. After the appearance of the first drops of condensate we started a continuous feed of solution. The rate of evaporation was 150 ± 10 ml/h. The feed solution contained molybdenum at known concentration (0.5-1.5 g/liter) and nitric acid at a concentration equal to that of the acid in the equilibrium vapor above the solution. Thus during the experiment the composition of the solution remained constant (to within ±10%) but the molybdenum concentration in it gradually increased. The experiment was terminated when a precipitate appeared in the solution. We also performed two parallel experiments with solution feed rates 5% greater and 5% less than in the original principal experiment. In the first parallel experiment no precipitate came down; in the second there was a precipitate which did not redissolve after prolonged boiling of the solution (for up to 6 h), and thus the principal experiment was regarded as correct, i.e., as representing equilibrium between the solution and the molybdenum in the precipitate. From the volume of the evaporated feed solution we calculated the molybdenum concentration in the solution of given composition at which the precipitate starts to come down.

As reagents we used 55-77% nitric acid, analytical reagent grade metal nitrates, and solutions of molybdenum nitrate obtained by dissolving the powdered metal in 2 M and 8 M HNO_3, kept for not more than two weeks, and carefully filtered.

From the results we plotted the molybdenum concentration at which a precipitate begins to appear vs the acidity of the solution and the amount of nitrates present (Fig. 1). We see that experimental curve 1 is similar in shape to the 100°C solubility isotherms of hydrated molybdenum trioxides dissolved in HNO_3. The ascending part of curve 1 practically coincides with the data on the solubility of $MoO_3 \cdot 0.5\ H_2O$ [6], while the descending part is similar† to the data on the solubility of $MoO_3 \cdot H_2O$ [7]. This strongly suggests that when we evaporate nitrate solutions containing molybdenum, $MoO_3 \cdot 0.5\ H_2O$ is precipitated if the HNO_3 concentration in

*The solutions were prepared from weighed amounts of the reagents.

†The more appreciable deviation from the data in [7] is apparently due to the fact that in the descending part of curve 1 the boiling points of the solutions were above 100°C (up to 112°C).

Translated from Atomnaya Énergiya, Vol. 42, No. 2, pp. 133-134, February, 1977. Original article submitted September 1, 1976.

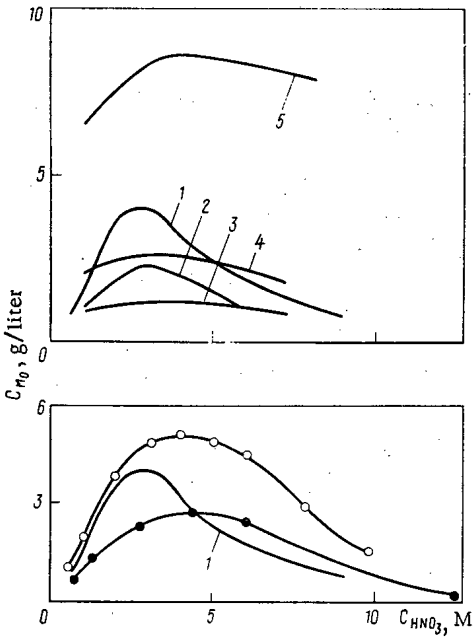

Fig. 1. Molybdenum concentration at which precipitate begins to come down vs composition of solution. 1) Solution with no salts; 2) solution containing 4.2 M $NaNO_3$; 3) 2 M $Al(NO_3)_3$; 4) 0.15 M $Ce(NO_3)_3$; 5) 1 M $Fe(NO_3)_3$; ○, ●) solubilities of $MoO_3 \cdot 0.5\ H_2O$ [6] and $MoO_3 \cdot H_2O$ [7] at 100°C.

the solution is less than about 3 M, but $MoO_3 \cdot H_2O$ is precipitated if the HNO_3 concentration in the solution is greater than about 3 M.

According to Jones [11], at nitric acid concentrations corresponding to the ascending part of curve 1 molybdenum is found in solution in the cationic form, but in the region of the descending part it is found in the anionic form. Therefore we should expect that metal nitrates could increase the solubility of molybdenum by forming complexes with the anionic forms, but reduce it by salting-out the cationic forms or by forming less soluble molybdates. Curves 2-5 agree with this hypothesis: The salting-out action of aluminum nitrate is stronger than that of sodium nitrate, while the complex-forming capacity is greatest in ferric nitrate, in agreement with the general properties of these cations. When solutions of sodium nitrate in nitric acid containing molybdenum are evaporated, the hydrates $MoO_3 \cdot 0.5\ H_2O$ and $MoO_3 \cdot H_2O$ will be precipitated, just as when sodium nitrate is absent. In the evaporation of solutions of aluminum, cerium (III) and iron (III) nitrates, other molybdenum compounds can be precipitated – e.g., molybdates and heteropolyacids.

LITERATURE CITED

1. In: Processing Fuel for Power Reactors [in Russian], Atomizdat, Moscow (1972).
2. Wastes from the Nuclear Power Industry [in Russian], Gosatomizdat, Moscow (1963).
3. In: Proc. Symp. on the Management of Radioactive Wastes from Fuel Reprocessing, OECD, Paris (1973).
4. D. Clelland, in: Proc. IAEA Symp. Treatment and Storage of High-Level Radioactive Wastes, Vienna (1963), p. 63.
5. P. Fangaras and T. Kikinday, Ibid., p. 119.
6. S. P. Vorob'ev and I. P. Davydov, Zh. Neorg. Khim., 11, 2031 (1966).
7. G. A. Meerson and V. G. Mikhailova, Zh. Neorg. Khim., 12, 1615 (1967).
8. L. Ferris, J. Chem. Eng. Data, 6, 600 (1961).
9. O. N. Krasnobaeva and I. N. Lepeshkov, Zh. Neorg. Khim., 17, 2855 (1972).
10. A. N. Efimov, M. I. Zhikharev, and Yu. P. Zhirnov, Radiokhimiya, 12, 766 (1970).
11. M. Jones, J. Am. Chem. Soc., 76, 4233 (1954).

BEHAVIOR OF EUROPIUM OXIDE IRRADIATED IN A FAST REACTOR

T. M. Guseva, V. R. Zolotukhin,
V. K. Nevorotin, S. A. Kuznetsov,
and V. V. Chësanov

UDC 621.039.54

Europium oxide is a promising absorbing material for control rods in fast reactors, owing to its valuable properties:

1. High capture cross section for fast neutrons. The efficiency of unit volume of europium oxide is only 3-4 times less than that of boron carbide with 80% enrichment with ^{10}B, and is equivalent to boron carbide with the natural contents of ^{10}B and ^{11}B [1].

2. High chemical stability.

3. No gas emission during irradiation (unlike boron compounds).

4. Efficiency is retained during prolonged irradiation owing to the formation of isotopes with large neutron capture cross sections.

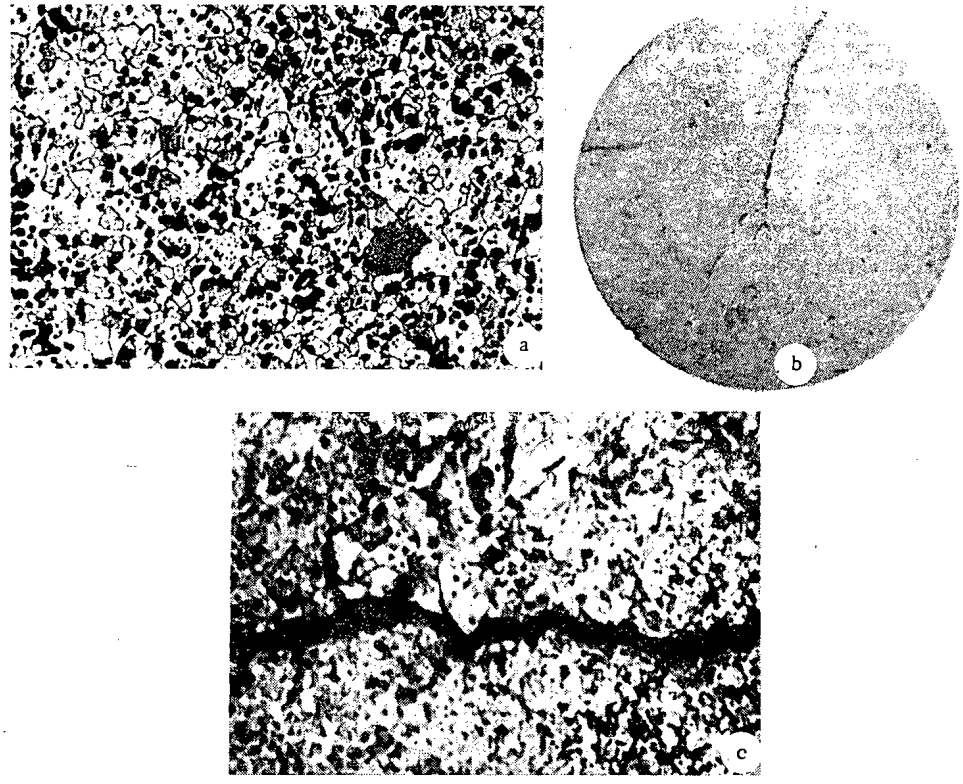

Fig. 1. Structure of europium oxide specimen No. 1: a) before irradiation (×200); b, c) after irradiation (×5; ×200).

Translated from Atomnaya Energiya, Vol. 42, No. 2, pp. 135-136, February, 1977. Original article submitted April 5, 1976; revision submitted September 14, 1976.

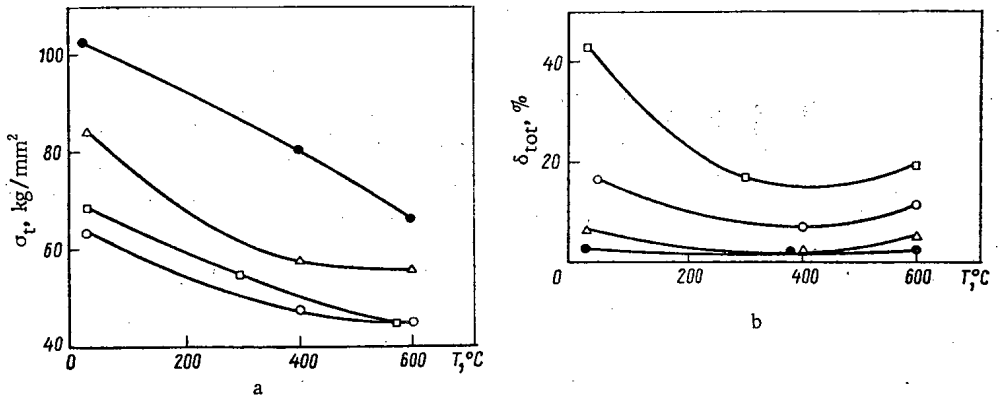

Fig. 2. Tensile strength (a) and relative elongation (b) of steel Kh16N15M3B vs test temperature. □) Unirradiated specimen; ○, △, ●) irradiated at 530, 450, and 370°C: nvt = $0.85 \cdot 10^{22}$, $27 \cdot 10^{22}$, and $4.7 \cdot 10^{22}$ neutrons/cm^2, respectively.

The extensive use of europium oxide for controlling fast reactors is being held up by the lack of information on its radiation behavior. There are only a few results known on the irradiation of europium in thermal reactors by fluences of $1.9 \cdot 10^{21}$ or 10^{22} neutrons/cm^2 at 150°C [2] or 350-600°C [3].

In this connection we investigated europium oxide after irradiation in a BOR-60 fast reactor.

The original europium oxide, with a density of 7.0-7.2 g/cm^3, had a mainly monoclinic structure, though some of the specimens also contained a cubic phase. Specimens in the form of tablets, 10.95 mm in diameter and 10 mm deep, were sealed in cans, 12 mm in diameter and 0.4 mm thick, Kh16N15M3B stainless steel.

Specimens Nos. 1, 2, and 3 were irradiated with fluences of $4.7 \cdot 10^{22}$, $2.7 \cdot 10^{22}$, and $0.85 \cdot 10^{22}$ neutrons/cm^2, respectively. The burn-up of ^{151}Eu was ^{153}Eu was 3.8%.

The energy emissions due to absorption of γ quanta from the core and of the reaction products of neutron absorption were 85, 54, and 31 W/cm^3 for specimens Nos. 1, 2, and 3, respectively. The calculated surface temperature of the specimens was 630°C. The difference between the surface and central temperatures was 210°C for No. 1, 135°C for No. 2, and 75°C for No. 3.

After irradiation in the reactor the specimens were examined by remote handling in "hot" chambers. They retained their geometrical integrity; there were no superficial defects.

The diameters of specimen Nos. 1, 2, and 3 increased by 1.2%, 0.5%, and 0.2% respectively.

Metallographic analysis revealed radial crooks in specimens Nos. 1 and 2, due to the marked temperature differences (Fig. 1b). There were no marked changes in the microstructure of the europium oxide, which was characterized by marked porosity (Figs. 1a and c).

X-ray structural investigations of the specimens irradiated with fluences of $4.7 \cdot 10^{22}$ and $0.85 \cdot 10^{22}$ neutrons/cm^2 revealed that the unit cell parameters of the cubic and monoclinic europium oxide were not altered. Irradiation reduces the intensity of the x-ray reflections and increases the diffuse background.

The compressive strength of the specimens was increased by irradiation from 25 to 30 kg/mm^2.

To study the compatibility of europium oxide with stainless steel we made a metallographic analysis of the can material. The calculated temperatures of the cans during irradiation were 370, 450, and 530°C for specimens Nos. 1, 2, and 3, respectively.

There were no appreciable changes in the structure of the cans after irradiation. No visible interaction was detected between the steel and the europium oxide. The mechanical properties of the can material was altered within the permissible limits – more markedly when the specimen was nearer to the central plane of the reactor core (Fig. 2).

LITERATURE CITED

1. V. Orlov et al., Kernenergie, 12, 112 (1969).
2. E. Hoyt, Rep. GEAP-3909 (1962).
3. V. P. Gol'tsev et al., Fourth Geneva Conference, Reports of USSR, No. 49/P/704 (1971).

DETERMINATION OF THE $^{56}Fe(n, p)^{56}Mn$ CROSS SECTION AT 14.8 MeV

Z. A. Ramendik, G. M. Stukov, and V. T. Shchebolev

UDC 539.172.4

The $^{56}Fe(n, p)^{56}Mn$ cross section can serve as a reference value in determining cross section for the interaction of neutrons in the energy range 14-15 MeV with various elements, for measuring the fast neutron flux density, and in activation analysis [1, 2]. It is used also in fission and fusion reactor calculations.

The accuracy of the determination of a cross section in most cases depends on the systematic and random errors in measuring the neutron flux density, the number of nuclei in the sample, the induced activity, and other quantities.

We used a neutron generator based on the $^3T(d, n)^4He$ reaction with a specially constructed target assembly which permitted the determination of the neutron flux density by the method of associated particles, the method of n–α coincidences, and a method based on the knowledge of the cross section for the scattering of neutrons in hydrogen with a total error of ~1% [3].

The foil samples were made of chemically pure iron of nearly natural isotopic composition. The samples were ~80 mg/cm^2 thick. During irradiation the foils were placed at an angle of ~ 8° with the direction of the deuteron beam at a distance of 30-70 mm from the generator target. The error in determining the angle and distance was ~0.1%. The mass, the geometry, and the density of the samples were known to $\leq$ 0.02%.

The irradiation time in each series of measurements was 8-10 h with periodic monitoring of the $^3T(d, n)^4He$ yield by the relative values of the number of associated α particles recorded in time intervals Δt = 1000 sec. A correction to the resulting activity of the sample due to the instability of the neutron flux during the total time of irradiation was introduced if for a maximum change of flux density within an interval Δt of ~1% the arithmetic and logarithmic methods of averaging differed by ~0.07%.

The neutron energy for the center of the detector is E_n = 14.80 MeV. The deviation from this value resulting from the thickness of the target and the geometrical factor varied from −0.11 to +0.02 MeV.

In this range of detector–target distances no corrections were necessary for effects related to the presence of scattered neutrons and the attenuation of the neutron flux in air. The induced activity of the foils

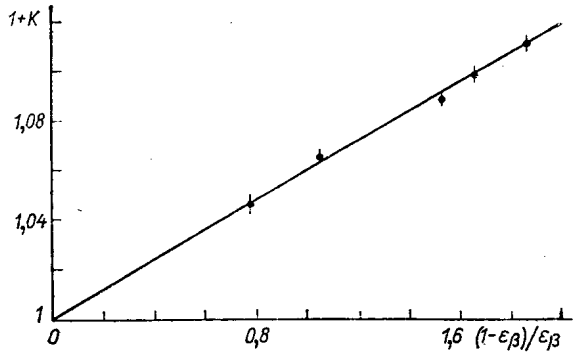

Fig. 1. 1 + K for Mn as a function of $(1 - \varepsilon_\beta)/\varepsilon_\beta$.

Translated from Atomnaya Énergiya, Vol. 42, No. 2, pp. 136-138, February, 1977. Original article submitted April 26, 1976.

TABLE 1. Experimental Values of Efficiency of Recording β Radiation, and Correction Factor

Sample No.	ε_β	$1 + K$
1	0,3767	1,0982
2	0,3817	1,0967
3	0,3825	1,0967

TABLE 2. Analysis of Errors

Source of error	Contrib. to error in determ. cross section	
	systematic	random
Neutron flux density	0,75	0,2
Correction factor K	0,3	—
Meas. of activity	—	0,1
Half-life and irradiation time	0,05	0,05
^{57}Fe + n reaction	0,05	—
Estimate of mean-square error	0,78	0,23

was measured by a low-background $\beta-\gamma$ coincidence system [4], with a $4\pi\beta$ counter [5], and by a BDBS-3-1eM-type γ spectrometer.

The complex decay scheme of ^{56}Mn and the rather high-energy β radiation necessitated the use of a 3-mm-thick copper filter between the foil and the γ counter, and required finding the dependence of the specific activity a on $(1 - \varepsilon_\beta)/\varepsilon_\beta$ where ε_β is the efficiency of the β counter, defined as N_c/N_γ, and N_c and N_γ are the counting rates minus background in the coincidence channel and in the the γ channel respectively.

This dependence was obtained by irradiating five manganese–nickel foils of various thicknesses in the same thermal neutron flux and subsequently measuring their activities with the $\beta-\gamma$ coincidence system. The results, shown in Fig. 1, are approximated by a straight line, from which the true specific activity corresponding to $\varepsilon_\beta = 1$ can be determined. Table 1 lists the values of the β efficiency and the correction factor $(1 + K)$ for the samples of iron used in the experiment.

A least-squares analysis of the experimental results (Fig. 1) gives a mean-square error of 0.3% for K. It should be noted that Axton's [6] calculation of K for ε_β close to unity gives the linear relation $A = f[(1 - \varepsilon_\beta)/\varepsilon_\beta]$. This conclusion was confirmed experimentally in [7]. However, the experimental value [8] of K is close to zero and does not depend on ε_β. We used still another method of determining the form of this relation.

Two manganese–nickel foils of the same thickness ($\varepsilon_{\beta_1} = \varepsilon_{\beta_2}$) were irradiated simultaneously in a standard thermal neutron flux. The activity of each foil $A_1(\varepsilon_{\beta_1})$ and $A_2(\varepsilon_{\beta_2})$ and that of the combination A_{1+2} $(\varepsilon_\beta^{1+2})$ were measured with the $\beta-\gamma$ coincidence system. Assuming that $\varepsilon_\beta^{1+2} \neq \varepsilon_{\beta_1}$, $A_{1+2} \neq A_1 + A_2$. The results showed that this assumption is true, and moreover, within the limits of error, the ratio $A_{1+2}/(A_1 + A_2)$ is equal to the value obtained from the graph for ε_{β_1} and ε_β^{1+2}.

The ^{56}Fe(n, p)^{56}Mn cross section was calculated by using the natural isotopic abundance of ^{56}Fe for the sample (0.9168), and 2.577 h for the half-life of ^{56}Mn. A correction was introduced for the contribution to the activity of the sample from the ^{57}Fe(n, d)^{56}Mn and ^{57}Fe(n, np)^{56}Mn reactions.

Table 2 lists the sources of error and their contribution to the resulting error, taking account of the statistical weight for the confidence coefficient 0.68. Taking for an estimate the linear superposition of the systematic and random errors, for a confidence coefficient of 0.99, we obtain an error of 1.5% for the measured result.

Our measured value of 110.9 ± 1.7 mb for the $^{56}Fe(n, p)^{56}Mn$ cross section for E_n = 14.80 MeV is in satisfactory agreement with the cross section 109.8 ± 2.9 mb for E_n = 14.78 MeV obtained by Robertson et al. [8] who also measured the activity by the $4\pi\beta-\gamma$ coincidence method.

LITERATURE CITED

1. E. Axton et al., Proc IAEA Symp. on Neutron Monitoring Rad. Prot. Purposes, Vol. 2, Vienna (1972), p. 431.
2. J. Robertson et al., J. Nucl. Energy, 27, 531 (1973).
3. V. T. Shchebolev et al., Metrologia No. 11, 65 (1973).
4. O. A. Andreev et al., in: Proc. Metrological Institute of the USSR, No. 145(205), Moscow (1973), p. 33.
5. A. A. Konstantinov and A. E. Kochin, in: Proc. Inst. of the Committee of Standards of Measures and Measuring Devices, No. 59 (129) [in Russian], Standartgiz, Moscow–Leningrad (1962), p. 13.
6. E. Axton, J. Nucl. Energy (Parts A/B), 17, 125 (1963).
7. A. DeVolpi and K. Porges, (ANL) RPD-EPM No. 95 (1968).
8. J. Robertson, B. Audric, and P. Kolkowski, J. Nucl. Energy, 27, 139 (1973).

BOUNDED ESTIMATE OF ABSORBED DOSE USING LINEAR PROGRAMMING

N. G. Volkov, V. K. Lyapidevskii, and Yu. I. Malekhov

UDC 539.1.074:519.83

Most of the nuclear-radiation detectors currently used in dosimetry have "operational inflexibilities" [1]. According to [2, 3], the inflexibility may be reduced by the simultaneous use of several detectors having different spectral sensitivites, the detectors being chosen so that a linear combination of their spectral sensitivities g_i

$$h(E)=\sum_{i=1}^{n} A_i g_i(E) \tag{1}$$

is equal to unity over the whole range of radiation energies. In practice, however, such a choice is impossible, and therefore the problem arises that the estimates of the absorbed dose obtained are not unique.

In [4, 5] a graphical method was proposed for the calculation of upper and lower bounds on the estimate of the absorbed dose in the case of two detectors. However, two detectors cannot always ensure sufficient accuracy in determining the absorbed dose, and it is necessary to use a larger number.

In this case, unfortunately, the graphical method is too unwieldy and moreover does not allow the random and systematic errors in the measured values to be correctly taken into account.

The aim of the present work is to develop and test an algorithm for deriving a bounded estimate using the linear-programming method, taking as an example the calculation of the absorbed dose of γ radiation in some materials of known composition.

The absorbed dose of γ radiation in the material is

$$W^{\gamma}=\Phi_{\gamma}\int_{E_{\min}}^{E_{\max}}\frac{\mu_a(E)}{\rho}E\varphi_{\gamma}(E)\,dE, \tag{2}$$

where Φ_γ is the γ-quantum flux density, quanta/cm^2·sec; E is the γ-quantum energy, eV/quantum; φ_γ is the differential γ-quantum energy spectrum (normalized to unity), quanta/eV; μ_a/ρ is the total mass coefficient of γ-energy absorption, cm^2/g.

Translated from Atomnaya Énergiya, Vol. 42, No. 2, pp. 138-139, February, 1977. Original article submitted April 26, 1976; revision submitted September 3, 1976.

TABLE 1. Estimate of Absorbed γ-Radiation Dose in Materials

Material	Exptl. value [6]	Materials providing data for estimate	Estimate	
			lower bound	upper bound
Pb	1,71	C—Al	1,8	1,64
Zr	1,4	C—Al	3,77	1,4
C	1,43	Fe—Zr	1,66	0,99
Pb	1,71	C—Al—Fe	1,75	1,70
Zr	1,4	C—Al—Fe	1,9	1,4

In [6-8], methods are proposed for determing the absorbed dose in the investigated material from the known absorbed doses in other materials W_i^γ (i = 1, 2, ...). The proposed methods rest on certain assumptions: the use of the mean γ-quantum energy, or an empirical dependence of the effective mass coefficient of γ-energy absorption for the investigated material on the difference in effective mass absorption coefficients of certain selected pairs of heavy materials.

The correct solution of this problem is to find an interval that is sure to contain the true value of the absorbed dose, taking into account the errors in determining the W_i^γ (i = 1, 2, ...).

It is usual to assume that the errors in W_i^γ (i = 1, 2, ...) do not exceed some given positive constant μ^2, characterizing the degree of reliability of the measurements. The error is taken from the norm in a particular metric. For our purposes, it is expedient to use a uniform metric, which allows the most reliable treatment of the errors in the experimental data, and in this metric the norm is given by the expression

$$\| x_i \|_{\Delta_i} = \max [x_i/\Delta_i], \tag{3}$$

where x_i is the quantity being estimated; Δ_i is the error in determining x_i.

In this case, the problem may be formulated mathematically as

$$W_{\min}^\gamma = \min \left\{ \Phi_\gamma \int_{E_{\min}}^{E_{\max}} \frac{\mu_a(E)}{\rho} E\varphi_\gamma(E)\, dE \quad \text{when} \right.$$

$$\left. \| W_i^\gamma - \Phi_\gamma \int_{E_{\min}}^{E_{\max}} \left[\frac{\mu_a(E)}{\rho} \right]_i E\varphi_\gamma(E)\, dE \|_{\Delta_i} \leqslant \mu^2 \right\}, \quad \varphi_j(E) \geqslant 0; \tag{4}$$

$$W_{\max}^\gamma = \max \left\{ \Phi_\gamma \int_{E_{\min}}^{E_{\max}} \frac{\mu_a(E)}{\rho} E\varphi_\gamma(E)\, dE \quad \text{when} \right.$$

$$\left. \| W_i^\gamma - \Phi_\gamma \int_{E_{\min}}^{E_{\max}} \left[\frac{\mu_a(E)}{\rho} \right]_i E\varphi_\gamma(E)\, dE \|_{\Delta_i} \leqslant \mu^2 \right\}, \quad \varphi_j(E) \geqslant 0, \tag{5}$$

where i = 1, 2, ...; $W_{\min}^\gamma$ and $W_{\max}^\gamma$ are respectively the minimum and maximum possible value of W^γ.

In [9] it was shown that Eqs. (4) and (5) are problems of linear programming, and specimen solutions of such problems were given.

A program was written to calculate the absorbed dose for a number of materials. Results obtained using the program are shown in Table 1, where the experimental data are taken from [10]. The estimates were obtained from experimentally known values of the absorbed dose for groups of two and three chosen materials.

The calculated values show that the proposed method of estimating the absorbed dose gives satisfactory results (see Table 1). The bounds of the estimate narrow as the number of experimental data used in the calculation is increased.

As is well known, one method of obtaining more accurate values of the absorbed dose is to determine experimentally the spectral composition of the radiation and hence to calculate the quantities of interest to us.

However, to measure the spectra using a multichannel spectrometer or a cutoff indicator is in many cases a technically complex operation, and the present work indicates that a satisfactory accuracy in determining the absorbed dose can be obtained more simply, by recording the output of a small number of detectors chosen according to their spectral characteristics.

It is simple to introduce a priori information on the spectral composition into the algorithm for the solution of Eqs. (4) and (5), thereby considerably narrowing the bounds on the estimate.

The authors would like to thank P. M. Rubtsov for discussions which were of considerable value in the conception of the present work.

LITERATURE CITED

1. V. I. Ivanov, Course of Dosimetry [in Russian], Atomizdat, Moscow (1970).
2. S. McGuire, Rep. LA-3435, Los Alamos (1965).
3. D. Nachtigall and F. Rohloff, Nucl. Instrum. Methods, No. 50, 137 (1967).
4. N. G. Volkov and V. K. Lyapidevskii, Prib. Tekh. Eksp., No. 5, 86 (1968).
5. H. Ryufuku and T. Nakayma, J. Appl. Phys. Jpn., 8, No. 10, 1142 (1969).
6. Yu. L. Tsoglin, Author's Abstract of Candidate's Dissertation [in Russian], Institute of Nuclear Research, Academy of Sciences of the Ukrainian SSR, Kiev (1975).
7. D. M. Richardson, Proc. First Geneva Conference [in Russian], Vol. 14, Gosatomizdat, Moscow (1956), p. 265.
8. P. Dyne and W. Thurston, CRC-696 (1957).
9. N. G. Volkov, V. K. Lyapidevskii, and Yu. I. Malakhov, Prib. Tekh. Eksp., No. 6 (1976).
10. A. Anderson and D. Linacre, in: Materials of a Symposium on Individual Problems of Dosimetry [in Russian], Gosatomizdat, Moscow (1962), p. 192.

THERMAL-NEUTRON TRANSFER FROM PULSE SOURCE IN MODERATOR WITH LARGE CYLINDRICAL CAVITY

Zh. M. Dzhilkibaev and M. V. Kazarnovskii

UDC 539.125.52:621.039.51.12

The nonsteady transfer of thermal neutrons in a moderator block with a large* cavity has been investigated theoretically for systems with spherical [1, 2] and plane [3] symmetry. However, for reactor physics and also for geometric applications, there is interest in the analogous problem for a moderator with a cylindrical cavity.

In the present work, this problem is considered for the particular case of a weakly absorbing moderator, for which the approach developed in [2] may be used.

Consider a moderator layer between two infinitely long coaxial cylinders of radii R and R + H, in which neutrons are emitted from a pulse source that is homogeneous with respect to the axis of the cylinders. Then, as in the case of spherical symmetry [2], it may be expected that, a certain time after the moment (t = 0) when the source is switched on, a quasisteady neutron distribution will be established in the system, dying away with time according to an approximately exponential law with an effective damping constant λ_0 related to the mean

*The characteristic dimension of the cavity is much larger than the transport free path.

Translated from Atomnaya Énergiya, Vol. 42, No. 2, pp. 139-140, February, 1977. Original article submitted May 19, 1976.

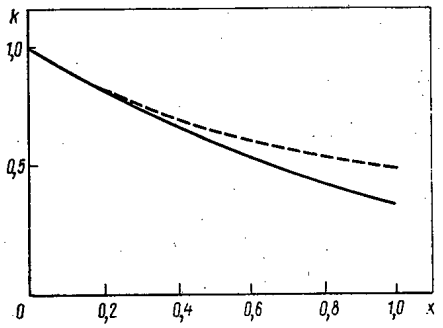

Fig. 1. Dependence of albedo on parameter x.

(over the angles of incidence and emission of the neutrons) albedo k at the internal moderator surface by the equation

$$\frac{1}{k}=\mathrm{Re}\left[\left\langle\exp\left\{\frac{\lambda_0}{v}l(\mathbf{v})\right\}\right\rangle\right].$$

Here v is the neutron velocity; $l(\mathbf{v})$ is the neutron path through the internal cylinder in the direction of v; $\langle\ldots\rangle$ denotes the mean over the neutron-velocity distribution at exit from the moderator.

In the considered case of a weakly absorbing moderator, the spectrum of neutrons leaving the moderator is close to Maxwellian, and their angular distribution is isotropic. The mean over the Maxwellian distribution corresponding to temperature T is of the form

$$\left\langle\exp\left\{\frac{1}{v}\lambda_0 l(\mathbf{v})\right\}\right\rangle=\frac{1}{\langle v\rangle_T}\left\langle vI\left(-\frac{2R\lambda_0}{v}\right)\right\rangle_T,$$

$$I(y)=\frac{2}{\pi}\int_{-1}^{1}d\mu\sqrt{1-\mu^2}\int_{0}^{\pi/2}d\varphi\cos\varphi\exp\left(-y\frac{\cos\varphi}{\sqrt{1-\mu^2}}\right).$$

It may be expected that as $y\to 0$

$$I(y)=1-y+\frac{1}{6}y^2+\frac{1}{8}y^3\left(\ln y+0{,}5772\ldots+\frac{38}{9\pi}-\frac{63}{16}\right)+O(y^4\ln y).$$

Averaging with respect to v gives the result

$$\frac{1}{k}=1+\frac{\sqrt{\pi}}{2}x+\frac{1}{6}x^2+\frac{\sqrt{\pi}}{8}x^3(\ln|x|+0{,}2621\ldots), \qquad (1)$$

where $x = 2R\lambda_0/v_T$; $v_T=\sqrt{2kT/m}$.

This dependence of k on x is shown in Fig. 1 and, for comparison, a graph is given for a spherically symmetric system [2] with $x = (4/3)(R_{sph}\lambda_0/v_T)$, where R_{sph} is the radius of the spherical cavity. This choice of the variable x facilitates the comparison, since in both cases x may then be represented in the same form: $x=\bar{l}\lambda_0/v_T$, where $\bar{l}$ is the mean neutron path in the cavity. For cylindrical geometry, the decrease in k with increase in x is slower, because in this case there is more prolonged damping due to the longer path in the cavity along a direction close to the axis.

Using Eq. (1) the mean albedo of thermal neutrons for a cylindrical cavity may be determined from experimental data on λ_0 for a homogeneous cylindrical layer of moderator and for a multilayer nonincreasing system, for example, the cells of a reactor (without fuel elements).

The following is a theoretical expression for a homogeneous cylindrical layer of moderator obtained in a diffusion approximation

$$k=(1-\varepsilon)/(1+\varepsilon);$$

$$\varepsilon=\sqrt{2\pi}\frac{D_0}{L(\lambda)v_T}\frac{I_1(\rho_1)K_0(\rho_2)-I_0(\rho_2)K_1(\rho_1)}{I_0(\rho_2)K_0(\rho_1)-I_0(\rho_1)K_0(\rho_2)};$$

$$\rho_1=\frac{R}{L(\lambda)};\quad \rho_2=\frac{R+H+z_0}{L(\lambda)};\quad L(\lambda)=L_0/\sqrt{1-\lambda_0'\alpha_0}.$$

Here D_0 is the diffusion coefficient, L_0 the diffusion length, and α_0 the rate of absorption in the inner cylinder with Maxwellian neutron distribution in the moderator; z_0 is the extrapolated length; $I_j(x)$ and $K_j(x)$ are j-th order Bessel functions with imaginary arguments.

LITERATURE CITED

1. K. D. Ilieva and M. V. Kazarnovskii, At. Energ., 35, No. 5, 346 (1973).
2. K. D. Ilieva and M. V. Kazarnovskii, At. Energ., 39, No. 3, 186 (1975).
3. K. D. Ilieva and M. V. Kazarnovskii, At. Energ., 35, No. 5, 347 (1973).

CROSS SECTIONS FOR (n, α_0), (n, α_1), (n, α_2), (n, α_3), AND (n, α_4) REACTIONS IN ^{28}Si AND (n, α_0), (n, α_1) IN ^{29}Si AT A NEUTRON ENERGY OF 14.1 MeV

L. I. Klochkova and B. S. Kovrigin

UDC 539.172.4

The present paper determines the cross sections for the ^{28}Si(n, α) ^{25}Mg and ^{29}Si (n, α) ^{26}Mg reaction at a neutron energy of 14.1 MeV for transitions to the ground and excited states of the residual nucleus.

The energy spectrum of α particles was measured by a lithium-drifted silicon semiconductor detector which was placed in a neutron flux and served as both target and detector at the same time. With this measuring technique, the α-particle peaks of a given spectrum were integrated over the angle of emission of the particles.

The high energy resolution of the semiconductor detector, the use of an appreciable mass of the material under study, as well as the practically 4π geometry of α-particle detection enables results to be obtained with a good accuracy in 15-30 min at a flux of 10^9 neutrons/sec. To obtain similar results by the counter telescope method, the angular distribution of the α particles would have to be measured and the exposure time would be ~300 h.

Neutrons with an energy of 14.1 MeV are obtained from the ^{3}H(d, n)^{4}He reaction in an HF-200 neutron generator. The interaction of neutrons with silicon nuclei of the semiconductor detector produces α particles and protons which are detected by a single-channel spectrometer consisting of the detector, an amplifier, and a pulse-height analyzer.

The lithium-drifted silicon semiconductor detectors used in the work had a sensitive region 260-2800 μ thick. To separate overlapping lines in the spectrum the spectrum was decomposed by using an instrumental line of the α_0 spectrum of the ^{28}Si(n, α_0)^{25}Mg reaction.

The cross section for the (n, α) reaction in the silicon nucleus for an individual transition is given by

$$\sigma = \frac{kAN_\alpha}{f\varphi N_A \rho SHt},$$

where A is the atomic mass of the silicon isotope; N_α is the number of α particles detected in the given peak of the energy spectrum; ρ is the neutron flux density; N_A is the Avogadro number; φ is the density of crystalline silicon; S is the working area of the semiconductor detector; H is the thickness of the sensitive region of the detector; t is the measuring time; f is the fraction of the given isotope in the mixture of the isotopes of the element; k is a correction factor associated with edge effects during the passage of α particles through the detector material.

Translated from Atomnaya Énergiya, Vol. 42, No. 2, p. 141, February, 1977. Original article submitted May 24, 1976.

By calculations it can be shown that the fraction of undetected α particles for a detector with a sensitive layer of thickness H is $\eta = 1/2(x/H)$, where x is the α-particle range in silicon. Then the correction factor is $k = 1/(1 - \eta)$.

The measured energy spectra and the ratio $\sigma = kAN_{\alpha}/(f\varphi N_A \rho SHt)$ were used to find the cross sections for the $^{28}Si(n, \alpha)^{25}Mg$ and $^{29}Si(n, \alpha)^{26}Mg$ reactions when $\varepsilon_n = 14.1$ MeV for transitions to the ground and excited states of the residual nucleus. The cross sections for the α_0, α_1, α_2, α_3, and α_4 spectral lines of the $^{28}Si(n, \alpha)^{25}Mg$ reaction have the following values: 14.3 ± 0.7, 6.6 ± 0.3, 9.0 ± 0.5, 12 ± 1, and 13.8 ± 0.7 mb. Cross sections of 2.4 ± 0.3 and 7.3 ± 0.9 mb have been obtained for the α_0 and α_1 spectral lines of the $^{29}Si(n, \alpha)^{26}Mg$ reaction.

The principal contribution to the error in the cross section is made by the errors of measuring the neutron flux density, the thickness of the sensitive region of the detector, and the procedure of decomposing overlapping peaks.

The values obtained for the cross sections can be used to find the density of the fast monochromatic neutron flux with silicon semiconductor detectors.

ACCELERATING CONVERGENCE IN PERTURBATION-THEORY PROBLEMS FOR NUCLEAR REACTORS

É. G. Sakhnovskii

UDC 621.039.51

For the radial Schrödinger equation [1] describes a perturbation theory in which the wave function is calculated in the m-th approximation to within ε^{2m}, where ε is the perturbation parameter. Convergence can also be similarly accelerated in perturbation-theory problems for the one-group model of nuclear reactors. In contrast to the usual representation of a perturbed neutron flux in the terms series, over the entire spectrum, in the eigenfunctions and eigenvalues of the unperturbed problem, the flux in the m-th approximation is expressed only in terms of functions of the (m − 1)-th approximation and is of a finite form.

Let us consider the one-group diffusion equation for a plane symmetric reactor without reflector, of width 2R:

$$\Phi''(x) + [\alpha_0^2 + \varepsilon\alpha^2(x) - \Delta]\,\Phi(x) = 0 \tag{1}$$

with the boundary conditions $\Phi'(0) = 0$ and $\Phi(R) = 0$. Here, $\varepsilon\alpha^2(x)$ is a given small nonuniform perturbation of the Laplacian $\alpha_0^2 = \text{const}$; $\Delta = \text{const}$ is a compensating factor keeping the critical dimension R of the unperturbed reactor ($\varepsilon = 0$, $\Delta = 0$) unchanged when $\varepsilon \neq 0$.

Assuming that

$$y(x) = \Phi'(x)/\Phi(x) \quad \text{or} \quad \Phi(x) = \Phi(0)\exp\int_0^x y(\xi)\,d\xi, \tag{2}$$

we apply the solution of Eq. (1) to the solution of the Riccati equation

$$y'(x) + y^2(x) + \alpha_0^2 + \varepsilon\alpha^2(x) - \Delta = 0 \tag{3}$$

for the boundary conditions $y(0) = 0$ and $y(R) \to -\infty$. Allowing for the quadratic character of the nonlinearity of Eq. (3) and subsequently linearizing it with respect to the small parameter ε, we arrive at the expansion

$$\begin{aligned} y &= y_0 + \varepsilon[y_1 + \varepsilon[y_2 + \varepsilon^2[y_3 + \varepsilon^4[y_4 + \ldots]]\ldots] = y_0 + \sum_{k=1}^{\infty}\varepsilon^{2k-1}y_k(\varepsilon); \\ \Delta &= \varepsilon[\Delta_1 + \varepsilon[\Delta_2 + \varepsilon^2[\Delta_3 + \varepsilon^4[\Delta_4 + \ldots]]\ldots] = \sum_{k=1}^{\infty}\varepsilon^{2^{k-1}}\Delta_k(\varepsilon). \end{aligned} \tag{4}$$

Translated from Atomnaya Énergiya, Vol. 42, No. 2, pp. 141-143, February, 1977. Original article submitted May 24, 1976.

The neutron flux in the m-th approximation on the basis of Eq. (2) is of the form

$$\Phi_m(x)=\Phi_m(0)\exp\int_0^x\left[y_0(\xi)+\sum_{k=1}^{m}\varepsilon^{2k-1}y_k(\xi)\right]d\xi. \tag{5}$$

Substituting Eq. (4) into Eq. (3) and discarding terms of the order of ε and higher we get an equation of the zeroth-order approximation (for the unperturbed reactor):

$$y_0'+y_0^2+\alpha_0^2=0. \tag{6}$$

When $y_k(0)=0$ and $y_0(r)\to-\infty$, as was to be expected we have

$$y_0(x)=-\alpha_0\operatorname{tg}\alpha_0x;\quad \Phi_0(x)=\Phi_0(0)\cos\alpha_0x;\quad \alpha_0=\pi/2R. \tag{7}$$

Solution of the equation of the first approximation,

$$y_1'+2y_0y_1+\alpha^2(x)-\Delta_1=0 \tag{8}$$

gives the familiar expression for the compensating factor Δ_1:

$$y_1=\Phi_0^{-2}\int_0^x\Phi_0^2(\Delta_1-\alpha^2)\,d\xi,$$
$$\Delta_1=\int_0^R\Phi_0^2\alpha^2\,dx\Big/\int_0^R\Phi_0^2\,dx. \tag{9}$$

From the equation of the m-th approximation,

$$y_m'+2(y_0+\varepsilon y_1+\ldots+\varepsilon^{2^{m-2}}y_{m-1})y_m+y_{m-1}^2-\Delta_m=0\qquad(m\geqslant 2) \tag{10}$$

we obtain

$$y_m(x)=\Phi_{m-1}^{-2}(x)\int_0^x\Phi_{m-1}^2(\xi)\,[\Delta_m-y_{m-1}^2(\xi)]\,d\xi\quad\text{for}\quad m\geqslant 2;$$

$$\Delta_m=\int_0^R\Phi_{m-1}^2(x)\,y_{m-1}^2(x)\,dx\Big/\int_0^R\Phi_{m-1}^2(x)\,dx\ \text{for}\ m\geqslant 2;$$

$$\Phi_m(x)=\Phi_m(0)\,\Phi_{m-1}^{-1}(0)\,\Phi_{m-1}(x)\left[1+\varepsilon^{2^{m-1}}\int_0^x y_m(\xi)\,d\xi\right]+0(\varepsilon^{2^m})\quad\text{for}\ m\geqslant 1, \tag{11}$$

where $\Phi_{m-1}(x)$ in the expression for $\Phi_m(x)$, representing $\Phi(x)$ to within quantities of the order of ε^{2m}, should also be calculated to within quantities of the order of ε^{2m}.

As a methodological example having an analytical solution let us consider a symmetric problem about a point perturbation of a reactor at the coordinate a of the active zone and a point compensation of the perturbation at another coordinate $b(0<a<b<R)$. Then $\alpha^2(x)=\delta(x-a)$, $\Delta=\Delta^*\delta(x-b)$, where $\Delta^*=\text{const}$. From Eqs. (8) and (9) in the first approximation we get

$$y_1=\cos^2\alpha_0a\,\frac{\theta(x-b)-\theta(x-a)}{\cos^2\alpha_0x};\quad \Delta^*=\varepsilon\Delta_1^*+0(\varepsilon^2), \tag{12}$$

where $\theta(x)=1$, if $x\geq 0$ and $\theta(x)=0$, if $x<0$, and $\Delta_1^*=\cos^2\alpha_0a/\cos^2\alpha_0b$.

Substituting Eq. (12) into Eq. (5) or Eq. (11), we get

$$\Phi_1(x)=\Phi_1(0)\cos\alpha_0x\,[1+\varepsilon J(x)]+0(\varepsilon^2), \tag{13}$$

where

$$J(x)=\frac{1}{\alpha_0}\cos^2\alpha_0a\,[\theta(x-b)(\operatorname{tg}\alpha_0x-\operatorname{tg}\alpha_0b)-\theta(x-a)(\operatorname{tg}\alpha_0x-\operatorname{tg}\alpha_0a)]. \tag{14}$$

In the second approximation, after simple rearrangements we find (to within quantities of the order ε^4 and not ε^3):

$$\Delta^* = \varepsilon\Delta_1^* [1 - \varepsilon J(b) + \varepsilon^2 J^2(b)] + 0(\varepsilon^4);$$
$$\Phi_2(x) = \Phi_2(0) \cos \alpha_0 x [1 + \varepsilon J(x)] + 0(\varepsilon^4). \quad (15)$$

Comparison of Eqs. (13) and (14) gives reason to suppose that the exact solution of the problem is of the form

$$\Delta^* = \varepsilon\Delta_1^* [1 + \varepsilon J(b)]^{-1};$$
$$\Phi(x) = \Phi(0) \cos \alpha_0 x [1 + \varepsilon J(x)]. \quad (16)$$

The latter is confirmed by the following iterations and alternative methods of solving the problem by using the generalized [2] Green's function $G(x, \xi)$ of the operator $L(\Phi) = \Phi''(x) + \alpha_0^2 \Phi(x)$, in which $\alpha_0 = \pi/2R$ is the eigenvalue

$$R\alpha_0 G(x, \xi) = \begin{cases} x \sin \alpha_0 x \cos \alpha_0 \xi + (\xi - R) \sin \alpha_0 \xi \cos \alpha_0 x, & x \leqslant \xi; \\ (x - R) \sin \alpha_0 x \cos \alpha_0 \xi + \xi \sin \alpha_0 \xi \cos \alpha_0 x, & x \geqslant \xi. \end{cases} \quad (17)$$

For comparison with the usual methods of expanding the perturbed neutron flux in the entire spectrum of eigenfunctions, we consider the classical example of the calculation [3] of the neutron flux variation due to the formation of fussion products and compensation of the reactivity by the addition of uranium so that

$$\Delta = -(\nu - 1 - \zeta)\, \delta\Sigma_f / D \quad \text{for} \quad \varepsilon\alpha^2(x) = -c\Phi_0(x)/D. \quad (18)$$

Here, ν is the mean number of fast neutrons liberated per fission event; ζ is the ratio of the cross section for radioactive capture to that for fission of the fuel; and D is the diffusion coefficient. The absorption in the fission products is taken to be proportional in the first approximation to the unperturbed neutron flux $\Phi_0(x)$ (c is a proportionality factor), and the sought variation of the macroscopic cross section $\delta\Sigma_f$ is uniform. Substitution of Eq. (18) into Eq. (9) yields

$$\delta\Sigma_f = (\nu - 1 - \zeta)^{-1} \int_0^R c\Phi_0^2\, dx \Big/ \int_0^R \Phi_0^2\, dx = \frac{8}{3\pi} c\gamma (\nu - 1 - \zeta)^{-1}, \quad (19)$$

where γ is the normalization for the eigenfunctions. The expression for $\delta\Sigma_f$ is in agreement with the formula given in [3]. Equation (11) for the perturbed neutron flux leads to the expression

$$\Phi_1(x) = \Phi_1(0) \left\{ \cos \alpha_0 x + \frac{c\delta}{3\alpha_0^2 D} \left[1 - \cos \alpha_0 x - \sin \alpha_0 x \left(2\frac{x}{R} - \sin \alpha_0 x \right) \right] \right\}, \quad |x| \leqslant R, \quad (20)$$

which in contrast to an infinite series, which cannot be summed directly, is in simple finite form. Going over in Eq. (20) to the coordinate system adopted in [3], i.e., setting $x' = x + R$ and expanding $\Phi_1(x)$ in a series in the eigenfunctions $\sin(n\pi x')/2R$, we can verify that the expressions for $\Phi_1(x)$ are identical. This leads, in particular, to a formula for the sum of an infinite series ($0 \leq z \leq \pi$):

$$\sum_{n=3,\ 5,\ 7\ldots} \frac{\sin nz}{(n^2-4)(n^2-1)n} = \frac{\pi}{12} \left[1 - \frac{5}{3\pi} \sin z - \left(1 - \frac{2z}{\pi} \cos z - \frac{1}{2} \sin^2 z \right) \right]. \quad (21)$$

The expressions for $\Phi_2(x)$ and higher approximations which according to Eq. (11) converge to a finite number of quadratures do not have a simple representation in elementary functions in this problem, but are easily found indirectly by numerical methods.

LITERATURE CITED

1. V. S. Polikanov, Zh. Eksp. Teor. Fiz., 52, No. 5, 1326 (1967).
2. V. I. Smirnov, A Course of Higher Mathematics, Vol. 4, Pergamon Press, Elmsford, New York.
3. A. Weinberg and E. Wigner, Physical Theory of Nuclear Chain Reactors, Univ. of Chicago Press, Chicago (1958).

OPTIMAL OPERATING CONDITIONS FOR ATOMIC POWER PLANT REACTORS

A. S. Gerasimov and A. P. Rudik

UDC 621.039.514.25

Formulation of the Problem. A large number of problems pertaining to the optimization of xenon processes in nuclear reactors has now been solved [1-3]. However, in solving them an isolated nuclear reactor was considered. As a rule, several reactors are installed in one atomic power plant so that the problem arises of optimizing them simultaneously. Let us formulate this problem.

The nominal total thermal power of n reactors in an atomic power plant is W. Periodically (once every 24 h) for a time τ the power of the plant has to be reduced to εW, where $\varepsilon < 1$. It is necessary to find what the time dependence of the partial power reductions should be for the i-th reactor, $\varepsilon_i(t) \geq 0$, $0 \leq t \leq \tau$, $1/n \sum_{i=1}^{n} \varepsilon_i(t) = \varepsilon$ so that the total neutron absorption in ^{135}Xe in all reactors in 24 h is a minimum.

This formulation of the problem differs from earlier ones in that, firstly, several reactors are considered at once and, secondly the neutron absorption in ^{135}Xe is minimized.*

Introducing the generally accepted notation [2, 3] and assuming that in the i-th reactor the neutron flux density is $\varepsilon_i(t)U$ when $0 \leq t \leq \tau$ and U when $\tau \leq t \leq T = 24\ h - U$, we write the equations for the concentration of ^{135}I and ^{135}Xe (normalized to the macroscopic cross section for fission of the nuclear fuel)†:

$$\begin{aligned} dI_i/dt &= \gamma_1 \varepsilon_i U - \lambda_1 I_i, \quad i = 1, 2, \ldots, n, \\ dX_i/dt &= \gamma_2 \varepsilon_i U + \lambda_1 I_i - (\sigma_2 \varepsilon_i U + \lambda_2) X_i, \end{aligned} \tag{1}$$

with $\varepsilon_i = \varepsilon_i(t)$, $0 \leq t \leq \tau$; $\varepsilon_i = 1$; and $\tau \leq t \leq T$.

The boundary conditions for $I_i(t)$ and $X_i(t)$ reduce to the cyclicity requirement

$$I_i(T) = I_i(0); \quad X_i(T) = X_i(0), \tag{2}$$

which in the formalism of the maximum principle [5] leads to transversality conditions for adjoint functions, similar to those used in [6] for reactor optimization problems with feedback.

*The formulation in [4] of the problem of minimizing neutron capture in ^{135}Xe without making allowance for the cyclical nature of reactor operation is not very convincing.

†One group of neutrons is under consideration. The problem is solved for a point model, i.e., the neutron flux density used is the value averaged over the reactor volume.

TABLE 1. Relay Modes

Parameters	θ, h					
	0	0,4	0,8	1,2	1,6	2,0
X_1^{max}, 10^{16} cm^{-2}	1,85	2,04	2,21	2,36	2,50	2,62
X_2^{max}, 10^{16} cm^{-2}	3,04	2,98	2,91	2,83	2,73	2,62
J, 10^{16} cm^{-2}	23,15	23,17	23,19	23,20	23,21	23,21
R, 10^{16} cm^{-2}	7,52	8,59	9,41	9,99	10,34	10,46

Translated from Atomnaya Énergiya, Vol. 42, No. 2, pp. 143-144, February, 1977. Original article submitted June 21, 1976.

TABLE 2. Modes with Constant $\varepsilon_i(t)$

Parameters	$\varepsilon_i(t)$					
	0	0,1	0,2	0,3	0,4	0,5
X_1^{max}, 10^{16} cm^{-2}	3,04	2,86	2,70	2,56	2,43	2,30
X_2^{max}, 10^{16} cm^{-2}	1,85	1,93	2,01	2,10	2,20	2,30
J, 10^{16} cm^{-2}	23,15	23,19	23,21	23,23	23,24	23,24
R, 10^{16} cm^{-2}	7,52	7,08	6,74	6,50	6,36	6,31

The functional J being minimized is of the form

$$J/\sigma_2 U = \sum_{i=1}^{n} \left\{ \int_0^{\tau} \varepsilon_i(t) X_i \, dt + \int_{\tau}^{T} X_i \, dt \right\}. \tag{3}$$

The Classical Optimal Mode. Let us consider the first n−1 functions $\varepsilon_i(t)$ as the control, and write $\varepsilon_n(t)$ as $\varepsilon_n t = n\varepsilon - \sum_{i=1}^{n-1} \varepsilon_i(t)$. Then the Hamiltonian $\mathscr{H}$ of the problem under consideration can be written as

$$\mathscr{H} = \chi + \sum_{i=1}^{n-1} \varepsilon_i(t) \varphi_i, \tag{4}$$

where the functions χ and φ_i do not depend explicitly on $\varepsilon_i(t)$, and when $0 \leq t \leq \tau$,

$$\varphi_i/U = \gamma_1 [\psi_i^{(1)} - \psi_n^{(1)}] + \gamma_2 [\psi_i^{(2)} - \psi_n^{(2)}] - \sigma_2 \{[\psi_i^{(2)} - \psi_0] X_i - [\psi_n^{(2)} - \psi_0] X_n\}, \tag{5}$$

where $\psi_0 = -1$; $\psi_i^{(1)}$ and $\psi_i^{(2)}$ are, respectively, the adjoint I_i and X_i functions.

It follows from Eq. (5) that all $\varphi_i = 0$; $0 \leq t \leq \tau$; $i = 1, 2, \ldots, n-1$ simultaneously if all $\varepsilon_i(t) = \varepsilon$, i.e., such a choice realizes the simultaneous classical mode over all controls. The existence of the classical mode results in an insensitivity to the choice of the mode of power reduction in an atomic power plant, although it is not clear whether this classical mode corresponds to a maximum or a minimum of the functional J. To explain the latter circumstance we give the results of alternative calculations.

The Results of Calculations. The following quantities were determined in the calculations: X_i^{max} for the i-th reactor, as well as the total neutron absorption J in ^{135}Xe; R in the system of control* for the atomic power plant. The quantity J is conveniently given in the form of a sum $J(T) = \sum_{i=1}^{n} J_i(T)$, the value of J for the i-th reactor with a constant neutron flux density U for a time t being of the form

$$J_i(t) = \sigma_2 U/(\sigma_2 U + \lambda_2)\,[(\gamma_1 + \gamma_2) Ut + I_i(0) + X_i(0) - I_i(t) - X_i(t)]. \tag{6}$$

The quantity R is defined by the expression

$$R/\sigma_2 U = \sum_{i=1}^{n} \left\{ \int_0^{\tau} \varepsilon_i(t) [X_i^{max} - X_i(t)]\, dt + \int_{\tau}^{T} [X_i^{max} - X_i(t)]\, dt \right\}. \tag{7}$$

The calculations were carried out with the following values of the physical constants which appear in Eq. (1): $\gamma_1 = 0.061$, $\gamma_2 = 0.002$, $\lambda_1 = 2.8525 \cdot 10^{-5}$ sec^{-1}; $\lambda_2 = 2.1088 \cdot 10^{-5}$ sec^{-1}; and $\sigma_2 = 2.7 \cdot 10^{-18}$ cm^2. The case of two (n = 2) was considered and it was assumed that $U = 3 \cdot 10^{-13}$ neutrons/cm^2·sec, $\varepsilon = 0.5$, and $\tau = 4$ h.

Table 1 gives the results of the calculation of relay modes in which $\varepsilon_i(t)$ is either 1 or 0. By θ we denote the time during which $\varepsilon_1(t) = 0$ (respectively, the time during which $\varepsilon_2(t) = 0$ is $\tau - \theta$).

Table 2 shows the results of calculation of modes in which $\varepsilon_i(t)$ is constant when $0 \leq t \leq \tau$; $\varepsilon_1(t) + \varepsilon_2(t) = 1$.

*A reactor, of course, has a control system for compensating reactivity losses when $X_i(t) < X_i^{max}$.

Thus, the classical control $\varepsilon_i(t) = \varepsilon$ leads to the maximum neutron absorption ^{135}Xe. Neutron absorption in ^{135}Xe is very insensitive to the choice of the mode of power reduction. In the examples considered, this quantity reaches a minimum for the case when one reactor has been shut down and the other is operating at full power. The neutron absorption in the control system varies appreciably with the mode of power reduction and reaches a minimum for the classical regime with $\varepsilon_i(t) = \varepsilon$.

The authors are grateful to A. D. Galanin for his interest in the work.

LITERATURE CITED

1. M. Ash, Optimal Shutdown Control of Nuclear Reactors, Academic Press, New York (1966).
2. A. P. Rudik, Nuclear Reactors and the Pontryagin Maximum Principle [in Russian], Atomizdat, Moscow (1971).
3. A. P. Rudik, Xenon Transient Processes in Nuclear Reactors [in Russian], Vol. 1, Atomizdat, Moscow (1974).
4. T. S. Zaritskaya and A. P. Rudik, ITEF Preprint, No. 52, Moscow (1974).
5. L. S. Pontryagin et al., Mathematical Theory of Optimal Processes [in Russian], Fizmatgiz, Moscow (1965).
6. A. S. Gerasimov, At. Energ., 42, No. 1, 126 (1977).

^{85}Kr CONCENTRATION IN THE ATMOSPHERE OVER THE USSR TERRITORRY IN 1971-1975

É. G. Tertyshnik, A. A. Siverin, and V. G. Baranov

UDC 621.039.75:551.594

Since man has adopted nuclear energy the concentration of ^{85}Kr in the atmosphere of our planet increases continually. The reason is that the krypton, being a noble gas, is hardly soluble in water; radioactive decay ($T_{1/2}$ = 10.76 yr) is the only mechanism by which ^{85}Kr is removed from the atmosphere. At the present time the concentration of this isotope in the air exceeds 10 times the concentration of tritium and almost 1000 times the total concentration of the other artificial radioisotopes.

Since 1971, the changes in the ^{85}Kr concentration in the atmosphere are regularly observed [1]. The measurements are based on the technological krypton which is released by industrial air separating units into the atmospheric layer close to ground. Krypton samples were taken once per month from units located in the European part of the USSR in the latitudinal zone between 54 and 59° N. The technological krypton contains about 5% xenon and a certain radon concentration; the activity resulting from ^{222}Rn ($T_{1/2}$ = 3.8 days) exceeds the ^{85}Kr activity several hundred times when the sample is taken. Therefore between the sampling and the measurements on the samples no more than two months elapse; the gas sample to be measured is introduced into the counter through a filter which separates the aerosol particles on which long-lived decay products of radon might precipitate.

The activity of the samples was determined with a scintillation counter [2]. Similar concentration values were obtained in control measurements made on several samples with the aid of a filled counter of the All-Union Scientific-Research Institute of Physicotechnical and Radiotechnical Measurements [3].

We indicate below the average annual ^{85}Kr concentration values at 0°C and a pressure of 101,320 N/m^2 (760 mm Hg).

The results of individual measurements deviated from the average level by at most 15%. In order to facilitate the comparison of the data with the results of other authors using various units for the formula of the ^{85}Kr

Translated from Atomnaya Énergiya, Vol. 42, No. 2, p. 145, February, 1977. Original article submitted July 26, 1976.

TABLE 1

Year	pCi/m^3 air	decays/min·mmole Kr
1971	13,6	590
1971	13,7 *	600 *
1972	14,1	620
1973	14,6	640
1974	14,6	640
1975	16,2	710

*The measurements were made in the All-Union Scientific-Research Institute of Physicotechnical and Radiotechnical Measurements.

volume concentration, we calculated the ^{85}Kr concentration per unit volume of dry air and per unit volume of natural krypton, the latter unit volume being equal to 22.4 cm^3 (1 mmole).

The results are in good agreement with the results of measurements made in the USA [4, 5]. Slightly higher concentration levels were obtained in the Federal Republic of Germany [6].

It is generally accepted that more than 97% of the global krypton are in the atmosphere, and that the atmosphere is the only main reservoir of ^{85}Kr. The total stored amount determined for this radioisotope at the end of 1973 in the atmosphere amounted to 53 MCi [5]; calculations indicate that the main fraction of the total originates from the ^{85}Kr released in the production of plutonium and from the waste of fuel reprocessing plants working on the fuel elements of atomic power stations [6]. The contribution which nuclear weapons tests render to the ^{85}Kr amounts at the present time to less than 2% of the global total of this radioisotope.

When the usefulness of measures limiting the release of ^{85}Kr into the atmosphere is evaluated, one must take into account not only the additional dose resulting from the effect upon the skin and the light contamination of the ground by the β particles of ^{85}Kr, but also the negative influence upon the climate of the planet; this influence can be caused in the future by the considerable ^{85}Kr-induced ionization of the entire atmospheric layer [7].* Since atmospheric electricity is important for processes causing the release of precipitation, a noticeable increase in the conductivity between the surface of oceans and the ionosphere may substantially change the atmospheric processes, and the consequences of these changes are hard to predict at the present time.

LITERATURE CITED

1. É. G. Tertyshnik and S. G. Malakhov, in: Trans. of the Inst. of Exper. Meteorology [in Russian], No. 3 (42), Gidrometeoizdat, Moscow (1974), p. 60.
2. É. G. Tertyshnik, in: Trans. of the Inst. of Exper. Meteorology [in Russian], No. 4(56), Gidrometeoizdat, Moscow (1976), p. 152.
3. V. I. Albul and V. G. Baranov, Prib. Tekhn. Eksp., No. 2, 43 (1973).
4. Radiat. Data Rep., 15, No. 11, 133 (1974).
5. K. Telegadas and G. Ferber, Science, 190, No. 4217, 882 (1975).
6. K. Schroder and W. Roether, in: Proc. IAEA Symp. Isotope Ratios as Pollutant Source and Behavior Indicators, Vienna, 18-15 Nov., SM-191/30 (1974).

*In Russian original, no reference No. 7 appears in the Literature Cited – Publishers.

NEUTRON LEAKAGE FROM A MANGANESE BATH

E. A. Zhagrov, Yu. A. Nemilov,
A. V. Platonov, and V. I. Fominykh

UDC 539.1.074.8

The most accurate and reliable existing method of measuring the neutron yield from various sources is that of the manganese bath, which has recently been improved significantly. A flow bath has been developed [1] and this method has been used to measure the neutron flux obtained in accelerators [2]. It is of particular interest to use the magnanese bath for intermediate neutrons, in which case the highest accuracy can be attained. Usually, the manganese baths employed in measurements are on a large scale, with a tank diameter of ~ 80 cm. This limits the application of the method in the calibration of weak intermediate-neutron sources in the case of isotopic photoneutron sources and in work with intermediate-neutron beams in accelerators. The dimensions of the manganese bath, therefore, must be optimized for measurements in the comparatively little-investigated area of intermediate neutrons with an energy ranging from several tons of keV to 250 keV. However, to do this one must know the distribution of neutrons in a manganese sulfate solution from monoenergetic sources of intermediate neutrons. These data are not available in the literature.

The $^{7}Li(p, n)^{7}Be$ reaction was used as a neutron source. A beam of protons accelerated in an electrostatic generator bombarded a lithium target (Fig. 1). Neutrons were detected at a 135° angle to the proton beam. Neutrons of 25 and 230 keV were used. The nonuniformity of the neutron energy was determined in the main by the thickness of the lithium target; the calculated width of the neutron energy distribution was ~10 and 24 keV for a neutron energy of 25 and 230 keV, respectively. The lithium target was surrounded by a 27-cm continuous shield consisting of a saturated solution of sodium tetraborate and boric acid. The neutron beam was shaped by a collimator of borated polyethylene. The neutron flux passing through the collimator monitored by an SNM-13 counter installed inside another, symmetrically situated collimator of similar construction. The direction of the proton beam was taken to be the axis of symmetry. The SNM-13 counter was surrounded by a polyethylene moderator 4 cm thick ensuring maximum detector sensitivity to intermediate neutrons. The distribution of slow neutrons was studied with a boron SNM-13 counter immersed in a 35 × 35 × 40-cm bath. The counter was moved along the axis of the neutron beam. Pulses from the neutron counter proceeded to an amplifier and then to a discriminator and scaler. The measuring channel was monitored with a specially prepared and calibrated antimony–beryllium neutron source.

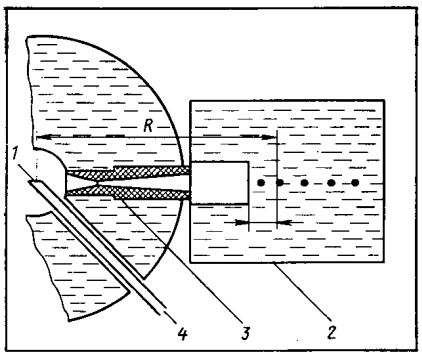

Fig. 1. Diagram of experimental arrangement: 1) LiF target; 2) bath; 3) collimator; 4) ion guide.

Translated from Atomnaya Énergiya, Vol. 42, No. 2, pp. 146-147, February, 1977. Original article submitted July 30, 1976.

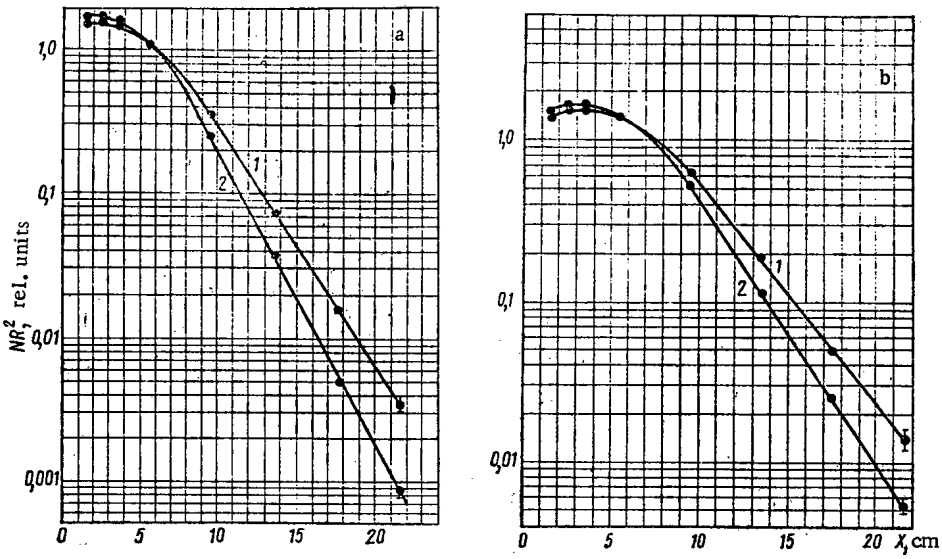

Fig. 2. Distribution of slow neutrons in water (1) and in manganese sulfate solution (2) from a neutron source with an energy E_n of: a) 25 keV; b) 230 keV.

TABLE 1. Relaxation Length for Water and Manganese Sulfate Solution

E_n, keV	L_{H_2O}, cm	L_{MnSO_4}, cm
25	2,59±0,09	2,06±0,08 3,46 [4]
230	3,11±0,09 3,34 [3]	2,58±0,09

Figure 2 presents the distribution of slow neutrons in water (curve 1) and in a 30% solution of manganese sulfate [curves at an initial energy of 25 keV (Fig. 2a) and 230 keV (Fig. 2b)]. The distributions obtained in the manganese sulfate solution were normalized to distributions in water at a 5.5-cm point. For all dependences at distances greater than 9 cm from the tank outlet, the distributions in the bath are described by an exponent. This makes it possible to determine the relaxation length and to calculate the maximum neutron leakage from a spherical moderator of known radius for an isotropic source. The distributions were processed by the least-squares technique. The relaxation length obtained is given in Table 1, along with the data obtained in [3] by using an isotopic photoneutron source based on ThC" + D with E_n = 194 keV, as well as the results of [4].

The neutron leakage from a spherical moderator of radius r and relaxation length L is estimated by the formula $f = A \exp(-r/L)$ which was used in [4-6]. The coefficient A was taken to be equal to 2 in accordance with the data in a report by the Bureau International des Poids et Mesures [6] which analyzed the leakage values for a number of various moderator dimensions and for various values of A and L. The calculated value of leakage for water and manganese sulfate solution is given in Table 2 which also lists data from [4, 7] for fission-spectrum neutrons of energy < 1 MeV.

Slow-neutron distributions in water obtained for 230-keV sources are in satisfactory agreement with the results of [3]. Some papers have shown that for neutron sources with an energy of several MeV the neutron distribution is practically the same in water as it is in manganese sulfate. Our measurements indicate that for the investigated range of intermediate neutrons these distributions differ substantially.

Thus, for radioactive sources of neutrons with an energy of up to 230 keV, a spherical manganese sulfate bath of radius 15 cm has a neutron leakage of < 1%.

In measurements with an antimony–beryllium neutron source at an energy of E_n = 25 keV, a value of L = 3.46 cm was obtained for a manganese sulfate solution [4] which is significantly larger than our results.

TABLE 2. Values of Leakage from Spherical Water Moderator and Manganese Sulfate Solution

r, cm	f, %				
	$\varepsilon_n = 25$ keV		$\varepsilon_n = 230$ keV		$\varepsilon_n < 1$ MeV
	H_2O	$MnSO_4$	H_2O	$MnSO_4$	$MnSO_4$
12	1,9	0,6	4,2	1,9	—
15	0,6	0,14 5,6 [4]	1,6	0,6	8,5 [7]
18	—	—	0,6	0,2	—
20	0,08	0,01	0,3	0,08	2,9 [7]

In the paper, the leakage was overevacuated at 5.6% for a 15-cm spherical manganese sulfate bath, as also been pointed out in [9].

LITERATURE CITED

1. E. Axton and P. Cross, J. Nucl. Energ, 15, 22 (1961).
2. I. Leroy, Nucl. Instrum. Methods, 88, 1 (1970).
3. K. A. Petrzhak (Pietrzak) and M. A. Bak, Trudy RIAN, 7, No. 1, 41 (1956).
4. D. Davy, J. Nucl. Energy A/B, 20, 277 (1966).
5. E. Axton, J. Nucl. Energy A/B, 19, 409 (1965).
6. V. Naggiar, Rapport B. I. P. M., Sevres (1967).
7. H. Goldstein, Trans. Am. Nucl. Soc., 5, No. 1, 89 (1962).
8. P. Wunderer, Z. Angew. Phys., 10, 537 (1958).
9. A. De Volpi and K. Porges, Metrologia, 5, No. 4, 28 (1969).

YIELDS OF ^{121m}Te, ^{121g}Te, AND ^{123m}Te IN THE BOMBARDMENT OF ANTIMONY BY PROTONS AND DEUTERONS

P. P. Dmitriev, M. V. Panarin, Z. P. Dmitrieva, and G. A. Molin

UDC 539.172.12

The radioisotopes ^{121m}Te, ^{121g}Te, and ^{123m}Te ($T_{1/2}$ = 154, 17, and 120 days, respectively) are used in applied and scientific research. The γ rays emitted in the decay of ^{121m}Te (37.18 keV) and ^{123m}Te (159.0 keV) are used in research with the Mössbauer effect.

The isotopes ^{121m}Te, ^{121g}Te, and ^{123m}Te decay into daughter nuclei in the following way:

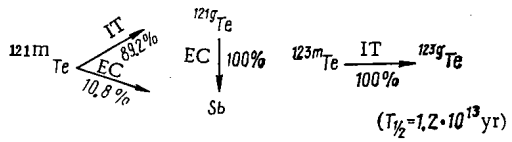

where IT denotes an isomeric transition and EC electron capture.

Translated from Atomnaya Énergiya, Vol. 42, No. 2, pp. 148-149, February, 1977. Original article submitted August 20, 1976.

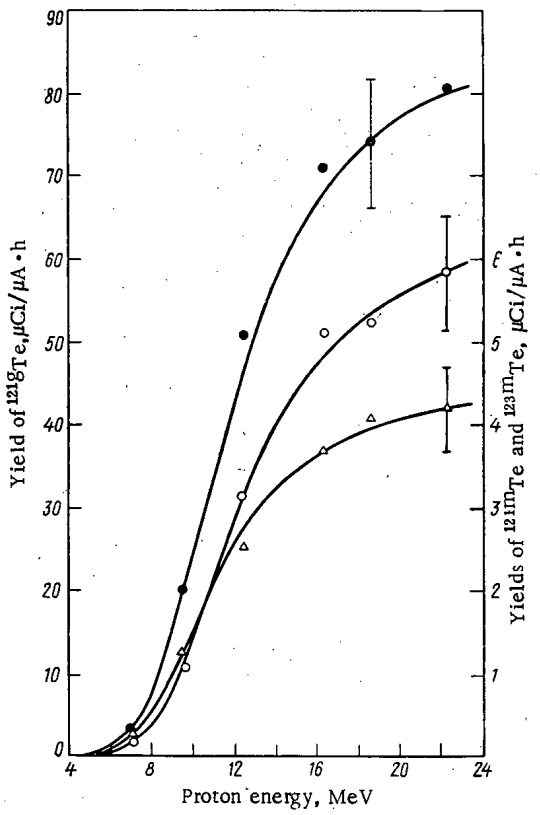

Fig. 1

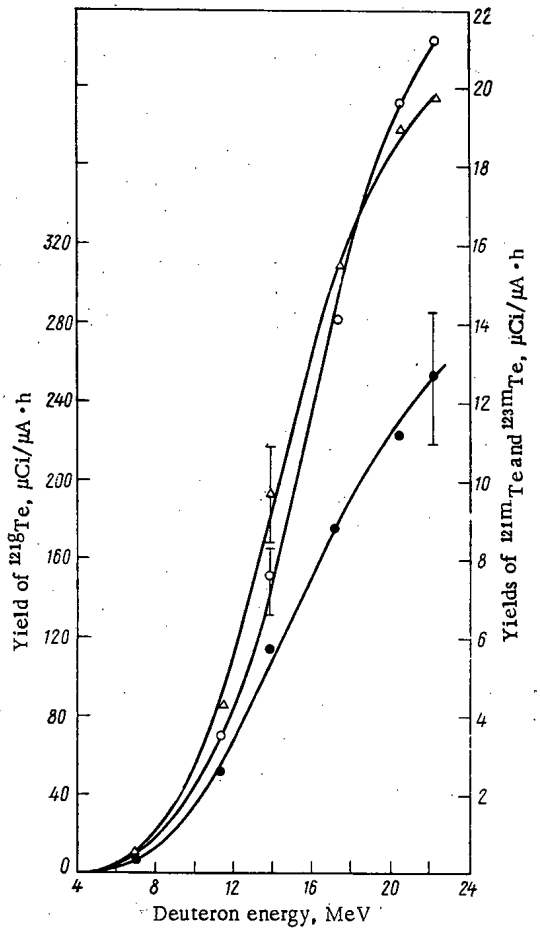

Fig. 2

Fig. 1. Yields of ^{121m}Te, ^{121g}Te, and ^{123m}Te as functions of proton energy for thick antimony targets: ●) ^{121m}Te; ○) ^{121g}Te; △) ^{123m}Te.

Fig. 2. Yields of ^{121m}Te, ^{121g}Te, and ^{123m}Te as functions of deuteron energy for thick antimony targets: ●) ^{121m}Te; ○) ^{121g}Te; △) ^{123m}Te.

TABLE 1. Energies and Quantum Yields of γ and X Rays

Radio isotope	Energy of radiation	Yield, %	Reference
^{121m}Te	γ 212,21	81,3	[2]
	K_β (Te) 31,13	6,7	Present work
	K_α (Te) 27,38	30,8	"
	K_β (Sb) 29,81	2,6	"
	K_α (Sb) 26,28	12,4	"
^{121g}Te	γ 573,08	79,0	[2]
	K_β (Sb) 29,81	13,4	Present work
	K_α (Sb) 26,28	62,6	"
^{123m}Te	γ 159,0	83,5	[3]
	K_β (Te) 31,13	8,8	[3]
	K_α (Te) 27,38	40,5	[3]

Thus ^{121g}Te is formed in the nuclear reaction and in the decay of the long-lived parent isotope ^{121m}Te. The ^{121g}Te obtained in the reaction practically disappears in 6-7 months after bombardment, and the isomeric pair ^{121m,g}Te is in equilibrium.

We have measured the yields of ^{121m}Te, ^{121g}Te, and ^{123m}Te as functions of the energy of protons and deuterons bombarding thick antimony targets. The radionuclides are formed in the following reactions: ^{121}Sb(p n) ^{121m,g}Te, ^{123}Sb(pn)^{123m}Te, ^{121}Sb(d2n)^{121m,g}Te, and ^{123}Sb(d2n)^{123m}Te. Samples of metallic antimony were bombarded with particles whose energies were varied by copper retarding foils. The method of bombardment and

TABLE 2. Yields of ^{121m}Te, ^{121g}Te, and ^{123m}Te

Method of obtaining and particle energies in MeV	Yield, μCi/μA·h		
	^{121m}Te	^{121g}Te	^{123m}Te
Sb + *p*:			
22,3±0,43	5,8±0,7	80,5±9,7	4,2±0,5
18,6±0,50	5,2±0,6	74,0±9,0	4,1±0,5
16,3±0,53	5,1±0,6	70,7±8,5	3,7±0,45
12,4±0,58	3,2±0,4	51,0±6,2	2,5±0,3
9,5±0,64	1,1±0,14	20,0±2,5	1,2±0,15
7,1±0,65	0,15±0,02	3,0±0,4	0,2±0,03
Sb + *d*:			
22,1±0,41	21,2±2,6	253±31	19,7±2,4
20,3±0,46	19,6±2,4	223±27	19,0±2,3
17,2±0,52	14,1±1,7	175±21	15,4±1,9
13,8±0,56	7,5±0,9	113±14	9,6±1,2
11,4±0,61	3,4±0,41	51±6,2	4,2±0,51
7,1±0,65	0,4±0,05	50±0,7	0,5±0,07

the measurement of the activity of the radionuclides and the integrated flux were similar to those described in [1].

The activity of ^{121g}Te was measured throughout the first ten days after bombardment ceased, and therefore the correction for the activity of the ^{121g}Te formed in the decay of ^{121m}Te was less than 10%.

As a result of K-capture and internal conversion in the K shell in the decay of ^{121m}Te, ^{121g}Te, and ^{123m}Te intense x rays are emitted.

Table 1 lists the energies and quantum yields of the γ rays used to measure the ^{121m}Te, ^{121g}Te, and ^{123m}Te activities and the K_α and K_β x-ray lines. The quantum yields of the ^{121m}Te and ^{121g}Te x rays were calculated as in [4] using the internal conversion coefficients for the K shell from [2].

The measured yields of ^{121m}Te, ^{121g}Te and ^{123m}Te are shown in Table 2 and Figs. 1 and 2. The 12-15% errors in the experimental yields are due mainly to systematic errors in measuring the activities of the radionuclides and the integrated flux of bombarding particles.

There are no data on cross sections or yields reported in the literature for reactions with the formation of ^{121m}Te, ^{121g}Te, and ^{123m}Te. The measured [6] values of the isomeric ratio σ_m/σ_g for the ^{121}Sb (d2n)^{121m,g}Te reaction are 0.56 and 0.793 for E_d = 9.2 and 27.3 MeV, respectively. No values are given for the cross sections σ_m and σ_g. By differentiating the yield curves for ^{121m}Te and ^{121g}Te (Fig. 2) the cross sections σ_m and σ_g can be estimated; their ratio σ_m/σ_g in the deuteron energy range ~10-22 MeV agrees with the data in [5] to within 20-30%.

Among other methods of obtaining carrier-free ^{121m}Te, ^{121g}Te, and ^{123m}Te can be mentioned the bombardment of tin with α particles in (αxn) reactions. For an α-particle energy of 44.0 ± 0.6 MeV the measured yields of ^{121m}Te, ^{121g}Te, and ^{123m}Te are 4.1 ± 0.5, 50 ± 8,and 1.0 ± 0.2 μCi/μA·h, respectively. These values are considerably lower than those for the bombardment of antimony by protons and deuterons. The radioisotopic purity in this case is sharply decreased as a result of the formation of other long-lived tellurium isotopes ^{118}Te, ^{119m}Te, ^{125m}Te, and ^{127m}Te ($T_{1/2}$ = 6, 4.7, 58, and 108 days, respectively) with appreciable yields. In order to obtain ^{121m,g}Te and ^{123m}Te of high radioisotropic purity it is necessary to bombard enriched isotopes ^{121}Sb and ^{123}Sb respectively.

The authors thank G. N. Grinenko for help with the work.

LITERATURE CITED

1. P. P. Dmitriev et al., At. Energ., 31, No. 2, 157 (1971); 32, No. 5, 426 (1972).
2. D. Horen, Nucl. Data Sheets, B6, No. 1 (1971).
3. M. Martin and P. Blechert-Toft, Nucl. Data Tables, A8, Nos. 1-2 (1970).
4. P. P. Dmitriev et al., At. Energ., 38, No. 2, 100 (1975).
5. A. Macoroa et al., J. Inorg. and Nucl. Chem., 28, 5 (1966).

THE FIRST MINÉNERGOMASH TECHNOLOGICAL CONFERENCE

A. I. Merenkov

In May 1976, the Ministry of Power Machine Construction (Minénergomash) held its First Technological Conference which summed up the filfulment, in the course of the Ninth Five-Year Plan, of the plan for the creation of a new technique for introducing the leading technology and for the mechanization and automation of manufacturing processes. The conference also noted the way in which the goals of the Ninth Five-Year Plan have been carried out in regard to accelerating the technical re-equipment of production facilities, the widespread introduction of progressive techniques and technology, which ensure improved quality of production and higher productivity, increasing the return on investment, the economy of material resources, and improving working conditions.

The two conference panels, technological and metallurgical, devoted much attention to the development of the atomic power machine building industry which should increase the production of equipment for atomic power plants 2.5-3 times during the Tenth Five-Year Plan while at the same time improving the production base and increasing the unit power plant, reliability, maneuverability, and economy of power plant produced.

The conference discussed the long-term research and design work. The most important projects were: development of plant for series-produced atomic power plants with VVÉR-1000 (water moderated water-cooled) reactors; replacement of VVÉR-440 reactor blocks by VVÉR-500, standardized with VVÉR-1000 blocks; development of reactor equipment for atomic power plants with an RBMK reactor rated up to 1500 MW; and creation and utilization of the equipment for atomic power plants with blocks of fast reactors.

The conference noted how extremely important it was that production capacity be introduced and mastered at the Volgodon Atommash factory and its metallurgical base in the Kamator foundry and foreshop during the Tenth Five-Year Plan. Accordingly, the conference urged all specialists in the relevant branches to cooperate in every possible way in constructing and outfitting these factories and also in training personnel. Once these factories are commissoned, the atomic power machine industry will have been elevated to a new level and stage of equipment of the production base.

In a resolution, the First Minénergomash Technological Conference urged that the production associations, enterprises, and branches of scientific-research, design and construction, and technological institutes ensure unconditional fulfilment of goals of the Tenth Five-Year Plan which were discussed at the conference in regard to the development of new techniques and the promotion of advanced technology, mechanization and automation of production processes, and automated control systems.

It was decided to hold the second technological conference in 1978.

Translated from Atomnaya Énergiya, Vol. 42, No. 2, p. 150, February, 1977.

SOVIET – BRITISH SEMINAR ON FAST REACTORS

Yu. V. Markov

The main program of the seminar, which was held in Great Britain in October 1976, dealt with various aspects of the design of equipment and monitoring and control instruments for the sodium-cooled fast reactors CFR and BN-600.

Two sodium-cooled fast reactors are in operation in Great Britain at the present time, the experimental DFR with an electrical power of 14 MW and the 250-MW prototype power reactor PFR which has attained 60% of its rated capacity. Minor leaks in the gas cavity of the steam generators and which were primarily responsible for difficulties in them have been eliminated and the further program of utilizing the PFR is associated with a gradual increase in power. The operation of the reactor at the power mastered is characterized by the stability of the principal controlled parameters. Now that the PFR at been mastered, it is proposed to halt operation of the DFR, as was reported, although at the present time it is being used to carry out experiments on safety related to the study of transient processes of reducing the sodium flow through the reactor as well as for irradiation material testing.

The development of a commercial fast reactor, the CFR, at the given stage is characterized by the imperfection of the individual assemblies. Firm dates have not been set for the construction and the construction site has not been selected. The design for a CFR with an electrical power of 1320 MW(E) envisages the use of a vessel of prestressed ferroconcrete as a protective jacket which surrounds a 25-m diameter reactor tank of austenitic steel. Cooling of the active zone is ensured by six main circulating pumps and eight intermediate heat exchangers inside the reactor tank.

The basic concept of the construction of such a reactor is that of factory fabrication of equipment and assemblies of units leading themselves to transport as much as possible. These would then be assemblied in a workshop built especially for the purpose on the atomic power plant site. The assembly technology envisaged is that of moving the root with an assembled weight of 3000 tons onto the reactor vessel; consequently, the vessel is sunk 30 m into the ground. The reactor equipment is installed in a hermetic shell designed to withstand a rise in internal pressure by 2 bars because of an accident and to withstand the external shock loads from an aircraft falling on it. The structures and the equipment also allow for the effect of seismic loads with accelerations of up to 0.25% g. It is assumed that the CFR will take six years to build, from the start of actual construction to filling with sodium, and one year will be required for finishing work.

Although some technical solutions common to the designs of the PFR and CFR can be traced, there are also major differences. For example, the packet-reloading system in the CFR has a direct mechanism and three rotating plugs instead of a pantograph and one rotating plug. The evaporators and superheaters of the steam generators are to have one-piece U-shaped tubes made of ferrite–pearlite steel containing 9% chromium; tube plants have been eliminated from the designs and individual tubes coming out of the lid of the module are brought together in group collectors. The CFR will use superheating of steam instead of sodium.

Both the operating PFR and the projected CFR are highly automated facilities where provision has been made for a large volume of in-pile measurements, the signals from these measurements being fed into the controlling computer system. This system of the PFR power block consists of two Argus-500 computers made by Ferranti and performs the functions of data processing and display, monitoring of the energy block, and reactor protection with respect to the parameters of in-pile monitoring (the basic protection of the reactor does not depend on the controlling computer system). In view of the low probability that both computers will malfunction the volume of individual monitoring and control of the technological equipment is insignificant, but sufficient to be used for controlled shutdown cooling of the reactor.

Translated from Atomnaya Énergiya, Vol. 42, No. 2, pp. 150-151, February, 1977.

Much attention is being paid in Britain to the construction of in-pile monitoring devices and to outfitting reactors with them so as to increase the shutdown safety. For example, positive results have been obtained in the development of coaxial thermocouples, measuring 1 mm in diameter and operating with the hot junction immersed right in sodium at a temperature of 600°C, possessing in inertia of no more than 0.1 sec, and measuring temperatures at a rate of 30°C in 0.1 sec. Development work is under way on small flow sensors based on the distortion of a magnetic field in the sodium flow, the response of these sensors being 50% in 0.1 sec. Structurally, these sensors may contain several thermocouples of the type indicated above. Such sensors, installed above each packet, can be used for the scram protection system. For the CFR, work is under way on neutron flux sensors and cables for them, to be placed in dry holes alongside the active zone and to operate at temperatures of up to 625°C, neutron flux densities of about 10^{11} neutrons/cm^2·sec, and γ-ray fields of the order of 10^5 R/h.

Work in the area of the safety of reactors and steam generators is being conducted on a quite wide scale in Risley and Winfrith Heath, both on model stands for experimental completion of design techniques and on sodium construction. The instrumentation and the devices for automated data collection and processing are based, as a rule, on standard manufactured elements.

Research on the safety of fast reactors with studied on the explosive processes in hypothetical accidents due to the interaction of molten fuel with sodium are being carried out on a complex of stands, introduced in Winfrith Heath at the end of 1975. In the experiments, scientists are studying the behavior of models of the reactor vessel, in -vessel devices, and the reactor shield with a sudden energy release for the purpose of developing design methods. Processes are recorded by strain gauges, piezoceramic pressure pickups, and high-speed filming. In the first stage the experiments are being carried out with the molten aluminum interacting with water.

It should said that the consideration of various aspects of reactor safety and environmental protection in connection with the effects of the undertakings of future large-scale nuclear power generation were the subject of a report by a committee headed by Prof. D. Flowers, which recently reported to the government on its work. Having considered the place and role of fast reactors in the overall structure of the fuel and energy balance of the country, the committee came to the conclusion that since the problems associated with the processing of irradiated fuel to extract the plutonium and with the storage of large quantities of radioactive waste have not yet found a satisfactory solution and do not ensure guaranteed safety and environmental protection, it would be premature to focus on a program of extensive use of fast reactors for power generation over a period of several decades (50 yr or thereabouts). This conclusion was evidently not made without taking account of the North Sea Oil resources and, although, as follows from the press, far from being indisputable, it does not negate the necessity of continuing studies on fast reactors and the development of the CFR commercial reactor.

On the whole, the meeting of Soviet and British specialists confirmed the existence of a broad spectrum of questions of mutual scientific and technical interest.

MEETING OF INTERNATIONAL WORKING GROUP ON FUTURE ACCELERATORS AND ON THE DEVELOPMENT OF HIGH-ENERGY PHYSICS

A. V. Vasil'ev

With unflagging interest scientists the world over have been following the results of basic research on energetic charged particles which is carried out on accelerators in order to obtain a deeper insight into the basic laws governing the structure of matter. The enormous interest taken in the physics of the nucleus and elementary particles is due to the fact that each new stage in deepening our knowledge of the properties of matter and the laws governing is associated with new purposeful practical uses of this knowledge for the welfare of mankind. The history of the development of this area of science in not much more than half a century provides many examples of how the discoveries by scientists and inventions by engineers consituted the basis for creating energy sources of unheard of power, new technological processes, fundamentally new engineering, and new methods of research in related sciences.

In a relatively short time there has been a significant development of the basic experimental base of physical research, i.e., accelerators of charged particles. In our day and age, to organize complicated physical experiments scientists have at their disposal various sorts of beams of elementary particles with an energy of up to hundreds of billions of eV and an intensity of up to 10^{12} particles/sec.

As a result of the historical development of the science physicists in all countries investigating the inner secrets of matter naturally began to actively collaborate with each other. Much success in research on the particles comprising our world and the laws which govern them has been achieved precisely because of such collaboration.

Further development of elementary-particle physics calls for even more sophisticated, powerful, and expensive facilities. For this reason it is desirable to coordinate efforts in the construction of facilities being developed at the present time on a regional scale or separately by the industrially most advanced countries. There is an obvious need of broader collaboration in the development of projects for new, more powerful accelerators and joint use of the experimental base in existence or under construction.

Just such questions of coordination and collaboration in the development of elementary-particle physics were discussed at the first meeting of the working group on future accelerators and the development of high-energy physics, which was held in May 1976, at the Institute of High-Energy Physics in Protvino. A resolution about the organization of a working group was adopted in March 1975, at a seminar which eminent physicists of the USSR, the USA, the Joint Institute of Nuclear Research (JINR, Dubna), and CERN held in New Orleans (USA). The working group consisted of: A. Ts. Amatunin, A. M. Budker, A. A. Logunov, A. A. Vasil'ev, V. A. Glukhikh, M. A. Markov, L. D. Solov'ev, A. N. Skrinskii, I. V. Chuvilo, and V. A. Yarba (USSR); V. Weisskopf, R. Wilson, M. Barton, J. Björken, R. Diebold, and L. Lederman (USA); V. P. Dzhelepov and K. Lanius (JINR); J. von Dardel, U. Amaldi, K. Jensen, A. Russe, D. Thomas, and D. Houseman (CERN); and J. Mamagauchi (Japan).

The working group prepared a report which reviews the present state of knowledge of the fundamental laws governing the structure of matter and problems requiring the construction of a more modern experimental base. The report also presents information about accelerators now under development (see Part II of Table 1). It is assumed that superconducting magnets will be used in proton machines and the latest advances in superconductivity make this assumption highly realistic. Examples of preliminary studies of large accelerators and storage rings with a mean radius of 5-15 km and a cost of about 1 billion dollars are listed in Part II of Table 1.

Translated from Atomnaya Énergiya, Vol. 42, No. 2, pp. 152-153, February, 1977.

TABLE 1. Existing and Planned Accelerator Projects for Superhigh Energies

Country or region	Name of facility	Energy in laboratory system, GeV		Energy of colliding particles in CM system, GeV				Perimeter of facility, km
		protons	electrons	proton–proton	proton–antiproton	proton–electron	electron–positron	
I-Japan	Tristan	180	17	360	—	~ 110	34	~ 2
GFR	PETRA *	—	19	—	—	—	38	2,3
CERN	LSR	400	20	800	800	180	—	6,4
	LEP	—	< 100	—	—	—	< 200	51
USA	PEP	200	18	—	—	100	36	2,2
	Doubler	1 000	—	—	—	—	—	~ 6
	ISABELLE	200	20	400	—	130	—	~ 3
	POPAE	1 000	20	2 000	—	280	—	5,5
USSR	VEPP-4*	—	7	—	—	—	14	
	Accelerator-storage complex	2 000	20	4 000	4 000	400	—	~ 18
II. International accelerator	With fixed target	10 000	—	20 000	20 000	—	—	30—60
VBA	With colliding electrons and positrons	—	> 100	—	—	—	> 200	> 50

*Under construction

These examples may be considered to be the initial stage in laying the foundations of an inter-regional experimental program on accelerator complexes in high-energy physics after 1990.

The members of the working group expressed confidence that the technological progress in coming decades would yield more economic and efficient solutions for high-energy accelerators under construction and on the drawing boards. The working group recommends continuous inter-regional collaboration and exchange of information, with the technological aspects of importance to projects for future accelerators being incorporated into existing research programs. Duplication can thus be reduced to a minimum.

A broad and active experimental program in high-energy physics can be carried out by applying present-day techniques, but improvements are to be expected in many physical methods. The use of integrated circuitry will significantly reduce the cost of multiwire proportional and drift chambers which already ensure a high accuracy of about ~ 50 μ and will be extremely useful for measuring angles and momenta. Calorimeters with liquid argon and uranium plates are convenient for work at high energies, especially in studying multiparticle processes over a wide range of angles. The Cerenkov-counter technique should be improved so as to provide better velocity resolution with an increase in the acceptance. At an energy running into hundreds of GeV or more detectors based on transient radiation will replace Cerenkov counters. An important role in the control, reception, and initial analysis of experimental data will be played by microprocessors, i.e., special-purpose computers. For efficient operation of large spectrometric magnets it is necessary to ensure that strong magnetic fields are obtained at lower power consumption per unit than in present-day magnets. Experimental data should be exchanged between physics centers throughout the world in the fastest and most efficient manner in order to optimize data analysis. In particular, it is proposed to study the possibility of transmitting data by satellite.

In its conclusions and recommendations, the working group proposes greater joint use of regional accelerators by scientists of various countries on the basis of existing or future new systems of accelerating understandings and agreements. At the same time, it is advisable that joint research be pursued on promising new systems of accelerating and experimental technique within regional accelerator projects now being worked out. International collaboration is also envisaged in investigations leading to the creation of the next generation of accelerators for superhigh energies after the regional projects listed in Table 1 are realized. These accelerators will be so large that they can be built only by the joint effort of all the regions concerned. As was noted in this report, the development of an accelerator complex for superhigh energies entails extremely complicated scientific, technical, and organizational problems that require systematic study and discussion. The working group recommends that such a discussion be started in the near future and proposed to the IUPAP commission that working groups and meetings similar to the one described be organized.

SECOND SYMPOSIUM ON COLLECTIVE METHODS OF ACCELERATION

V. P. Sarantsev

The symposium, which was held in Dubna from September 29 to October 2, 1976, was attended by 120 specialists from various scientific centers the world over. The largest number of participants came from the USSR and the USA. The 85 papers discussed at the symposium dealt with three main areas: accelerators with electron beams, and production and shaping of high-current electron and ion beams.

Accelerators with Electron Storage Rings. The work done in this area in Garching (GFR), and at the Institute of Theoretical and Experimental Physics and in Dubna (USSR) is developing the well-known initial scheme envisaging injection of electrons already possessing relativistic energy into a magnetic field into an orbit of large radius and then compressing the ring to the required size in a growing magnetic field. The electron bunch so prepared can then be accelerated along its axis.

A group at the University of Maryland (USA) is developing a scheme with longitudinal compression of a tubular beam into a ring. And, finally, a group at the Scientific-Research Institute of Nuclear Physics at the S. M. Kirov Polytechnic Institute of Tomsk is experimenting with "mirror" capture of a compensated electron beam near a conducting wall. The goal of the work is to obtain rings of electrons of maximum density and high accelerating fields for ions. In the traditional area employing radial adiabatic compression of the electron ring in a magnetic field, the greatest impression was made by the results of starting up the prototype of a heavy-ion accelerator in Dubna. This facility has produced electron rings with maximum parameters with respect to both the number of electrons and the electron density in the rings. The features of the facility are: metal walls near the ring, a quite high conductivity, a high coefficient of compression of the electron ring in a pulsed field (~10), and a good quality of the beam of injected electrons ($\Delta E/E \sim 1$-2% and emittance 30 mrd·cm). These features determined the parameters of the electron ring after compression: radius R = 3.5 cm, section half-size a = 1.5-2 mm, number of electrons in ring 10^{13}, field of ring 50 MW/m. Such rings are being envisaged for accelerating xenon ions in a decreasing magnetic field over a length of 85 cm. The proposed ion energy is 1.5-2.MeV/nucleon and the intensity 10^{11} ions/ring.

In work carried out over the past several years on the Schuko facility, constituting a single-coil system for the rapid compression of the electron ring (~10 sec), the Garching group performed experiments on the compression of an electron ring and its acceleration with hydrogen and helium atoms. As a result, optimal conditions of compression were found for the given facility. And although the inadequate quality of the ring (the field strength in the compressed ring was 5 MW/m) and the short accelerating length (~5 cm) did not permit an accelerator to be built for the experiment, this facility did make possible a cycle of investigations which underlay the Pustorex designed for physical experiments with heavy ions at energies of 10-100 MeV/nucleon. Structurally, it has several distinctive features. The principal one is the combination of a fast system of ring compression (35 μsec) with a system of acceleration in a decaying time-constant field produced by a superconducting solenoid. Consideration has been given to the possibility of obtaining highly ionized ion states in the ring. Nevertheless, the accelerating field of the ring is taken equal to 16 MW/m, primarily because of the insufficiently good qualities of the beam.

An interesting scheme for an ion-accelerating facility was presented at the symposium by the group from the Institute of Theoretical and Experimental Physics (ITEP). This group carried out calculations on optimizing the acceleration of a ring bunch with a magnetic core of varying cross section inside the ring. Good results were obtained concerning the transmission of transfer of the stored electron energy to ions in the accelerating process (50%). On the basis of the calculations a scheme was proposed for a facility to accelerate rings by using a rebuilt induction electron accelerator and a compressor with ring parameters $a/R = 10^{-1}$, providing for acceleration of protons to 1 GeV and uranium ions Z/A = 0.2 to 0.1 GeV/nucleon.

Translated from Atomnaya Énergiya, Vol. 42, No. 2, pp. 153-154, February, 1977.

A scheme of longitudinal compression for obtaining ring bunches is being developed by the University of Maryland group. For the purpose, the group is using a one-gap accelerator, especially adapted to produce a hollow cylindrical beam. The electron energy is 0.5-3 MeV, the beam current is 1-60 kA, and the pulse duration is 30 nsec.

The main experiments were carried out for a beam with an energy of 2.5 MeV and a current of 1-8 kA. In the first stage, the kinetic energy of the electrons was transformed into rotational energy of the electrons by means of a magnetic field gradient. Here the longitudinal velocity was reduced to 0.1 of the speed of light and the pulse duration was shortened to 1 nsec. The cylinder radius was 6 cm and the radial thickness was $\Delta R = 0.5$-1 cm. The longitudinal dimension of the cylinder decreased to 10 cm. The number of electrons in this formation was $(1-8) \cdot 10^{13}$.

In the near future this group is to carry out experiments in conjunction with the Garching group on further compression by using retardation near a conducting wall and also to effect the capture of ions in an electron ring and acceleration in a decreasing field over a 2-m length.

Acceleration of Ions in Electron Beams. Another attempt to sum up the experimental data and to interpret them from the point of view of well-known representations of the mechanism of acceleration was made at the symposium by K. Olson (USA). Having analyzed the data of the principal experimental work, he presented an improved model of the potential well formed at the ionization front produced by a high-current beam in a gas. The main conclusion from such a model was that the acceleration process could not take place at a beam current below a critical value for the given geometry of the drift space and that the energy of the accelerated particles was independent of the electron current at a current above the critical value. Indeed, in experiments for electron currents ranging from 6 to 230 kA no significant difference was observed in the accelerated-ion energy. However, this model ran into serious difficulties. A paper by S. Putnam and B. Akker (USA) presented the latest experimental data on determining the dependence of the accelerated-ion energy on the electron current and the electron-beam energy. A pronounced difference from the Olson model was obtained. Thus, the mechanism by which the ions in a gas are accelerated in a high-current electron beam remains an open question. The high quality of the experiments carried out in the P. N. Lebedev Institute of Physics, Academy of Sciences, USSR, as well as in American Institutes gives reason to hope that in coming years control experiments will be performed, making it possible unambiguously to determine the mechanism of acceleration of such ions.

Obtaining and Shaping High-Current Electron and Ion Beams. High-current electron accelerators have become quite common instruments enabling research to be conducted on collective acceleration, wave generation, plasma heating, etc. Many problems in applications are being solved on these accelerators. The symposium devoted much attention to the discussion of projects for new accelerators with a pulse power of 10^{14} W which enable scientists to draw near to the solution of problems of the beam thermonucleus. Particular interest was aroused by the project of the Angara facility presented by the I. V. Kurchatov Institute of Atomic Energy.

However, interest in high-current electron accelerators as such was somewhat diminished at the symposium primarily because of the progress made in constructing high-current ion accelerators. Just a few years ago it was still difficult to employ conventional electronics to obtain ion streams because of the low coefficients of energy transfer by electrons to ions in an ordinary diode. However, in the past two years research and trials have produced a whole class of ion diodes which can be used to obtain proton streams with an energy of ~1 MeV and a pulsed current of 200 kA. And, what is especially important, the efficiency has been increased practically to 100%. A group from Cornell University (USA) reported on this work. In particular, the group gave data on research on reflex diodes and with magnetic insulation in which maximum efficiency has been attained.

The discussion on the problems involved in the use of ion beams noted three aspects: obtaining a thermonuclear reaction, generating neutrons, and producing an Astron-type configuration for plasma heating. To accomplish the latter, a number of experiments have been carried out on injection of ions into a magnetic field and compression of the resulting ion rings to obtain a rotation of the magnetic field because of the magnetic self-field of the ring. And although no rotation of the field has yet been achieved, the results in storing $6 \cdot 10^{16}$ ions in such a ring speak for themselves.

In the general opinion of the participants, the symposium was interesting and useful.

FOURTH INTERNATIONAL IAEA CONFERENCE ON PLASMA PHYSICS AND CONTROLLED THERMONUCLEAR FUSION

É. I. Kuznetsov

More than 400 delegates from 26 countries attended the latest IAEA conference on controlled thermonuclear fusion held in Berchtesgaden (GFR) from October 6-13, 1976. The 165 original papers presented at the conference sessions covered practically all areas of research in the physics of high-temperature plasmas and reflected the latest results of work on thermonuclear power reactors. They discussed theoretical and experimental research on closed installations of the tokamak and stellerator type, including the influence of impurities on the plasma behavior, plasma heating by the injection of atomic hydrogen and by radio-frequency and turbulent methods; the results of work on open magnetic traps, equipment of the plasma focus type and various pinches; radio-frequency methods of plasma confinement and stabilization; initiation of controlled thermonuclear reactions by laser radiation and relativistic electron beams; the interaction of beams with plasma; the properties of plasma with thermonuclear parameters and projects for future thermonuclear reactors.

More than a third of the papers were devoted to tokamaks which are continuing to be developed successfully and, as before, remain the most reliable prototype of the quasistationary thermonuclear reactor. The large tokamaks were built in 1975, the T-10 (USSR) and the PLT (USA). At a longitudinal magnetic field strength of 35 kG and a discharge current of 0.4 mA the T-10 produced a plasma with a density of $6 \cdot 10^{13}$ cm^{-3} with electron and ion concentration of 1 and 0.7 keV, respectively, and a plasma confinement time of up to 0.06 sec in better modes. A yield of up to $3 \cdot 10^{9}$ thermonuclear neutrons per discharge was observed when the chamber was filled with deuterium. The amount of impurity in plasma proved to be very insignificant (effective charge < 2). Similar results were obtained at a similar discharge current and strength of longitudinal magnetic field in the PLT facility, which came into service somewhat later; the plasma, it is true, proved to be highly contaminated with impurities (effective charge about 5-6) and power time about 0.03 sec.

Important physical results were produced by experiments performed on the T-11 (USSR), ORMAC (USA), TFR (FRANCE), and DITE (Great Britain) installations to study the processes of plasma heating by the injection of fast hydrogen atoms. In the TFR the ion temperature was successfully doubled with an injected deuterium beam power of 450 kW and a record ion temperature of 1.9 keV was obtained.

In the American installation Alcator, with a longitudinal magnetic field of 81 kG it proved possible to increase the plasma density in the center to $6.6 \cdot 10^{14}$ cm^{-3}, with the power confinement time increasing to 18 msec and the effective charge decreasing. Encouraging results were given by Doublet IIA (USA), by a tokamak with a plasma pinch of elliptical section, and the analogous TNT system (Japan). Adiabatic compression by a growing magnetic field in Tuman-2 (USSR) significantly increased the plasma parameters, and in particular increased the power confinement time fivefold. Experiments designed to study the operation of a diverter, a device for removing contaminants from plasma, have begun on DITE (Great Britain).

Much attention at the conference was devoted to the problem of stripping instability which hinders an increase in the plasma density in tokamaks. Experimental data obtained on the Pulsator (GFR), T-4 (USSR), and TFR coupled with theoretical analysis clarified the picture of the onset of instability and led to the conclusion that the critical plasma density, above which instability arises, depends on the heating power. This means that the density required for the effective operation of a thermonuclear reactor can be obtained with an appropriate increase in the heating power. Significant advances have recently been made in the theoretical investigations and as evidenced by papers presented to the conference on the nonlinear theory of the development of helical magnetohydrodynamic and drift instabilities as well as on the numerical simulation of plasma behavior in tokamaks.

Translated from Atomnaya Énergiya, Vol. 42, No. 2, pp. 155-156, February, 1977.

The discussion of the experimental and theoretical research that took place at the official and numerous unofficial meetings permits the assertion that plasma with thermonuclear parameters will be obtained in tokamaks in the near future and that a physical fusion reaction will be realized.

Interesting and important results have been obtained on the large new stellarators Liven'-2 (USSR), Cleo (Great Britain), Vandelstein-VIIA (GFR), and IPP-TP (Japan).

In Liven'-2, with ohmic heating at a discharge current of 20 kA and magnetic field of 14 kG the plasma had a density of about 10^{13} cm^{-3}, an electron temperature of 0.4 keV, and a power confinement time of 8 msec. Experiments with Cleo, which was operated in both the stellarator and tokamak modes, showed that a poloidal magnetic field in a stellarator leads to an improvement in plasma confinement. Earlier studies on plasma confinement obtained on the Stellarator-C (USA) proved to be wrong because of mistakes in the design of the machine. Although technically complicated, stellarators deserve to be developed further.

Research on ion-cyclotron heating is continuing on the stellarators Uragan-2 (USSR) and Heliotron-D (Japan) and stable plasma with a density of 10^{12} cm^{-3} has been produced on the toroidal machine Elmo Bampi Torus (USA) with heating by electron cyclotron resonance. Work has been recently undertaken on a new method of plasma buildup, i.e., by injection of solid granules of deuterium. It may be expected that with a radius of 200-400 μ and a velocity of 10^5-10^6 cm/sec, the injection of these granules will enable the parameters of plasma in closed systems to be improved substantially.

The few papers on open magnetic traps included a noteworthy one about work on the 2XP B (USA). Thanks to a new method of feeding cold ions through a magnetic mirror externally to stabilize hot plasma in a trap, it was possible to obtain a stable plasma with a density of $1.5 \cdot 10^{14}$ cm^{-3}, an ion temperature of 10 keV and a lifetime of 0.3 msec. Great interest was aroused by a new system presented by scientists of the Institute of Nuclear Physics, Academy of Sciences, USSR; this was a magnetic trap with double mirrors which makes it possible to appreciably increase the ratio of the thermonuclear energy yield to the energy input.

The conference heard papers from practically all laboratories of the USA, the USSR, Japan, France, and Great Britain engaged in research on plasma heating by laser radiation, especially in research on the absorption and reflection of light, production of fast electrons and ions, anomalous energy transfer in plasma, in well as compression of glass microspheres filled with deuterium and tritium. Although quite extensive experimental data are available there is, as yet, no complete clear picture of the mechanism of absorption of radiation and production of fast particles. Noteworthy among the latest results is the finding that with a radiation flux of more than 10^{12} W/cm^2 the entire energy contribution (more than 50% of the incident energy) is due to resonance absorption, the character of the interaction remaining practically unchanged with variation in the wavelength, which is equal to 1 or 10 cm (USA, Japan, USSR).

In experiments American scientists (the KMS-Fuji Laboratory) subjected microspheres to a cubic compression of up to 2000 times, the temperature after the compression being 1.5 keV in the center of the target.

Numerical calculations performed for quite large multilayer hollow targets in a number of laboratories (USSR, USA) indicated the possibility of achieving a value of 1000 for the ratio of thermonuclear energy yield to energy input at a laser radiation energy of 0.1-1 MJ provided that the instabilities which destroy the thin shells can be eliminated.

As reported in a number of papers, installations employing neodymium-glass lasers with an energy of 10 kJ (USA, USSR) and CO_2 lasers with an energy of up to 10 kJ will go into service in coming years for use in initiating the physical reaction of fusion.

In work on heating with electron and ion beams, a study has been made of the heating of targets and plasma in a magnetic field as well as the information of electron and ion rings to confine plasma in open magnetic traps and systems of the Astron type. A new approach to heating targets, by relativistic electron beams, was presented and demonstrated by Soviet scientists (I. V. Kurchatov Institute of Nuclear Physics). A dense deuterium target has been heated by a 1.5-kJ beam in the Triton installation and a yield of $3 \cdot 10^6$ thermonuclear neutrons was recorded. A beam heated the outer shell of a conical model of a target with $Z \gg 1$. As a result of radiative heat conduction a significant part of the energy was transferred to the inner shell with an effective charge of 1. In the process, because of the smaller mass of the inner shell it was possible to achieve a velocity sufficient to ignite the deuterium fuel with a significantly smaller energy contribution to the first shell than in the usual heating methods. American scientists (Sandia laboratories) reported in their papers that they had obtained a current density of 1 MA/cm^2 in electron beams and a velocity of $3.5 \cdot 10^6$ cm/sec for the shell of a one-layer target, and also that they had observed an anomalous energy contribution to the thin shell.

When plasma was heated by electron beams in open magnetic traps (USA, Great Britain), the temperature exceeded 1 keV, the density was 10^{16} cm^{-3} (at a pressure of 0.1 torr). The beam current density was 20 kA/cm^2 and the pulse duration was 150 nsec. The nature of the effects which result in heating is not yet clear.

Serious attention at the conference was paid to work on obtaining high-current ions beam with reflex triodes and with coaxial diodes with magnetic insulation and planar diodes with magnetic self-insulation (USA). Ion beams with a maximum current of 200 kA at an energy of 0.6-1.2 MeV and a power of more than $2 \cdot 10^{11}$ W were reported. The number of protons accelerated during a pulse was $3 \cdot 10^{16}$ and the angular divergence of the beam was 3-6°. It is proposed to use ion beams to produce ion rings and to heat the target shell. In the latter case, the energy required to ignite deuterium fuel proves to be several times smaller than in the case of electron beams.

Although they occupy an important place in the thermonuclear research program, investigations on systems with a high ratio of plasma pressure to the confining magnetic field have not thus far led to significant results. It may be hoped that the high level of the theoretical and experimental work being conducted in this area in the USSR, GFR, the USA, Great Britain, and Japan will make it possible to obtain high-temperature plasma and to effect its confinement with a more efficient use of magnetic fields.

As a previous conferences, one sesson was devoted to a discussion of projects for thermonuclear reactors for power generation. American scientists (Wisconsin University) presented a project for a thermonuclear reactor of the tokamak type, Uvmak III, taking the latest experimental data into account. In this version the walls were assumed to receive a higher thermal load from thermonuclear neutrons, i.e., 2 MW/m^2.

Projects for thermonuclear power reactors with a thermal power of 400-500 MW were also presented by the Argonne and Oak Ridge National Laboratories and by General Atomic (USA), and a project for a smaller one, about 100 MW, was presented by Japan. In a paper, British scientists (Culham research establishment) made a detailed analysis of the cost of building and operating a tokamak thermonuclear reactor.

The results of the conference testify to the rapid advances made in research on the physics of high-temperature plasma, in the qualitative comprehension of the processes which occur in various experimental facilities, and a significant extension of engineering and technological developments, necessary for creating the next generation of large thermonuclear reactors and for the future thermonuclear power industry.

EUROPEAN NUCLEAR PHYSICS CONFERENCE ON HEAVY IONS

V. V. Volkov

An international conference devoted to the nuclear physics of heavy ions was held in Cannes (France) from September 6-10, 1976. Although the conference was officially called European (it was organized by the European Physical Society) it was attended by scientists from all continents who are actively working in this area of physics.

Attention was centered on the interaction of two complex nuclei at relativistic and nonrelativistic energies. The largest number of papers (three reviews and 13 brief communications) were devoted to a new type of reaction between complex nuclei, deeply inelastic transitions (DIT), discovered several years ago in Dubna and the Laboratory of Nuclear Reactions. The strong coupling between the entrance and exit channels of the reaction is conserved in DIT, as in direct processes. Products of DIT "do not forget" either the direction of motion of the initial nuclei or their atomic numbers and mass numbers. The angular distributions of DIT are highly asymmetric: light products emerge primarily at low angles to the beam. The charge and mass distributions have a maximum near A and Z of the initial nuclei. Moreover, their kinetic energy is close to the height

Translated from Atomnaya Énergiya, Vol. 42, No. 2, pp. 157-158, February, 1977.

of the exit Coulomb barrier and does not depend on the energy of the bombarding ions just as is observed in fission reactions. The laws established in the cross sections for the formation of DIT products indicate that a partial statistical equilibrium has been realized in the system of two interacting nuclei in regard to exchange of thermal energy and excited nucleons. Figuratively speaking, DIT is a "physical centaur" among the known mechanisms of reactions with heavy ions. The peculiarity of these reactions is related to the formation of a dual nuclear system (DNS) in deeply inelastic collisions. Other names for it are composition system and intermediate nuclear complex. In a DNS the surfaces of the nuclei strongly overlap and their relative velocity is low. The nuclei of the system intensively exchange energy and nucleons with each other and, at the same time, retain their individuality within wide limits because of strongly coupled inner-shell nucleons. Possessing appreciable magnetic moments, DNS rotate as a whole like a dumbbell. The lifetime of such a system in deeply inelastic reactions is shorter than the time of one rotation of the system but is ten times the characteristic nuclear time ($\sim 1 \cdot 10^{-22}$ sec). As a result, a partial statistical equilibrium manages to establish itself in the DNS with respect to exchange of energy and excited nucleons. In deeply inelastic transitions a significant part of the orbital angular momentum in the process of dissipation of kinetic energy goes over into the spins of the nuclei in the system. As a result, rapidly rotating nuclei with angular momenta running into hundreds of $\hbar$ units are formed as DIT fragments. Experiments in which γ radiation of DIT products (multiplicity of γ quanta) were observed confirmed the conclusion that there is total dissipation of the tangential part of the kinetic energy in deeply inelastic collisions of nuclei.

Deeply inelastic transitions gave impetus to the development of a new nuclear physics approach to the description of the interaction of two complex nuclei. A characteristic feature of dual nuclear systems is that they evolve in time, continuously going from one state to another in a configuration corresponding to the minimum potential energy of the system. Therein lies the fundamental difference of DNS from nuclear molecules for which the quasistationary nature of states is characteristic. The theoretical models used to describe reactions and the reactions of the decay of an excited compound nucleus are incapable of describing the evolution of DNS since a time dependence of their state is characteristic of them. Papers read at the conference considered theoretical approaches based on the mathematical apparatus of nonequilibrium statistics: master equation and Fokker–Planck equation. In this approach the exchange of energy and nucleons between DNS nuclei is considered as a process of transfer and diffusion.

Experiments with krypton, xenon, and uranium ions showed that for the heaviest ions DIT are the dominant nuclear process, making the principal contributions to the reaction cross section. It is evidently altogether impossible for uranium nuclei to amalgamate in a collision to form a compound nucleus. Coulomb repulsion increases so much that the nuclear forces are no longer capable of keeping the two nuclei in contact. They manage only to exchange a number of nucleons.

Unfortunately, the information available about the interaction of nuclei at relativistic energies is still very meager and contradictory, and does not yet permit definite conclusions to be made about the formation of shock waves in the collision of two fast nuclei. Theoretical consideration of such collisions within a statistically microscopic approach did not confirm the formation of a shock wave front, unlike the conclusions of the group led by V. Greiher (GFR). New data obtained in Berkeley (USA) about the interaction of neon ions possessing an energy of 250, 400, and 2100 MeV/nucleons with uranium nuclei, yielding protons, deuterons, tritons, α particles, and ^{3}He nuclei, were interpreted without invoking the hypothesis of the shock-wave formation.

Reactions with heavy ions provide unique possibilities for obtaining rapidly rotating nuclei with spin, measured in tens of $\hbar$ units. A paper by Z. Szymanski (Polish People's Republic) showed that when the shell structure of nuclei is taken into account, their deformation as a function of the angular momentum by no means varies nonmonotonically as follows from consideration of the variation in the form within the framework of the liquid-drop model.

The possibility of isomeric states existing with large angular momentum is of particular interest. Such an isomeric state has been found in ^{152}Dy at an excitation energy of ~ 5 MeV.

The program of the conference in Cannes did not envisage discussion of the search for superheavy elements in nature and their synthesis in reactions with heavy ions; these topics were discussed in May 1976, as the third conference on the properties of nuclei far from the β-stability line. However, by the time the conference in Cannes began, a number of new investigations in this area had been carried out and the organizing committee decided to hold a special session on superheavy elements.

Let us recall that the July 1976 issue of Physics Review Letters carried a paper by American scientists (R. Gentry et al.) who reported that they had observed stimulated α radiation from nuclei of superheavy elements. Small crystals of the mineral monazite, found in the center of gigantic "halos" discovered in mica from

Madagascar, were exposed to irradiation by fine proton beams. The gigantic "halos" might have been produced by the α decay of superheavy elements and, if these elements have a sufficiently long lifetime, a number of their atoms might have survived to our time. The authors observed weak peaks of fluorescent x radiation in the interval between the Kx radiation of thorium and uranium and the Lx radiation of the rare earths, products of the spontaneous fission of uranium. The conclusion was that this is the fluorescent Lx radiation of superheavy nuclei that have not yet decayed. Proceeding from the energies of these nuclei, the authors obtained the atomic numbers of superheavy elements 126 and 124. The number of superheavy nuclei in the samples was estimated from the intensity of the peaks; a quite impressive quantity was obtained, hundreds of pg. By way of comparison let us point out that in the course of a search for natural superheavy elements over the past nine years at the Nuclear Physics Laboratory of the Joint Institute of Nuclear Research a sensitivity of one-thousandth of a pg/g of mineral in the samples studied was achieved. With this sensitivity, as a result of painstaking work it has thus far only been possible to map a promising direction for a search which could lead to the discovery of superheavy elements in nature.

The work of the American scientists was widely advertised by the American press. However, as shown by control experiments conducted in a number of laboratories and reported at the Canne conference, the paper by R. Gentry et al. proved to be wrong.

In Darmstadt (GFR) D. Schwalm et al. showed that when monazite is irradiated with protons of lower energy no additional peaks appear in the interval between the Lx radiation of uranium and thorium and the Kx radiation of rare earths. If the proton energy is increased, a peak corresponding to the Lx radiation of element 126 is indeed formed, but it is associated with nuclear radiation from the $^{140}Ce(p, n)^{140}Pr$ reaction. In Orsay (France) as well a negative result was obtained in an attempt to isolate superheavy elements from Madagascar monazite with a mass separator. It was shown that the content of superhigh elements in monazite relative to uranium is less than 10^{-12}. The Darmstadt scientists subjected about 20 g of monazite to chemical treatment, isolation of various fractions being followed by x-ray fluorescence analysis. No traces of superhigh elements were found. In Oxford (Great Britain) an attempt was made to use the back scattering of 50-MeV iodine ions in a search for super-heavy elements. When scattered from thorium and uranium nuclei at an angle of 170° iodine ions possess an energy of ~4 MeV, and when scattered from superheavy nuclei, ~10 MeV, Once again, no traces of superheavy elements were detected in monazite.

At the conference G. Seaborg (USA) presented provisional data about the synthesis of superheavy elements in reactions with ^{48}Ca ions. It should be noted that the first experiments on the synthesis of superheavy nuclei on a beam of ^{48}Ca ions were carried out by the NFL JINR. Numerous combinations were investigated in these experiments: targets of ^{232}Th, ^{231}Pa, ^{233}U, and $^{246-248}Cm$ were irradiated with ^{48}Ca ions. The American experiments used a ^{248}Cm target. Irradiation was carried out with 267-MeV ^{48}Ca ions, the energy of the extracted beam being about 1 μA. It was expected that at this energy the main contribution to the cross section for the formation of superheavy elements comes from the ^{248}Cm $(^{48}Ca, 3n)^{293}116$ reaction. The reaction products were subjected to chemical treatment and various fractions were separated, including inert gas fractions. The chemical treatment took about an hour, after which attempts were made to detect spontaneous fission, α decay, or β decay of superheavy elements. Superheavy elements were not detected at a cross section of $2 \cdot 10^{-34}$ cm^2. Since a superheavy element may prove to be short-lived, it is proposed to increase the speed of the techniques in subsequent experiments.

The conference in Cannes showed once again that the physics of heavy ions (nonrelativistic and relativistic) is one of the most dynamically developing areas of nuclear physics, opening up ever new opportunities to acquire fundamental knowledge.

THE 25th SESSION OF THE UN SCIENTIFIC COMMITTEE ON THE EFFECT OF ATOMIC RADIATION

R. M. Aleksakhin

Delegates from 20 member countries as well as representatives of a number of international organizations (IAEA, ICRP, FAO, UN Program on Environmental Research, etc.) participated in the work of the session which was held in Vienna (Austria) from September 6-16, 1976. This was the most representatives of all sessions held in 1969-1976, the period covered by the latest report of the UN General Assembly.

At its meetings, the physics subgroup (Chairman A. Jamme, France) discussed the conceptions and principal notions used to evaluate the effect of radiation on man. At the present time, the basic point of view in determining the consequences of irradiation of man rests on keeping a linear dose-effect relation (i.e., existence of the principle that there is no threshold in the effect of ionizing radiation) with extrapolation of the relevant data to zero irradiation dose. At the same time the deficiencies of this principle are quite obvious today. To date, no satisfactory experimental basis has been obtained for evaluating the effects of the effect of ionization radiation in small doses (up to 5-10 rd). Extrapolation of the irradiation risk, calculated from experimental data for large doses and their power, to doses close to or slightly above the background is of an especially formal character. The only argument in favor of such extrapolation is that it excludes the possibility of the irradiation hazard being underestimated. However, such a risk can, naturally, be overestimated. With the considerable expansion of the nuclear power industry, such an overestimation is undesirable since it hinders an objective analysis of the effect of atomic power plants on the natural environment and man.

More precise values have been given for the mean annual dose of radiation received by a person from the natural radiation background, these values for the gonads, lungs, cells lining the bone marrow, and bone marrow being 81, 130, 88, and 95 Grd, respectively. The principal sources of the natural radiation background are cosmic rays (about 31% contribution to the total dose), external irradiation from radionuclides present in the earth's crust (32%) and internal irradiation from ^{40}K incorporated into tissue. The global annual collective dose from the background of natural radiation for the population of the Earth is $3 \cdot 10^8$ man · rd (for lungs, this dose is approximately 30% lower).

Analysis of much experimental data on the dispersion in the biosphere of artificial radionuclides from nuclear weapons tests and the migration of these radionuclides through the biological chains into the environment was used to estimate the additional irradiation of the population from this source. The expected irradiation doses (i.e., those which will be produced by the time of the complete decay of the radionuclides introduced into the environment by nuclear tests) from explosions carried out up to 1975 is equal to a doubled natural radiation background over a period of 16 months for lungs and the gonads, 22 months for bone marrow, and 24 months for the cells lining the bone marrow. The greatest contribution to the expected dose from the fallout is from ^{14}C (7-32 Grd by the year 2000), the contribution ^{137}Cs as a source of external and internal irradiation is 38 and 16 Grd, respectively, that of ^{90}Sr as a source of irradiation of the bone marrow is 51-70 Grd, and that of ^{106}Ru and ^{144}Ce in external irradiation is 30 Grd.

The UN Scientific Committee on the Effect of Atomic Radiation (SCEAR) made an estimate of the collective irradiation doses (global, regional – to distances of 100-1000 km from the source, and local – within a 100-km radius) at all stages of the full nuclear-fuel cycle, from extracting nuclear raw material to storage of waste. The local and regional whole-body doses are (man · rd/MW(E) · yr): mining 0.003, fuel element fabrication 0.0001, nuclear power plant operation 0.03-0.5 (depending on the type of nuclear reactor), fuel-element reprocessing 0.025, and transportation of radioactive materials 0.003. Global collective doses in obtaining electricity from atomic power plants (in these units) are equal to ^{3}H 0.1, ^{85}Kr 0.2, ^{14}C 2.5, and ^{129}I 0.02 (on thyroid

Translated from Atomnaya Énergiya, Vol. 42, No. 2, pp. 158-159, February, 1977.

gland). Thus, the global collective doses are greater than the local or regional doses with world-wide use of nuclear energy. In 1974, when the production of electricity in atomic power plants was 59.5 GW(E), the global collective annual dose of irradiation (without account for local and regional doses) was $\sim 1.6 \cdot 10^5$ man·rd (i.e., was smaller than the collective dose from the natural background by a factor of more than 2000, e.g.

The meetings of the biological subgroup (chairman E. Pochin, Great Britain) considered a number of documents concerning estimates of the biological effect of radiation. In the discussion of radiation carcinogenesis in animals from the theoretical aspect, it was noted that the classical ideas of the role of somatic mutations and the activation of the oncogenous virus in the formation of cancer had drawn closer together. It was acknowledged that internal irradiation, especially from α radiation, was highly efficient but an increase in the cancer incidence in the event of internal irradiation is not identified directly from the relative biological effectiveness. Particular attention was paid to the propert diagnosis of tumours in experimental animals, critical evaluation of the nontumorous origin of the reduction in the lifespan and choice of the dose parameter for comparison with the effect.

A detailed analysis of the state of radiation carcinogenesis in man was given with the example of experimental results on cancer induced in Japanese who survived the nuclear explosions in Hiroshima and Nagasaki, data about thyroid gland tumors in Marshall Island inhabitants, and lung cancer in uranium miners (USA, France).

Extensive experimental data were generalized in the estimation of irradiation doses and possible effects from the use of ionizing radiation in medicine. It was pointed out that the term "collective irradiation dose" was inadmissible in the therapeutic application of radiation, and a more adequate parameter is the calculated mean internal dose on the gonads, bone marrow, and other critical organs. The effects of ionizing radiation on embryonic development were discussed thoroughly. It was noted that direct extrapolations of experimental data obtained with animals on the consequences of irradiation, especially for the later stages in the development of the embryo, are invalid. The level of professional irradiation at all stages of the complete nuclear-fuel was considered separately.

The genetic subgroup (Chairman A. Sobels, Beglium), working with a biological composition, considered the genetic effects of radiation. It was emphasized that the diverse processes occurring in the mammalian organism between the inception of a mutation and its manifestation do not provide a basis for extrapolating data on the radiosensitivity of one form of organism to another. The Committee took 100 rd for the dose which doubles the genetic damage in man. Hence, in the case of chronic irradiation in small dosages for a dose of 1 rd over 30 yr, it may be expected that in the first generation there will be 10 to 70 persons with various genetic deviations, including 2 to 20 persons with serious genetic defects. The insignificance of this figure is due to the fact that at the present time, because of all factors causing genetic deviations from the norm, 40,000 such cases arise spontaneously for every million births.

It was decided to convene the 26th session of the SCEAR in Vienna in April 1977; M. Klimek (Czechoslovak Socialist Republic) was elected chairman and F. Schtive (GFR), vice chairman.

POWERFUL SOURCES OF IONIZING RADIATION IN RADIATION TECHNIQUE

B. M. Terent'ev

An All-Union seminar on the application of powerful sources of ionizing radiation in radiation technique was held from September 12-16, 1976, at the Exhibition of the Achievements of the National Economy of the USSR. It was attended by 170 representatives of 50 organizations. They heard and discussed some 90 papers on the latest developments in radiation apparatus and processes employing various forms of ionizing radiation, and effective trends in the development and promotion of radiation technology were indicated.

The papers read at the seminar covered the following aspects: 1) the development and application of radiation processes with electron accelerators and radioisotopic sources; 2) methods and devices for determining the parameters and characteristics of radiation apparatus and processes; 3) and the efficiency of the development and industrial promotion of radiation processes and apparatus. Moreover, five papers reviewed the basic areas of radiation technology and equipment, including the experience and development trends in the production of radiation apparatus; radioisotopic γ-ray sources and electron accelerators in radiation-chemistry technology; safety and provision of metrological instrumentation for radiation-technological processes.

The seminar showed that considerable success has been achieved in radiation technology in the Soviet Union in recent years. In particular, various branches of the national economy of the country have introduced or are mastering industrial processes employing radiation apparatus for:

radiation-chemical synthesis (telomerization of ethylene, sulfochlorination of a hydrocarbon, etc.);

vulcanization of rubber (since 1972, e.g., a pilot plant has been producing thermostable self-adhesive electrical tape);

sterilization of medical supplies (the first commercial γ-ray unit Sterilizatsiya III has been built and two more are under construction);

graft polymerization of monomers (the first radiation-chemical cloth-finishing line using an electron accelerator);

processing of gaseous and liquid wastes;

processing of agricultural and food products.

The main trend at present is to create basic and standard designs of radiation apparatus that increase the economic effectiveness of the introduction of radiation technology in the relevant fields. Some of the more noteworthy among the developments which have resulted in pilot radiation installations and lines with electron accelerators (of the Élektron, ILU, ÉLIT, UÉ-0.4-600, Avrora, and other types) are: radiation modification of the thermosetting polyolefin film Termoplen, polyethylene flexible tubing and pipes for hot water supplies; application of pain and varnish coatings to metal, plastics, and wood; elasticization of synthetic materials in the production of artificial leathers; gas–liquid processes (removal of hydrogen from chlorine, preliminary purification of sewage). A paper by B. I. Al'bertinskii on the production of Portland clinker was interesting from the point of view of the search for promising applications of electron accelerators in power-consuming chemical processes. The temperature developed during the fast radiation synthesis of clinker is several hundred degrees lower than in the conventional method and the resulting product corresponds to high-grade Portland cement. Of other original papers in this area, particular mention should be made of "Promising uses of the electron accelerator for the production of lightweight conveyor belts" by M. Ya. Kaplunov et al. and "The technology of radiation modification of filled polymers by the use of electron accelerators" by R. E. Il'chenko et al.

Translated from Atomnaya Énergiya, Vol. 42, No. 2, p. 160, February, 1977.

The seminar noted that along with the production of radiation apparatus for individual processes on an industrial scale, it is desirable to organize the production of testing equipment and standard apparatus based on β sources and with effective ranges of application and extending the base of radiation research. Work should be continued on standardizing types and sizes and improving the technical and operating parameters of β and γ sources, particularly increasing the life, radiation yield, reliability, temperature stability, etc. There should be more research on the development and application of new radiation sources (for example, isotopic γ sources), ensuring that new effects are obtained when carrying out radiation-physical processes in solids (e.g., treating the microsurface of materials and products). The seminar felt that there was promise in creating apparatus with short-lived γ sources, i.e., with the working media of hot loops in atomic power plants in the case of the industrial-scale realization of processes requiring sources with a power of 100 kW or more, when the radiation component makes an appreciable contribution to reduced costs.

In reviews presented by V. V. Generalovoi, B. M. Tolkachev and Yu. D. Kozlov gave an evaluation of the methods and devices for determining the parameters and characteristics of radiation apparatus and processes. Their choice and concrete development depend on the problems being solved, the requirements with respect to the radiation process, the form, intensity, and quality of the source of ionizing radiation. A characteristic feature of this direction of work is that of solving the problem of standardization of methods for measuring the basic parameters of radiation fields in radiation technology.

The seminar recommended the adoption of unique methods of technological dosimetry suitable for work on radiation apparatus. Moreover, it drew attention to the necessity of commercial production of dosimetric systems, including systems for radiation installations with electron accelerators and with radioisotopic α and β sources, and noted the need of compulsory metrological expertise on dosimetric systems at various stages of development and commercial manufacture.

The theses of the papers presented at the All-Union scientific and technical seminar have been published and the collected reviews and original papers are to be published.

BOOK REVIEWS

A. K. Sledzyuk, N. S. Khlopkin,

B. G. Pologikh, A. M. Goloviznin,

and V. A. Kuznetsov

MARINE NUCLEAR POWER PLANTS*

Reviewed by V. S. Aleshin

The book under review is a new textbook for marine engineering students. The first of its eight chapters considers the physical foundations of nuclear power engineering: nuclear structure, radioactivity, nuclear reactions, and fission chain reactions and the conditions for their occurrence.

Chapter 2 presents the operating principles of the nuclear reactor, the classification of reactors by various features, the principal thermal circuits of steam-generating and steam turbine plants. The connection between the parameters of the primary and secondary circuits is considered and the parameters of the heat carriers of present-day atomic power plants are presented.

Chapter 3 describes the construction of various reactors, including those of the icebreaker Lenin, the ore carrier Otto Hahn, etc. This chapter considers the distinctive features of the design of fuel elements, technological channels, operating controls, and their actuators, as well as the design of the steam generators, circulating pumps of the primary circuit, volume compensators, ion-exchange filters, etc.

Chapter 4 presents the fundamentals of reactor physics. It discusses the principal propositions of the theory of neutron moderation and diffusion, the basics of the theory of homogeneous reactors and the distinctive features of heterogeneous reactors. It also gives some idea of the variation in the isotopic composition during reactor operation, reactor poisoning, and methods of compensating for excess reactivity. The characteristic features of heat exchange are presented, but they should have been considered in somewhat greater detail. A grasp of the physical essence of these processes is as important for operating personnel as knowledge of reactor physics is.

Chapter 5 gives the physical fundamentals of reactor control, presents the principal automatic control systems and safety systems, and describes and briefly analyzes programs for reactor power control.

Chapter 6 is devoted to dosimetry and the technique of radiation safety. Here the authors consider radioactive radiation and biological protection and give some general notions of the deactivation of equipment and organization of radiation safety on board ship.

The fundamentals of the operation of marine nuclear power plants are given in Chapter 7: preparation of steam generating plant for start-up, physical start-up of reactor, putting the plant into operation, changing the operating conditions of the reactor, stopping the operation of the plant, recharging the active zones, sustaining the required water conditions in the plant circuits, and some organizational aspects of the operation and maintenance of the atomic power plant.

Chapter 8 presents the general prospects for the development of economic indices for marine plants.

Thus, the textbook considers a wide range of topics and gives a full presentation of the design of reactors, the layout of steam-generating plants and steam turbine plants and auxiliary systems ensuring normal operation of the steam-generating systems, and also discusses the fundamentals of the theory and operation of steam-generating plant and radiation safety measures.

*V. A. Kuznetsov (editor), Atomizdat, Moscow (1976).

Translated from Atomnaya Énergiya, Vol. 42, No. 2, p. 161, February, 1977.

All topics are presented at the present scientific level, and complex physical phenomena are described in a readable form. The book is written in a lucid, precise langugage, is not overloaded with complicated mathematical formulas, and has the required graphs and tables illustrating the presentation.

The textbook does have some shortcomings. The inappropriate title of the book would better be replaced by another. "Marine Steam-Generating Atomic Plant," since it does not consider steam turbine plant which, along with steam-generating plant, forms part of an atomic power plant. The book is somewhat too long for the number of hours devoted to the subject and this will in some measure hinder the use of the text in the teaching process. Some topics in the textbook are repeated. For example, Chapter 1 (Sec. 1.8) deals with the principles of control but this topic is taken up in greater detail in Chap. 5. Ion-exchange filters are considered in Chap. 3 as well as Chap. 2. Some of the terms are not generally accepted, e.g., "poly-block steam-generating plant," "effective thermal efficiency," etc.

Notwithstanding the shortcomings mentioned above, the textbook conforms to the present curriculum and will contribute to an improvement in the training of students of marine engineering in marine colleges and can also be used by engineering and technical personnel operating marine atomic power plants.

B. A. Briskman

COMPONENTS OF ABSORBED ENERGY OF REACTION RADIATION*

Reviewed by Yu. I. Bregadze

Research on the effect that ionizing radiation has on various materials and substances is acquiring ever-increasing practical importance. The study of the behavior of materials in intensive γ-neutron fields is being highly topical in connection with the accelerated development of reaction construction for nuclear power.

Reactor radiation is complex in composition. The composition differs not only at various points in the apparatus during operation in the steady-state mode, but may also vary when the apparatus is in service. Moreover, the specific nature of the interaction of reactor radiation with matter is such that variations in the radiation in materials with different elements in their composition, placed at one and the same point in the radiation field, may be due to different components of the mixed radiation. Hence the understandable interest in the development of methods of measuring physical quantities which specify the degree of the effect of the reactor radiation on materials and substances.

The investigations are being carried out in two principle directions:

I. Development of methods of measuring the characteristics of radiation fields, i.e., quantities such as neutron fluence, and the differential energy dependence of the density of the neutron and γ-neutron fluxes.

II. Creation of methods of measuring the radiation energy released in the materials studied, including the breakdown of the energy into components due to different forms of mixed reaction radiation.

The book under review is devoted to a critical generalization of published works on the development of methods of measuring radiation energy. The book describes experiments conducted on concrete reactors in the USSR and elsewhere, illustrating various methods of measurement.

Reference data are given about the characteristics of the interaction of radiation with matter, data which are of interest to dosimetry experts. The monograph also generalized such results of original research which have made a large contribution to the development of methods for the dosimetry of reactor radiation.

*Atomizdat, Moscow (1976).

Translated from Atomnaya Énergiya, Vol. 42, No. 2, pp. 161-162, February, 1977.

Much attention has been paid to the reliability of the results of measurement and an analysis is made of possible sources of error of measurement and methods of estimating corrections so as to ensure a higher accuracy of measurement.

The monograph draws upon extensive factual and bibliographical material.

The book will prove useful to specialists in the dosimetry of ionizing radiation.

I. V. Goryachev, V. I. Kukhtevich,
and L. A. Trykov

DESIGN AND TESTING OF SHIELDING AGAINST RADIATION FROM NUCLEAR EXPLOSION*

Reviewed by S. G. Tsypin

As its preface states, the book under review constitutes a supplement to and extension of the book "Shielding against Penetration from an Atomic Explosion," published by Atomizdat in 1970. Therefore, the present review should be considered as a review of both books.

Designing shielding against nuclear explosions does not differ fundamentally from designing biological shielding for reactors but it does have some distinctive features due to the specific geometrical conditions and the characteristics of the radiation field.

The 1970 book presented in detail the characteristics of a nuclear explosion as a source of penetrating radiation as well as the radiation field near the surface of the Earth. The authors did not consider the generally accepted definition and physical treatment of some well-known phenomena; this made it possible in a small book to elucidate the features of the field of neutrons and γ radiation during and after a nuclear explosion. This chapter is supplemented by the first chapter of the second book which describes the principal characteristics in time. The need to know the latter is due to the fact that the efficiency of some forms of apparatus is more often determined by the instantaneous than be the integrated parameters of the radiation.

The fourth and fifth chapters of the 1970 book are devoted to the calculation of the characteristics of the passage of neutrons and γ radiation through shielding. They are supplemented by Chapter 3 of the 1976 book which describes the methods and experimental arrangements for studying the characteristics of the passage of the radiations from a nuclear explosion through flat elements for shielding and their reflection from those elements.

The basic merit of the authors is their systematic exposition of the theory and methods of calculating the shielding capability of equipment against penetrating radiation produced by a nuclear explosion. Some methods have won recognition in the Soviet and foreign literature.

The method of calculating the shielding capability of simple equipment (1970) has been developed further in the 1976 book which presents the analytic apparatus for calculating complex equipment. Moreover, a method is presented for the oriented design of shielding, making it possible to synthesize the equipment design which will ensure the required protection for the personnel of equipment and apparatus on the ground.

For the first time in the literature, there is a presentation of the experimental testing of shielding against radiation from a nuclear explosion under natural conditions, and especially under model conditions.

*Atomizdat, Moscow (1976).

Translated from Atomnaya Énergiya, Vol. 42, No. 2, p. 162, February, 1977.

Here, the main attention has been focused on the choice of suitable radiation sources and geometric conditions for the measurement. The 1976 book gives a detailed description of the methods and experimental arrangements for imitating the characteristics of the field of ionizing radiation during an explosion and at the sites of radioactive fallout. Individual chapters are devoted to the methodological aspects of measuring the characteristics of the field of reaction from imitator-sources and the data of such measurements for well-known experimental arrangements, as well as interpretation of the results in such tests.

The principal propositions associated with the reproduction of the field of ionizing radiation and the testing of the shielding capability of equipment are compared with well-known results of the actual testing of nuclear weapons.

Having noted the theoretical virtues, and especially the practical virtues of both books, one must point out that the material is somewhat disconnected. The use of different systems of physical units hinders their practical application. The data on the penetration of radiation through shielding need to be supplemented and updated. The chapters on the experimental testing of the shielding capability of equipment would be advisably supplemented with a presentation of the characteristics and distinctive features of the design of the recording instrumentation employed for these purposes as well as with data about the characteristics of fields of penetrating radiation during underground explosions.

Both books are well written and they make a significant contribution to the elucidation of one of the current problems of physics today.

engineering science

continued from back cover

Title	# of Issues	Subscription Price
Metallurgist *Metallurg*	12	$225.00
Metal Science and Heat Treatment *Metallovedenie i termicheskaya obrabotka metallov*	12	$215.00
Polymer Mechanics *Mekhanika polimerov*	6	$195.00
Problems of Information Transmission *Problemy peredachi informatsii*	4	$175.00
Programming and Computer Software *Programmirovanie*	6	$95.00
Protection of Metals *Zashchita metallov*	6	$195.00
Radiophysics and Quantum Electronics (Formerly Soviet Radiophysics) *Izvestiya VUZ. radiofizika*	12	$225.00
Refractories *Ogneupory*	12	$195.00
Soil Mechanics and Foundation Engineering *Osnovaniya, fundamenty i mekhanika gruntov*	6	$195.00
Soviet Applied Mechanics *Prikladnaya mekhanika*	12	$225.00
Soviet Atomic Energy *Atomnaya energiya*	12 (2 vols./yr. 6 issues ea.)	$235.00
Soviet Journal of Glass Physics and Chemistry *Fizika i khimiya stekla*	6	$ 95.00
Soviet Journal of Nondestructive Testing (Formerly Defectoscopy) *Defektoskopiya*	6	$225.00
Soviet Materials Science *Fiziko-khimicheskaya mekhanika materialov*	6	$195.00
Soviet Microelectronics *Mikroélektronika*	6	$135.00
Soviet Mining Science *Fiziko-tekhnicheskie problemy razrabotki poleznykh iskopaemykh*	6	$225.00
Soviet Powder Metallurgy and Metal Ceramics *Poroshkovaya metallurgiya*	12	$245.00
Strength of Materials *Problemy prochnosti*	12	$295.00
Theoretical Foundations of Chemical Engineering *Teoreticheskie osnovy khimicheskoi tekhnologii*	6	$195.00
Water Resources *Vodnye Resursy*	6	$190.00

SEND FOR YOUR
FREE EXAMINATION COPIES

Plenum Publishing Corporation
Plenum Press • Consultants Bureau
• IFI/Plenum Data Corporation
227 WEST 17th STREET
NEW YORK, N. Y. 10011

United Kingdom: Black Arrow House
2 Chandos Road, London NW10 6NR England

Back volumes are available. For further information, please contact the Publishers.

breaking the language barrier

WITH COVER-TO-COVER
ENGLISH TRANSLATIONS
OF SOVIET JOURNALS

in engineering science

Title	# of Issues	Subscription Price
Automation and Remote Control *Avtomatika i telemekhanika*	24	$260.00
Biomedical Engineering *Meditsinskaya tekhnika*	6	$195.00
Chemical and Petroleum Engineering *Khimicheskoe i neftyanoe mashinostroenie*	12	$275.00
Chemistry and Technology of Fuels and Oils *Khimiya i tekhnologiya topliv i masel*	12	$275.00
Combustion, Explosion, and Shock Waves *Fizika goreniya i vzryva*	6	$195.00
Cosmic Research (Formerly Artificial Earth Satellites) *Kosmicheskie issledovaniya*	6	$215.00
Cybernetics *Kibernetika*	6	$195.00
Doklady Chemical Technology *Doklady Akademii Nauk SSSR*	2	$65.00
Fibre Chemistry *Khimicheskie volokna*	6	$175.00
Fluid Dynamics *Izvestiya Akademii Nauk SSSR mekhanika zhidkosti i gaza*	6	$225.00
Functional Analysis and Its Applications *Funktsional'nyi analiz i ego prilozheniya*	4	$150.00
Glass and Ceramics *Steklo i keramika*	12	$245.00
High Temperature *Teplofizika vysokikh temperatur*	6	$195.00
Industrial Laboratory *Zavodskaya laboratoriya*	12	$215.00
Inorganic Materials *Izvestiya Akademii Nauk SSSR, Seriya neorganicheskie materialy*	12	$275.00
Instruments and Experimental Techniques *Pribory i tekhnika eksperimenta*	12	$265.00
Journal of Applied Mechanics and Technical Physics *Zhurnal prikladnoi mekhaniki i tekhnicheskoi fiziki*	6	$225.00
Journal of Engineering Physics *Inzhenerno-fizicheskii zhurnal*	12 (2 vols./yr. 6 issues ea.)	$225.00
Magnetohydrodynamics *Magnitnaya gidrodinamika*	4	$175.00
Measurement Techniques *Izmeritel'naya tekhnika*	12	$195.00

SEND FOR YOUR FREE EXAMINATION COPIES

Back volumes are available.
For further information,
please contact the Publishers.

continued on inside back cover

Declassified and Approved For Release 2013/04/01 : CIA-RDP10-02196R000700090002-7